Proceeding
Of
International Conference on Computer Science and Information Technology (ICCIT 2014),

International Conference on Electrical Power control And Electronics Engineering. (ICEPEE- 2014)
&
International Conference on Civil & Chemical Engineering (ICCCE- 2014)

Date: 7th December 2014
Goa

Editor-in-Chief

PROF. (DR.) ARJUN PRALHAD GHATULE
Sinhgad Institute of Computer Sciences,
Pandharpu(MS),India

Organized by:

TECHNICAL RESEARCH ORGANISATION INDIA
Website: www.troindia.in

ISBN: 978-81-930280-3-2

About Conference

Technical Research Organisation India (TROI) is pleased to organize the International Conference on Computer Science and Information Technology (ICCIT 2014), International Conference on Electrical Power control And Electronics Engineering. (ICEPEE- 2014) & International Conference on Civil & Chemical Engineering (ICCCE- 2014)

ICCIT & ICEPEE is a comprehensive conference covering the various topics of Engineering & Technology such as Computer Science, Electrical and IT. The aim of the conference is to gather scholars from all over the world to present advances in the aforementioned fields and to foster an environment conducive to exchanging ideas and information. This conference will also provide a golden opportunity to develop new collaborations and meet experts on the fundamentals, applications, and products of Computer science and Electrical. We believe inclusive and wide-ranging conferences such as ICCIT can have significant impacts by bringing together experts from the different and often separated fields of Computer & IT. It creating unique opportunities for collaborations and shaping new ideas for experts and researchers. This conference provide an opportunity for delegates to exchange new ideas and application experiences, we also publish their research achievements. ICEPEE & ICCCE shall provide a plat form to present the strong methodological approach and application focus on Electrical, civil & chemical engineering that will concentrate on various techniques and applications. The conference cover all new theoretical and experimental findings in the fields of Electrical, Civil & Chemical engineering or any closely related fields.

Topics of interest for submission include, but are not limited to:

Computer Science & Engineering
Information Technology
Electrical Engineering
Electronics Engineering
Chemical Engineering
Aeronautical Engineering
Environmental Engineering
Nano-Technology,
Genetic Engineering
Materials and Metallurgical Engineering
Soft computing
Aeronautical Engineering
Agricultural engineering
Civil engineering
Engineering Science
Network Engineering
Software Engineering
Structural Engineering
System Engineering
Telecommunication Engineering
And many more....

Organizing Committee

Editor-in-Chief:
Prof. (Dr.) Arjun P. Ghatule
Director, Sinhgad Institute of Computer Sciences (MCA),Solapur(MS)

Programme Committee Members:

Dr. Dariusz Jacek Jakóbczak
Assistant Professor , Computer Science & Management .
Technical University of Koszalin, Poland

Dr. Hansa Jeswani
Asso. Professor.,
Sardar Patel College of Engineering, Mumbai- 58

Dr. S.P.ANANDARAJ.,
M.Tech(Hon's),Ph.D.,
Sr.Assistant Professor In Cse Dept,
Srec, Warangal

Prof O. V. Krishnaiah Chetty
Dean, Mechanical Engineering
Sri Venkateswara College of Engineering and Technology
Chittoor- Tirupati

Dr. D.J. Ravi
Professor & HOD, Department of ECE
Vidyavardhaka College of Engineering, Mysore

Prof. Roshan Lal
PEC University of Technology/Civil Engineering Department,
Chandigarh, India
rlal_pec@yahoo.co.in

Dr. Bhasker Gupta
Assistant Professor. Jaypee University of Information Technology, Himachal Pradesh

Dr. A. Lakshmi Devi,
Professor, department of electrical engineering,
SVU college of Engineering, Sri Venkateswara university, Tirupati

Prof. Shravani Badiganchala

Assistant professor, Shiridi sai institute of science and engineering

Prof. Surjan Balwinder Singh

Associate Professor in the Electrical Engineering Department,
PEC University of Technology, Chandigarh.

Dr. Shilpa Jindal ,
PEC University of Technology (Deemed University), Chandigarh
ji_shilpa@yahoo.co.in

Prof. S. V. Viraktamath
Dept. of E&CE S.D.M. College of Engg. & Technology Dhavalagiri, Dharwad

Subzar Ahmad Bhat
Assistant Professor, Gla University
Dr. G.Suresh Babu
Professor,Dept. of EEE,CBIT, Hyderabad

Prof .Ramesh
Associate Professor in Mechanical Engineering,
St.Joseph's Institute of Technology

Prof.Amit R. Wasnik
Sinhgad Institute of Technology, Pune, Maharashtra

IIT KHARAGPUR
Prof. Rajakumar R. V.
DEAN Acadedemic, rkumar @ ece.iitkgp.ernet.in
Prof. Datta D., ddatta @ ece.iitkgp.ernet.in
Prof. Pathak S S,r,ssp @ ece.iitkgp.ernet.in

XIMB,BHUBANESWAR
Prof Dr. Subhajyoti Ray.M-Stat, (ISI); Fellow, IIM(A),
Dean academic,XIMB-subhajyoti@ximb.ac.in ,
Prof.Andrew Dutta

Prof. Saveeta Mohanty

Dr. S. Peppin

Prof. Dipak Misra

Dr. W.S. William

Prof. Sunil agrawal

TABLE OF CONTENTS

Editorial

The conference is designed to stimulate the young minds including Research Scholars, Academicians, and Practitioners to contribute their ideas, thoughts and nobility in these two integrated disciplines. Even a fraction of active participation deeply influences the magnanimity of this international event. I must acknowledge your response to this conference. I ought to convey that this conference is only a little step towards knowledge, network and relationship.

The conference is first of its kind and gets granted with lot of blessings. I wish all success to the paper presenters.

I congratulate the participants for getting selected at this conference. I extend heart full thanks to members of faculty from different institutions, research scholars, delegates, TROI Family members, members of the technical and organizing committee. Above all I note the salutation towards the almighty.

Editor-in-Chief:
Prof. (Dr.) Arjun P. Ghatule
Director, Sinhgad Institute of Computer Sciences (MCA),
Solapur(MS)

ADVANCED MULTIMODALITY IMAGE FUSION TECHNIQUE USING DDWT AND PSO

[1]Mr.Pradeep Patil, *Student*, IOKCOE, Pune
[2] Prof.Ritesh Thakur, H.O.D (Computer Engg.), IOKCOE, Pune
E-mail: [1]patil.pr00@gmail.com, [2]ritraj_t@yahoo.com

Abstract— Image fusion is a process where multiple images (more than one) from different or same source are combined to form a single resultant fused image. This fused image is more productive, informative, descriptive and qualitative as compared to its original input images or than individual images. The fusion technique in medical images is useful for resourceful disease diagnosis purpose and robot surgery for doctors. This paper illustrates multimodality medical image fusion techniques and their results assessed with various quantitative metrics. Firstly two registered images CT and MRI-T2 are taken as input.

In this paper, a multimodal image fusion algorithm based on Dual tree discrete wavelet transform and particle swarm optimization (PSO) is proposed. Firstly, the source images are divided into low-frequency coefficients and high-frequency coefficients by the dual-tree discrete wavelet transform (DDWT). The low-frequency coefficients are fused by weighted average method based on regions, and PSO is used to determine to obtain proper fusion weight parameter from high-frequency coefficients from segmented images by DDWT. Also PSO is used to determine α parameter called scalar weight. Finally, the fused image is reconstructed by the inverse DDWT.

Index Terms: DDWT, PSO, Image fusion, Quantitative Metrics.

I. INTRODUCTION

Medical imaging field require highly productive, descriptive, informative image with high resolution and having high information content with respect bones, tissues and visualization for Necessary disease diagnosis for doctors and experts. This is impossible using single modality medical Images as X-ray computed tomography (CT) is best suited only for recognizing bones structure, where as MRI giving better information about the soft tissues. In reality we require corresponding information from different modalities for correctly diagnosis of disease of patient. For the same reason, Medical image fusion is the only promising technique which is successful to attract researchers, scientist to guide the doctors by producing high quality fused images and by extracting suitable information from a variety of modalities say CT, MRI, SPET, PET etc. In the area of medical image fusion, there are various fusion techniques, but these techniques have certain limitations [2]. For example, Wavelet transform is famous technique but suffers from Shift variance and additive noise which can be reduced by Using DDWT (Dual Tree Discrete Wavelet Transform). Thus multimodality medical image fusion has emerged as a promising research area in the recent years.

Image fusion basically aims at extracting and combining information from the source images on pixel basis thus resulting a more precise and complete information about an object. The actual fusion process can be carried out at several levels. Under this, in the pixel-level image fusion the fused images provided all relevant information present in original images with no artifacts or inconsistencies.

The pixel-level image fusion was classified into two type one as spatial domain fusions

and second as transform domain fusion. Spatial domain fusion is directly applied on the source images which results in reduce the signal to-noise ratio of the resultant image with simple averaging technique but causes spatial distortion in the resulting fused image. Improvement in fused image is carried out by using PSO (Particle Swarm Optimization) a population based algorithm inspired by natural behaviors of bird flocking, Ant colony etc.PSO gives optimal fused image also it is used to select proper scalar weight from high-coefficient intensities pixel from decomposed source images [11]. The quality of fused image is assessed by quantitative metrics like Entropy (EN), Root Mean Square Error (RMSE), Mutual Information (MI), and Peak Signal to Noise Ratio (PSNR) and Signal to Noise Ratio (SNR).

II. Literature Survey

The traditional Wavelet transform (WT) is based on Mallat algorithm. Basically wavelets transform carries out in three steps: 1) Decomposition of registered input images in to high and low frequency sub-bands, 2) To obtain new image, combination of approximate (low frequency part) and detail (high frequency part) is done and lastly 3) inverse wavelet transform is applied to construct fused image. The traditional wavelet is complex and it requires more storage space for read and writes an operation which is not suitable for real time applications [4]. The second generation of wavelet transform is called as Lifting Wavelet transforms (LWT) algorithm proposed in [10].It reduces the running time and storage space of image fusion. Lifting scheme consists of three phases: Split phase,2)Prediction phase and3)Update phase. Reconstruction of the image in LWT is also having three phases: Anti-update phase, Anti-Prediction phase and Merger phase which is opposite process of decomposition [10]. In LWT algorithm, first approximation coefficients and detail coefficients are computed by applying LWT, feature selection rule is applied on wavelet coefficients to obtain fused coefficients groups and finally the inverse LWT (ILWT) is applied to obtain fused image.

Discrete Wavelet Transform proposed in [7] frequently apply two channel filter bank out of which low pass band at the lowest resolution and high pass band at each step iteratively. In this Wavelet environment, firstly the K-level decomposition based on WT is performed on registered source images. K level decomposition consist of one low frequency band and 3K high frequency bands, then fused coefficients are obtained and lastly inverse DWT is carried out to get the fused image. The DWT gives better fused image with less computational cost and no loss of information.

III. Implementation Details

DDWT Algorithm:

It stands for Dual Tree Discrete Wavelet Transform. DDWT proposed by Kingsbury is only potential tools with the following advantages: direction selectivity, limited redundancy, and shift invariance. It is a complex transform whose wavelet function is restrained to have single-sided spectrum. Either the real part or the imaginary part can be used as a individual transform since both guarantee perfect reconstruction. Thus, DDWT is an over complete transform with redundancy of 2*m*:1 for *m*-dimensional signals. Only the real part of DDWT is taken in coding applications to reduce the introduced redundancy. For example, the resulting repeated information will be reduced to 2:1 from 4:1 i.e. by twice for 2-D case. The real part of DDWT is simply referred to as DDWT hereafter, unless otherwise stated. The implementation of 2-D DDWT follows two steps procedure. Firstly, an input image is divided up to a desired level by two separable 2-D DWT braches, branch *a* and branch *b*, whose filters are purposely designed to meet the Hilbert pair requirements. Thus six high-pass sub bands are generated: *HL*a, *LH*a, *HH*a, *HL*b, *LH*b, and *HH*b, at each level. Secondly, every two corresponding sub bands which have the same pass-bands are linearly combined by either averaging method or differencing method. We have result, sub bands of 2-D DDWT at each level are obtained as $(HL_a + HL_b)/2$, $(HL_a - HL_b)/2$, $(LH_a + LH_b)/2$, $(LH_a - LH_b)/2$, $(HH_a + HH_b)/2$, $(HH_a + HH_b)/2$ [5].

PSO Algorithm:

PSO stands for Particle Swarm Optimization is a population based optimization algorithm exhibits natural behaviors of animal such as bird flocking, Ant colony etc. which is useful to find scalar weight (α parameter).

The processing steps of PSO are given as follows.

Step 1: Set off the population. Each particle has its own random velocity and position.

Step 2: Determine the fitness function value of each particle.

Step 3: Find the best position of each particle by its own experience.

Step 4: Find the position of the best particle.

Step 5: Update the velocity and position of each particle by following equation no. (1) And equation no. (2).

$$V^d_i(t+1) = \omega.(t) + c1.r1(t).(p^d_i(t)-x^d_i(t)) + c2.r2(t).(p^d_g(t)-x^d_i(t)) \quad (1)$$

$$x^d_i(t+1)=x^d_i(t)+V^d_i(t+1) \quad (2)$$

Where t = iteration counter, ω = is the inertia weight controlling the impact of the previous velocity,c1 and c2 = learning constant , r1 and r2=random variables in the range[0,1],p_i=best position of particle i, p_g=best position of all particles within iteration t.

Step 6: Stop if the current approximate solution can be accepted or the stopping criterion is satisfied. Otherwise, jump to Step 2 [11].

Proposed fusion method model:

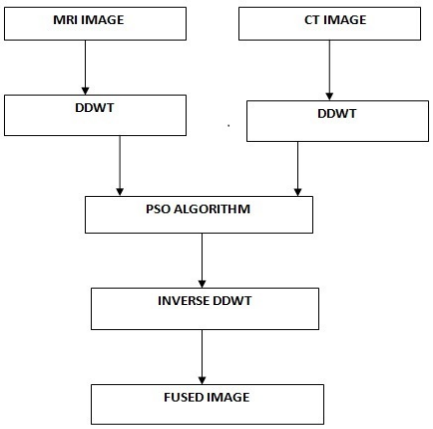

Fig.1. Proposed fusion method Design

This proposed fusion method accepts two input images of different modality say CT and MRI. Then those input images are decomposed into high sub band and low sub band respectively using DDWT algorithm and high coefficient are selected using either averaging method and PSO is used to find scalar weight to find optimal coefficient for fused image. finally inverse DDWT is performed to get resultant fused image.

IV. RESULTS

Dataset description:

This section describes different modality input images for experimental or demonstration purpose. Images of modality like MRI considered for fusion process one is MRI-T1 and MRI-T2 of which are gray scale images. Both input images are having GIF format and of size 9.06KB and 9.36KB respectively. Also images have dimensions of 169×204 pixels and 166×201 pixels which are registered images.

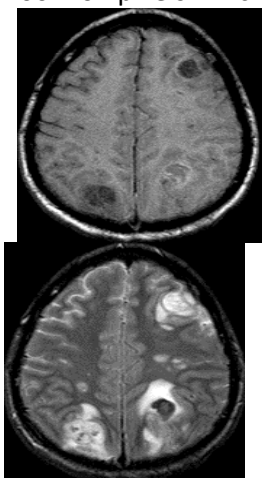

Fig.2.MRI-T1.gif
Fig.3.MRI-T2.gif

Similarly gray scale images of CT and CT-1 modality can be used for same process with size of 9.79KB and 6.89KB respectively with dimensions of 177×228 pixels and 164×207 pixels.

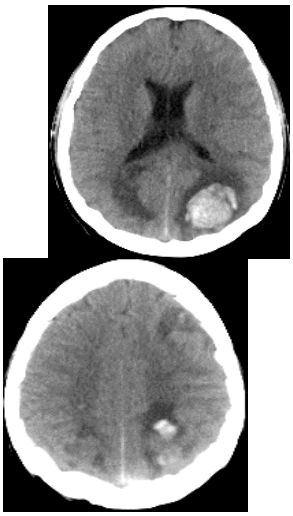

Fig.4. CT.gif
Fig.5.CT-1.gif

Result Description:

This section briefly describes several quantitative measure for visual as well quality evaluation of resultant fused image. The visual analysis alone cannot be only the criteria for quality evaluation.

1. Peak signal to noise ratio (PSNR): PSNR is defined as the ratio between the signal and the noise. PSNR is computed as[2]

$$PSNR=20\log_{10}[L^2/1(m\times n)\sum_{i=1}^{m}\sum_{j=1}^{n}[R(i,j)-(i,j)]^2] \quad (3)$$

A higher value of PSNR gives better fusion results.

2. Signal to Noise Ratio (SNR): It is defined as the ratio of mean pixel value to that of standard deviation of the corresponding pixel values. It gives the contrast information of the image Higher value of SNR indicates more contrast.[2]

$$SNR=Mean/StandardDeviation \quad (4)$$

3. Overall cross entropy (OCE): OCE measure difference between the input images and the fused image. Lower the value better is the fusion results obtained. It is given as[2]

$$OCE(I_A,I_B,F)=(CE(I_A,F)+CE(I_B,F))/2 \quad (5)$$

4. Root Mean Square Error (RMSE): RMSE value is calculated between the reconstructed image and original image for every fusion performed and present resulting error as a percentage of the mean intensity of the original image [6].

$$RMSE=\sqrt{(1/(M/N))[\sum X\sum Y(I_{true(x,y)-used(x,y)})]} \quad (6)$$

5. Entropy (EN): Entropy is often calculated to measure the information content of the image. A higher value of entropy display better fusion results. The entropy of an image is calculated using the formulae:[9]

$$EN=-\sum_{i=0}^{L-1}p_i\log_2 p_i \quad (7)$$

From above qualitative measure we can predict expected result will be as follows: Exiting result and Expected results are provided by considering dataset images of Brain say MRI-T1.gif and CT.gif

TABLE I
EXPECTED RESULTS

Quality Measure	Exiting Result	Expected result with proposed model
PSNR	47.6414	>47.6414
SNR	0.4576	>0.4576
OCE	1.0705	<1.0705
RMSE	5.6665	<5.6665
EN	6.6090	>6.6090

V. CONCLUSION AND FUTURE SCOPE

In our paper new technique of multimodality image fusion which combines the DDWT and PSO is presented. Our proposed method will give outperformed result using DDWT and PSO. Also proposed system overcome shift

invarience effect and ensures better quality fused image. Also researcher has scope to develop more reliable fusion technique using Multifocus images or Multiresolution images for motion picture and in scene mixing as well as we can extend our research for 3D image fusion.

VI. Acknowledgement

I would like to thank my colleagues to solve many queries that I had taken to them. In particular, I would like to thank my guide Prof. Ritesh Thakur for supporting my work.

VII. Reference

[1] Bhatnagar, G.; Wu, Q.M.J.; Liu, Z., "Directive Contrast Based Multimodal Medical Image Fusion in NSCT Domain," *Multimedia*, IEEE Transactions on, vol.15, no.5, pp.1014, 1024, Aug. 2013.

[2] Chandra Prakash, S Rajkumar, P.V.S.S.R.Chandra Mouli"Medical Image Fusion Based on Redundancy DWT and Mandani Type Min-Sum-Mean-of-Max Techniques with Quantitative Analysis"IEEE, 978-1-4673-0255-5/2012.

[3] Da Cunha, A.L.; Jianping Zhou; Do, M.N., "The Nonsubsampled Contourlet Transform: Theory, Design, and Applications," *Image Processing*, IEEE Transactions on, vol.15, no.10, pp.3089, 3101, Oct.2006.

[4] Hsuan-Ying Chen & Jin-Jang Leou," Multispectral and Multiresolution image fusion using particle swarm optimization" Springer, 2011.

[5] Jingyu Yang, Jizheng Xu, Feng Wu, Qionghai Dai1 and Yao Wang" image coding using 2-d anisotropic dual-tree discrete wavelet transform, "*ICIP,IEEE 1-4244-1437/7,*2007

[6] Kiran Parmar,Rahul k Kher, Falgun N Thakkar,"Analysis of CT and MRI image fusion using wavelet transform" *International Conference on Communication Systems and Network technologies*,IEEE,2012.

[7] Parmar, K.; Kher, R., "A Comparative Analysis of Multimodality Medical Image Fusion Methods," *Modelling Symposium* (AMS), 2012 Sixth Asia , vol., no., pp.93,97, 29-31 May 2012.

[8] Po, D.D.-Y.; Do, M.N., "Directional multiscale modelling of images using the contourlet transform," *Image Processing*, IEEE Transactions on, vol.15, no.6, pp.1610,1620, June 2006.

[9] Shrey Gupta,S Rajkumar, V Vijayarajan, K Marimuthu, "Quantitative Analysis of various image fusion techniques based on various metrics using different multimodality medical images", *International journal of engineering and technology* ,IJET, 0975-4024,2013.

[10] Wei Li; Xuefeng Zhu; Shaocheng Wu, "A Novel Approach to Fast Medical Image Fusion Based on Lifting Wavelet Transform," *Intelligent Control and Automation*, 2006. WCICA 2006. The Sixth World Congress on, vol.2, no., pp.9881, 9884.

[11] Yushu Liu, Mingyan Jiang "Multifocus image fusion Based on Multiresolution Transform and Particle Swarm Optimization" *Proceedings of the second International Conference on Computer and Information Application*, 2012(ICCIA 2012).

[12] Zhao Wencang; Cheng Lin, "Medical image fusion method based on wavelet multi-resolution and entropy," *Automation and Logistics*, ICAL, IEEE International Conference on, vol., no., pp.2329, 2333, 1-3 Sept. 2008.

APPROACHES TO IMPROVE CLOUD COMPUTING PERFORMANCE

[1]Akshay M Murshilli, [2]Dr. Sarojadevi Hande
PG Scholar at NMAMIT Nitte
Email: [1]ak.murshilli@gmail.com, [2]sarojadevi@nitte.edu.in

Abstract— Cloud Computing is the delivery of computing services over the Internet. Cloud computing at present generation aims to provide the data centers and enables application service providers to lease data center capabilities for deploying applications, depending on user Quality of Service (QOS) requirements. Cloud applications have different configurations, compositions and deployment requirements. Measuring the performance of resource allocation policies and application scheduling algorithms at finer details in Cloud computing environments is one of the challenging problems to tackle. In this paper the CloudSim architecture, CloudSim life cycle is explained and also the scheduling methods like Time-Space shared scheduling method and FIFO based scheduling method are proposed and evaluated. This analysis helps in virtual to real deployment and would be easier and accurate.

Index Terms—CloudSim, Cloud Computing, Cloud Applications, Application Scheduling.

I. INTRODUCTION

Cloud Computing is one of the technologies which provides secured and efficient services over the internet. Cloud computing at present generation aims to provide the data centers and it enables the application service providers to lease data center capabilities for deploying applications depending on users QOS requirements. Cloud services which are now available allow businesses and individuals to use software and hardware which are managed by third parties somewhere located at remote locations. Cloud Computing is mainly used for providing a service to the consumer, it is "pay as per use" service. Cloud Computing provides services such as Software as a Service (SaaS), Platform as a service (PaaS) and Infrastructure as a service (IaaS). Now a day's the internet is fast growing, the individuals and big organizations are finding new ways to reduce the cost of implementation, storage or communication.

Cloud Computing has basically two parts, the First part is of Client Side and the second part is of Server Side. The Client Side requests to the Servers and the Server responds to the Clients. The request from the client firstly goes to the Master Processor of the Server Side. The Master Processor have many Slave Processors, the master processor sends that request to any one of the Slave Processor which is free at that time. All Processors are busy in their assigned job and none of the Processor gets Idle.

In Cloud Computing Job Scheduling is a very difficult due to its parallel and distributed environment. The order in which work is performed in the computer system is called Scheduling. Job may be distributed among more than one virtual machine, so it is difficult to determine the job completion time.

To host an application in cloud environment requires complex deployment and composition, and to evaluate the implemented model in repeated manner is very tedious and

costly process. So simulation tools like CloudSim are used to model Cloud Computing systems and application environment. The CloudSim is an extensible simulation toolkit that enables simulation and modeling of Cloud Computing environments. The CloudSim toolkit supports for modeling and creation of one or more virtual machines (VMs) on a simulated node of a Data Center, jobs, and their mapping to suitable VMs. It also allows simulation of multiple Data Centers to enable a study on federation and associated policies for migration of VMs for reliability and automatic scaling of applications.

CloudSim provides lots of benefits to IT companies or an individual who wants to deploy his services through cloud. CloudSim has the following important properties [09]:

- CloudSim helps to simulate and model the data center, Cloud Computing environments.
- CloudSim provides a self-contained platform for modelling clouds, provisioning, service brokers and allocation policies.
- CloudSim provides support for simulation of network connections among the simulated system resources.
- CloudSim provides facility for simulation of federated cloud environment that inter-networks resources.

These features show that CloudSim aids in developing the cloud environments and it uses sequential algorithms [10] like FCFS to allocate the resources. This sequential way may not match with the real world requirements because there are different types of requirement in the real world that must be categorized and allocation should be done based on different categories. So there is need to refine the algorithm and architecture of CloudSim so that every experiment using this simulator can be compared directly to the physical set up of cloud environment. By doing this the cost and time of cloud implementation can be reduced.

CloudSim Simulation Environment: CloudSim frame work does the following things, firstly entity will be created which is named as CIS (Cloud Information Service), and this is the kind of registry that contains the resources that are available on the cloud. So CIS takes care of registry of the data center. Now data center is required to be registered and this registration process will be done with the CIS. Data center will be having some characteristics. Characteristics are basically for the hosts, each host will have some hardware configurations like number of processing elements, RAM, Bandwidth etc.

The cloud environment basically works on virtualization which differs from other technologies like parallel computing, grid computing etc. So virtualization says that the host will be virtualized into the number of machines, so each virtual machine will have the parameter.

It requires registering the datacenter with the CIS, as per the CloudSim frame work. Once above all process is done it is required to have the broker which will submit tasks to the data centers. Broker is basically an entity which at the initial stage talks to CIS and retrieves the resource information which is registered with the CIS about data centers, so the information so passed is called data center characteristics, now the broker will be having all the characteristics of the data centers. Refer to the **Figure 01** below:

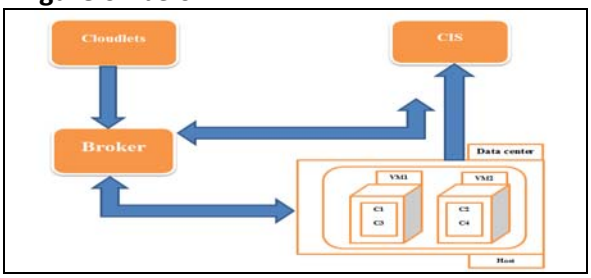

Figure 01: CloudSim Simulation Environment

Broker will have some tasks which are named as **Cloudlet(s)**, so set of cloudlets will be submitted to the broker. The broker directly interacts with the data center and assigns the cloudlet to some of the virtual machines which are running on the host. This is the basic framework or basic model which the CloudSim simulation tool which provide us. CloudSim

simulation tool takes care of lot of behavior's which are connected to all of the components, so the components are basically called as entities.

The above model works on various kinds of policies. We can submit more than one task to the virtual machines but overall processing is to be done is on the physical machine because the virtual machines share the resource of the physical machine. All the resources will be provided to the virtual machines on the basis of the policies i.e. virtual machine scheduler policies. So there are three different kinds of policies.

1. VM allocation policy.
2. VM scheduler policy.
3. Cloudlet scheduler policy.

So all the policies are either time shared or space shared.

II. RELATED WORK

Harjit Singh has discussed about the evolution process of cloud computing, characteristics of Cloud, current technologies adopted in cloud computing and they also presented a comparative study of cloud computing platforms (Amazon, Google and Microsoft), and its challenges. Cloud computing is the delivery of computing services over the Internet [01].

Qi Zhang has presented a survey of cloud computing, highlighting its key concepts, architectural principles and state-of-the-art implementation as well as research challenges. The aim of the paper is to provide a better understanding of the design challenges of cloud computing and identify important research directions in this increasingly important area [02].

Monica Gahlawat, Priyanka Sharma have described about the basic information about the Cloud Computing and its various services and models like SaaS, IaaS and PaaS. They also described about the deploying models of Cloud Computing and Virtualization services [03].

Rodrigo N. Calheiros, Rajiv Ranja, Anton Beloglazov, Rajkumar Buyya, A. F. De Rose have described about the various web based application related to Cloud Computing [04].

Anthony Sulistio, Rajkumar Buyya have described about the Scheduling. They said Scheduling is a process of finding the efficient mapping of tasks to the suitable resources so that execution can be completed such as minimization of execution time as specified by customers. They described various types of Scheduling like Static, Dynamic, Centralized, Hierarchical, Distributed, Cooperative, Non-Cooperative Scheduling. They also described Scheduling problem in Cloud and the types of users like CCU (Cloud Computing Customers) and CCSP (Cloud Computing Service Providers) [05].

Catalin L. Dumitrescu, Ian Foster have described about the Simulation techniques and the CloudSim. They described the various features of CloudSim like it supports for modeling and simulation for large scale of cloud computing infrastructure including data centers on a single physical computing node [06].

Henri Casanova, Arnaud Legrand have described about the optimization criterion that is used when making scheduling decision and represents the goals of the scheduling process. The criterion is expressed by the value of objective function which allows us to measure the quality of computed solution and compare it with different solution [07].

Saul Berman, Lynn Kesterson-Townes, Anthony Marshall and Rohini Srivathsa have described about the Quality of Service that is the ability to provide different jobs and users, or to guarantee a certain level of performance to a job. If the QoS mechanism is supported it allows the user to specify desired performance for their jobs. In system with limited resources the QoS support results in additional cost which is related to the complexity of QoS requests and the efficiency of the scheduler when dealing with them [08].

III. SIMULATION WORK

Here it is explained about how actually the simulation works and for each module the code is included. Initially it is required to set the number of users; this will directly correlates with the broker count.

1. Requires the initialization of common variables.
   CloudSim.*init*(num_user, calendar, trace_flag);
2. Data center must be created, this in turn will lead to the creation of host, characteristics (Parameters: Processing Elements, RAM, BW etc.)
   Datacenter datacenter0 = *createDatacenter*("Datacenter_0");
3. Datacenter broker instance is required to be created.
   DatacenterBroker broker = *createBroker*();
   int brokerId = broker.getId();
4. Virtual machines (Parameters: Processing Elements, RAM, BW etc.) instances is required to be created.
   Vm vm1 = **new** Vm(vmid, brokerId, mips, pesNumber, ram, bw, size, vmm, **new** CloudletSchedulerSpaceShared());
5. Virtual machines which are created are submitted to the broker.
   broker.submitVmList(*vmlist*);
6. Requires specifying the cloudlet(s) which are created with the certain parameters.
   Cloudlet cloudlet = **new** Cloudlet(id, length, pesNumber, fileSize, outputSize, utilizationModel, utilizationModel, utilizationModel);
7. Cloudlets which are created are submitted to the broker. So now broker has both Cloudlets and Virtual machines. Cloudlets will be mapped to the virtual machines through broker.
   broker.submitCloudletList(*cloudletList*);
   broker.bindCloudletToVm(cloudlet.getCloudletId(),vm.getId());
8. Start Simulation function is called.
9. Stop Simulation function is called.
10. Prints the status of the simulation.

Data Center consists of different Hosts and the Host manages the VM Scheduler and VMs. Cloudlet Scheduler determines how the available CPU resources of virtual machine are divided among Cloudlets. There are two types of policies:

1**] Space-Shared** (Cloudlet Scheduler Space Shared): This is used for assigning specific CPU cores to specific VMs.

2] **Time-Shared** (Cloudlet Scheduler Time Shared): This is used to dynamically distribute the capacity of a core among VMs.

Whenever the cloudlets are deployed on VMs, both the Time shared and Space Shared is incorporated.

IV. PROPOSED FRAMEWORK

Cloud computing is a “pay as you go” service. It is not easy to deploy the simulated work directly to the real world because cloud services are layered services and it takes additional scenarios also into consideration. For example when we are providing a service as cloud, we have several tasks that have higher priorities and needed to be finished first and there will be some other tasks which are defined earlier and needed to be performed according to the scheduled time. In the CloudSim simulation toolkit, the VMs are created and are allocated based on the requirement of the hosts. An application is developed which simulates the cloud and performs Tasks Allocation to the VMs on the basis of FCFS (First-Come-First-Served) Scheduling Policy, in the Cloud.

The proposed architecture is given as **Figure 02**:

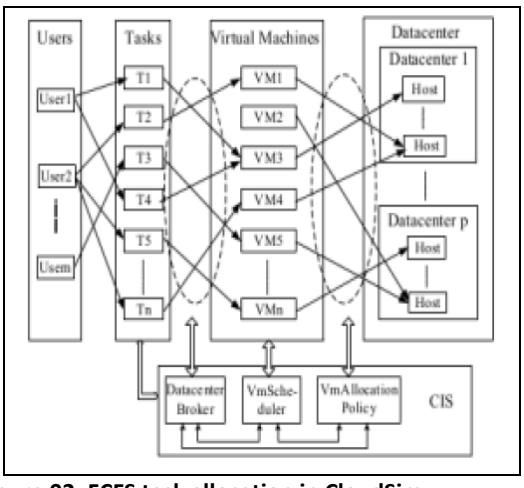

Figure 02: FCFS task allocation in CloudSim

Our FCFS scheduling will be having a Datacenter Broker that implements the FCFS

Task Scheduling Policy. The different Entities in our application are:

- FCFS
- FCFS Broker
- Datacenter Creator
- VMs Creator
- Tasks or Cloudlet Creator

FCFS: This entity creates the Datacenter and creates the VMs and creates the Cloudlets or Tasks by calling respective other entities. Once all of them are created, VMs and Tasks are submitted to the FCFS Broker.

FCFS Broker: This is a Datacenter Broker and it schedules the tasks to the VMs on the basis of FCFS policy. The tasks are got from the FCFS Entity.

Datacenter Creator: This entity is used to create Datacenter(s).

VMs Creator: This entity creates the specified number of VMs given by the user.

Cloudlet Creator: This entity creates the specified number of tasks.

Thus, we can perform task allocation to the VMs on the basis of FCFS (First-Come-First Served) Scheduling Policy in the Cloud.

V. RESULTS AND ANALYSIS

The type of scheduling policy used here is Time shared /Space Shared allocation policy. The simulation gives the timing performance as shown in the **Table 01,** referring to this table and considering the cloudlet performance of 3200sec, compared to the one without multiple cloudlets sharing the work, we get a speed up of 2. The speed up is given by the ratio of timing measurement without using multiple cloudlets sharing the work, over the timing with sharing.

Therefore Speedup = 800*8/3200

= 6400/3200

= 2

Total No. of Cloudlets	Timing Performance (Sec)
1	**800**
2	**1600**
8	**3200**

Table 01: Timing performance of different number of cloudlets

Speed up obtained is low compared to the ideal speed up. Therefore alternate mechanisms for improving performance such as FCFS method is experimented in CloudSim.

The FCFS scheduling is implemented and comparison of which is made with the performance of Time-Space shared scheduling of 8 cloudlets is given in **Table 02.** These simulation runs are carried out for 8 cloudlets and 2 VMs.

Scheduling Policy	Timing(Sec)
Time-Shared Scheduling	3200
FCFS	20.1

Table 02: Time taken to execute the cloudlets based on the scheduling policy.

The FCFS Scheduling takes 20.1sec for executing all 8 cloudlets. Further we can improve the execution time by using different scheduling policies like priority based scheduling policy.

Screen Shots for the Simulation runs corresponding to the results shown in **Table 02** are given below in **Figure 03** and **Figure 04**:

The simulation output displays the following information. The CloudSim toolkit is initialized and then datacenters are started, broker will be starting, Entities are started. Broker creates the VMs in the Datacenter and is created in the particular Host. Broker sends the cloudlets to the VMs. Cloudlets get executed and time at which the cloudlets got executed is sent back to broker. After when all cloudlets are executed all VMs are destroyed. Broker shuts down. Cloud Information Service (CIS) notifies to all entities to shut down. Simulation gets completed and status about the simulation is displayed.

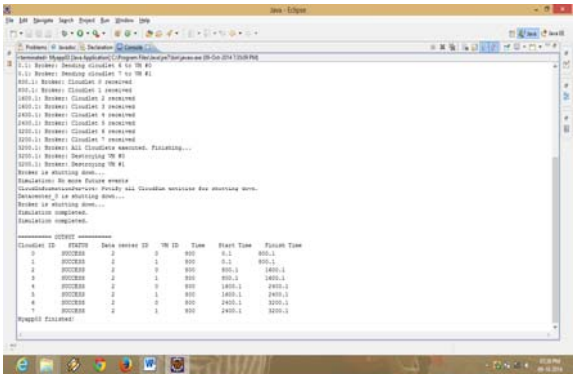

Figure 03: Time-Space Shared Scheduling

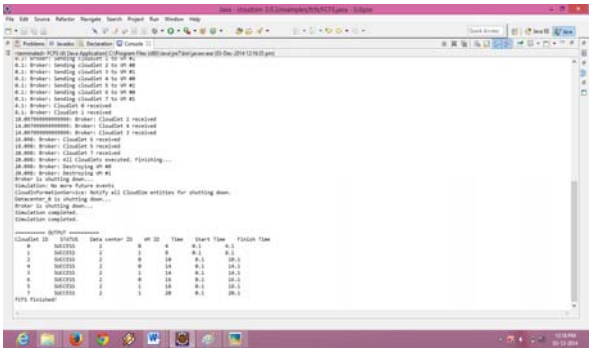

Figure 04: FCFS Scheduling

VI. CONCLUSION

Recently many efforts have been done in cloud technology to develop various techniques and have been presented to make it more efficient. CloudSim has been developed to help the organization and researcher to evaluate their experimental model before deployment in the real world. If the deployment is different from what we hypothyse then it causes heavy implementation and cost time. So in this paper simulation strategy is defined in real world manner so that the experiment what is being executed using CloudSim can be deployed directly in the cloud environment. Approaches to improve the performance of applications in Cloud Computing are discussed in this paper. An evaluation of the Scheduling mechanisms such as FCFS and Time-Space Scheduling are done in CloudSim environment. The results obtained indicate the scope for further improvement of the performance.

REFERENCES

[1] *Harjit Singh,* "Current Trends in Cloud Computing a Survey of Cloud Computing Systems", 2009.

[2] *Qi Zhang*, "Cloud computing: state-of-the-art and Research Challenges", 2010.

[3] Monica Gahlawat, Priyanka Sharma, "Analysis and Performance Assessment of CPU Scheduling Algorithms in Cloud using CloudSim", International Journal of Applied Information Systems (IJAIS) – ISSN: 2249-0868, 2013.

[4] Rodrigo N. Calheiros, Rajiv Ranja, Anton Beloglazov, Rajkumar Buyya, A. F. De Rose, "CloudSim: a toolkit for modelling and simulation of cloud computing environments and evaluation of resource provisioning algorithms", 2010.

[5] Anthony Sulistio, Rajkumar Buyya, "A Grid Simulation Infrastructure Supporting Advance Reservation".

[6] Catalin L. Dumitrescu, Ian Foster, "GangSim: A Simulator for Grid Scheduling Studies", 2005.

[7] Henri Casanova, Arnaud Legrand, Martin Quinson, "SimGrid: a Generic Framework for Large-Scale Distributed Experiments", 2006.

[8] Saul Berman, Lynn Kesterson-Townes, Anthony Marshall and Rohini Srivathsa, "The power of cloud: Driving business model innovation", IBM Global Business Services Executive Report.

[9] Rodrigo N. Calheiros, Rajiv Ranja, Anton Beloglazov, Rajkumar Buyya, A. F.De Rose, "CloudSim: a toolkit for modeling and simulation of cloud computing environments and evaluation of resource provisioning algorithms", 2010.

[10] Monica Gahlawat, Priyanka Sharma, "Analysis and Performance Assessment of CPU Scheduling Algorithms in Cloud using CloudSim", International Journal of Applied Information Systems (IJAIS) – ISSN: 2249-0868, 2013.

A REVIEW OF METHODS FOR SECURING LINUX OPERATING SYSTEM

[1]V.A.Injamuri
Govt. College of Engineering,Aurangabad, India
[1]Shri.injamuri@gmail.com

Abstract— This paper is focused on practical securing Linux production systems. It discusses basic Linux Security requirements for systems that need to pass various audits in an enterprise environment. This Linux Security is intended for a technical audience, Linux system administrators, and security people in corporations and organizations that have to use commercial Linux distributions for their production environment

***Index Terms*— iptables,RPM,inittab , boot script**

INTRODUCTION

There is a need to make Linux production systems compliant with various audit requirements; the system can offer a good baseline and starting point. The main objective of the system is to discuss basic Linux security requirements including account policies for production systems that are being audited [1].

Physical Security

Physical security should be of the utmost concern. Linux production servers should be in locked datacenters where only people with passed security checks have access. But physical security is out of scope for this article.

Verifying Security Action Items

To improve security, there are scripts available which can verify that all security action items have been executed. Even the best sys admins can make mistakes and miss steps. In case of larger Linux environment, it would be a good investment to write scripts for checking Linux security action items.

Retiring Linux Servers with Sensitive Data

To retire servers with sensitive data, it is important to ensure that data cannot be recovered from the hard disks. To ensure that all traces of data are removed, the Disk Sanitizer tool can be used...

Backups

In the event of the system being compromised, the backups become invaluable. In cases like bugs, accidents etc. backups can be used to compare you current system against your backed-up system. For production systems it is very important to take some Backups offsite for cases like disasters. For legal reasons, some firms and organizations must be careful about backing up too much information and holding it too long.

Disk Partitions

Servers should have separate partitions for at least /, /boot, /usr, /var, /tmp, and /home. It is not desirable to fill logging and temporary space under /var and /tmp using up space of all the root partition. Third party applications should be on separate file systems as well, e.g. under /opt.

Firewall (iptables)

The system will not cover iptablesmost companies use hardware based firewalls to protect their servers in a production network, which is strongly recommended for such environments.

Kernel Security Features

Virtual Address Space Randomization:

Starting with the 2.6.x kernel releases Linux now uses address-space randomization technique to mitigate buffer overflows.

SELinux

SELinux is an advanced technology for securing Linux systems. Hardening Linux using SELinux technology, on its own, warrants its own security[2] .

FTP, telnet, and rlogin (rsh)

FTP, telnet, and rlogin (rsh) are vulnerable to eavesdropping, which is one of the reasons why SSH/SCP/SFTP should be used.

I. PROBLEM STATEMENT

At the heart of Linux system is the Linux kernel and operating system. Combined, these form the base level of the system on which all the applications run. Comparatively speaking, the Linux operating system and kernel are actually reasonably secure. A large number of security features are built in the kernel, and a variety of security-related tools and features come with most distributions or are available in open-source form. Additionally, Linux offers exceptional control over whom, how, and what resources and applications users can access.

The security of the system depends on a wide variety of configuration elements both at the operating system level and at the application level [3].

Additionally, the Linux operating system and kernel are complex and not always easy to configure. In fact, Linux systems are nearly infinitely configurable, and subtle configuration changes can have significant security implications. Thus, some security exposures and vulnerabilities are not always immediately obvious, and a lack of understanding about the global impact of changing configuration elements can lead to inadvertent exposures. Furthermore, security on Linux systems never stays static. Once secured, the system does not perpetually stay secure. Indeed, the longer the system runs, the less secure it becomes. This can happen through operational or functional changes exposing the threats or through new exploits being discovered in packages and applications. Securing the system is an ongoing and living process.

Many distributions come prepackaged or preconfigured with a recommended default set of packages, applications, and settings. Usually this configuration is based on the author or vendor understanding what their end user requires of the distribution. Generally speaking, a lot of this preconfiguration is useful and enhances the potential security of the system; for example, Red Hat comes preconfigured to use Pluggable Authentication Modules (or PAM) for a variety of authentication processes. But sometimes this preconfiguration opens security holes or is poorly designed from a security perspective [4].

For example, as a result of the vendor's desire to make it easy to set the system up the vendors may install, configure, and start applications or services. Red Hat automatically configures and starts Send mail as part of the default installation options.

To be able to address different security issues, there is a need to have a solid understanding of the underlying basic security requirements of the system [5].

II. LITERATURE SURVEY

Thus we found that the linux security is centred on the how these security parameters are set and how configurations files are configured. Each server has its own configuration file and proper configuration of these files lead to good security of particular server. To achieve high security admin need to have very careful about configuring all security related configuration attributes and there high security attributes values[6][7][8].Thus high security is achieves through proper configuration of system, server and services configuration files and applying security related parameters. The summary of the vulnerabilities, attacks and defense mechanisms is given below:

Table 1: Vulnerabilities of workstation security and remedy

Sr No	Vulnerability	Attacks	Countermeasure
1.	No separate partition for /boot, /, /home, /tmp, and /var/tmp	System crash and data loss	Create separate partition for /boot, /, /home, /tmp, and /var/tmp
2.	Unnecessary software's	Software vulnerability attack	Install minimum software's
3.	maliciously altered package	System instability ,System crash and data loss, data still	Install Signed Packages
4.	No BIOS password	Stealing/Changing Data Using a Bootable Linux CD	Give BIOS password
5.	Single User Mode access	Access as root user without password	Password protecting BIOS
6.	Access to the GRUB Console	change its configuration or to gather information using the ***cat*** command.	Password protecting GRUB
7	Access to Insecure Operating Systems	If it is a dual-boot system, an attacker can select an operating system at boot time (for example, DOS)	Password protecting GRUB

Table 2: Network Security vulnerabilities and countermeasures

Sr No	Vulnerability	Attacks	Countermeasure
1.	OS fingerprinting	Get os information like OS version etc.	Place login banner
2.	Local log monitoring	Remove of log entries and log files	Remote log monitoring
3.	Insecure Services FTP , Telnet Transmit Usernames and Passwords Over a Network Unencrypted	1) Get user name and password. 2) Denial of Service Attacks (DoS)	1) Avoid these services and use behind the firewall 2) Use tcp_wrappers and xinetd 3) Use SSH
4.	/etc/sysctl.conf configuration file vulnerability	1) SYN Attack 2) IP Source Routing 3) IP Spoofing 4) Broadcasts Request	Properly configure /etc/sysctl.conf

Table 3: Server Security vulnerabilities and countermeasures.

Sr No	Vulnerability	Attacks	Countermeasure
1.	**FTP** i) Anonymous access ii) Too many user access	1) Unauthorized access 2) Denial of Service Attacks (DoS*)*	1) Apply proper security parameter 2) Apply DOS security parameters
2.	ssh password	Cracking of password	Use passphrase
3.	Unauthorized websites	Unauthorized access	Authenticate the website

IV. PROPOSED SYSTEM

The Linux security is centered on how the configuration is made. Configuration files for various system processes, application and servers play the vital role in hardening the Linux. Configuration file contains various security related attributes that need to be considered while at the time of configuration of particular application, process and server.

The authors have focused on various configuration files that are critical from security perspective and security attributes present in such configuration files. The following Fig. 1.1 shows the detail description about how to make Linux more secure so that impact of security breach can be minimum.
The Linux Hardening model consists of three modules which makes the Linux more secure from the attackers which are:

1. Vulnerability check module
2. Log Analysis Module
3. Security Module

1. Vulnerability check module

As Mentioned in the literature survey there are various configuration files such as system configuration file and server configuration files which contains attributes that are critical. This module will check such configuration files and scan for attribute which are important from security perspective. This module check current attribute value with best security value required for that attribute. If current configured value is not a best security value then it will consider it as vulnerability and generates the vulnerability report. Generated report is given to the security module.

2. Log Analysis Module

Linux system consists of very strong logging mechanism maintains the log for kernel, servers, users, system processes etc. These entire logs by default placed at different location. This module collects the log from these various places and generates report. This generated report is useful for finding the vulnerability. Generated report is given to the security module.

3. Security Module

This module collects the vulnerability report and log analysis report and applies security. By looking vulnerability report this module get the vulnerable configuration files and modify them with best security practice. Similarly by looking log analysis report this module apply the security attributes accordingly. This model is actually responsible for modifying the configuration files and making the Linux more secure.

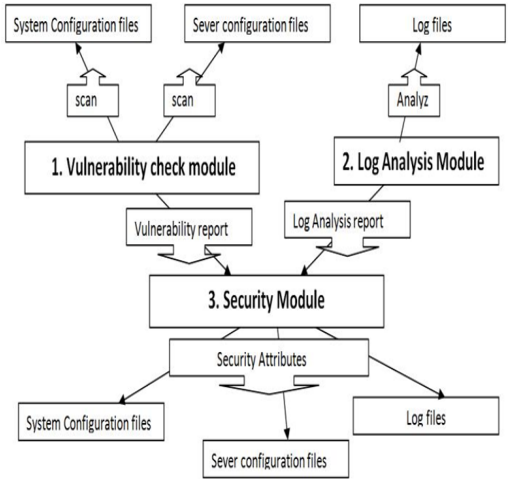

Figure : Linux Hardening Model

V. CONCLUSION

To increase reliance on powerful, networked computers to help run businesses and keep track of personal information, entire industries have been formed around the practice of network and computer security. Enterprises have solicited the knowledge and skills of security experts to properly audit systems and tailor solutions to fit the operating requirements of their organization Most of the organizations are increasingly dynamic in

nature, their workers are accessing critical company IT resources locally and remotely, hence the need for secure computing environments has become more pronounced. This paper describes how to simply, consistently, and practically secure the Linux environment.

Thus the Linux security is centered on proper system.

REFERENCES:

[1] P. A. Loscocco, S. D. Smalley, P. A. Muckelbauer, R. C. Taylor, S. J. Turner, and J. F. Farrell ," The Inevitability of Failure: The Flawed Assumption of Security in Modern Computing Environments ",21st National Information Systems Security Conference, NSA, 1998,PP 303– 314

[2] C. J. PeBenito, F. Mayer, and K. MacMillan. Refer-ence Policy for Security Enhanced Linux. In SELinux Symposium, 2006.

[3] R. Wita and Y. Teng-Amnuay. Vulnerability profile for linux. In Proceedings of the 19th International Conference on Advanced Information Networking and Applications, pages 953–958. IEEE, 2005.

[4] R. Spencer, S. Smalley, P. Loscocco, M. Hibler, D. An-dersen, and J. Lepreau. The Flask Security Architec-ture:System Support for Diverse Security Policies. In The Eighth USENIX Security Symposium, pages 123–139, August 1999.

[5] Nigel Edwards, Joubert Berger, and TseHoungChoo. A Secure Linux Platform. In Proceedings of the 5th Annual Linux Showcase and Conference, November 2001

[6] Crispin Cowan, Steve Beattie, Calton Pu, PerryWagle, and Virgil Gligor. SubDomain: Parsimonious ServerSecurity. In USENIX 14th Systems Administration Conference (LISA), New Orleans, LA, December 2000.

[7] Red hat enterprise linux 6 security guide (Red Hat
Engineering Content Services).

[8] Afinidad, T. E. Levin, C. E. Irvine, and T. D.Nguyen, "A model for temporal interval authorizations," inHawaii International Conference on System Sciences, Software Technology Track, Information Security Education and Foundational Research, (Kauai, Hawaii), p. to appear, January 2006.

3T XOR GATE DESIGN USING IDDG MOSFET

[1]Kriti Sharma, [2]Tripti Sharma,[3]K. G. Sharma
ECE Department, FET, Mody University of Science and Technology
Lakshmangarh-332311, Rajasthan, India
[1]sharmakriti92@gmail.com, [2]tripsha@gmail.com , [3]sharma.kg@gmail.com

Abstract— This paper presents a new design of 3 transistor XOR by using Double Gate MOSFET. Proposed gate has been designed using Independent Driven Double Gate and compared with 3T XOR implemented using Symmetrical Driven Double Gate in sub threshold region. The simulation and comparison analysis results in to low power consumption of the proposed design with various performance parameters. The entire simulation has been carried out on EDA tool at 45nm process technology.

Index Terms—3T XOR, IDDG, MOSFET, SDDG

I. INTRODUCTION

In 1965 Gordon Moore [1] predicted that the number of transistors per chip mould be just doubled in approximately two years. When channel length of the device shrinks, the close proximity between Drain to Source reduce the ability of the Gate electrode to control the potential distribution and flow of current in the channel. So, conventional bulk MOSFET cannot be scaled down at lower nanometer technologies to achieve low power systems.

The Double Gate MOSFET is electrostatically superior to a Single Gate MOSFET because two gates are used to control the channel from both sides. The two gates together control roughly twice as much current as a single gate [2]. The current driving capability of Double Gate MOSFET is twice that of planner CMOS and hence Double Gate MOSFET can be operated at much lower input and threshold voltage [3]. Depending upon the way that gate voltage are applied, Double Gate MOSFET may be categorized as 2 types: A Double Gate MOSFET is said to be symmetric when both gates have the same work function and a single input voltage is applied to both gates, otherwise it is called Asymmetric Double Gate MOSFET [4].

As MOS integrated circuit technology has evolved to exploit smaller device structures, it has become progressively more important in recent years to look more closely at the minority carriers present under the gate when the gate voltage is less than threshold voltage, i.e. in what is called the “Sub-threshold” region [5]. These carriers cannot be totally neglected, and play an important role in device and circuit performance. It is recognized that they also enable a very useful mode of MOSFET operation, and that the sub-threshold region of operation is an important as the traditional cut-off, linear and saturation region of operation. XOR gate is basic building block of digital circuits like 1-bit Full-Adder, Subtractor, and Multiplier [6]. The new proposed 3T XOR Gate with IDDG MOSFET fulfill the demand of sub threshold operation at various operating conditions. To construct Double Gate, two single gate MOSFET Transistors have been connected in parallel in such a way their Source and Drain are connected together [7].

The paper ordered as follows: Basic introduction about Double Gate MOSFET is including in session I. Session II illustrates the 3T XOR Gate by using SDDG MOSFET. Session III contain new design of 3T XOR Gate driven by Independent Driven Double Gate MOSFET. Session VI show simulations and comparison of SDDG and IDDG MOSFET designs and session V conclude the paper.

II. 3T XOR GATE DESIGN USING SYMMETRICALLY DRIVEN DOUBLE GATE MOSFET

Fig. 1 show the 3T XOR Gate circuit Design using Symmetrically Driven Double Gate MOSFET. This SDDG XOR Gate has been designed as the modified version of single Gate 3T XOR Gate design [8].

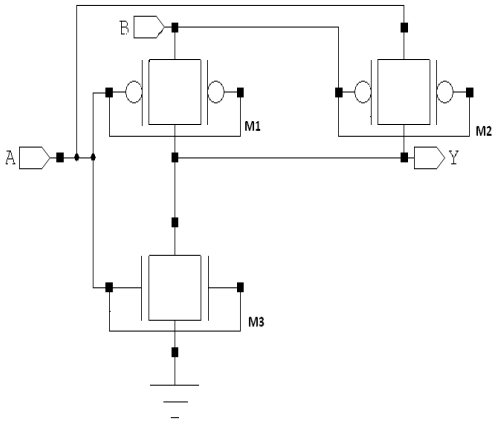

Fig. 1 Schematic of 3T XOR gate using SDDG MOSFET

The operation of SDDG design is like a 2-input XOR Gate. Unlike conventional single gate MOSFET in SDDG design has double control of gate of both n-SDDG MOSFET and p-SDDG MOSFET that leads to enhance the performance in term of I_{on} and I_{off} current. In this circuit minimum sizing is used for n-SDDG MOSFET and p-SDDG MOSFET transistors are taken as 1/1.

III. PROPOSED 3T XOR GATE DESIGN USING INDEPENDENT DRIVEN DOUBLE GATE MOSFET

Fig. 2 shows the schematic of 3T XOR Gate designed using Independent Driven Double Gate MOSFET. This design comprises of two p-types Double Gate MOSFET and one n-type Double Gate MOSFET. As IDDG gives the liberty of biasing the two gates independently therefore taking such benefit in the proposed design, the two gates of M2 transistor has been connected with each other whereas M1 and M3 have different gate biasing.

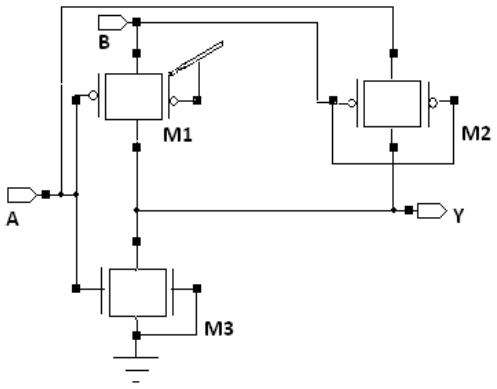

Fig. 2 Schematic of 3T XOR gate using IDDG MOSFET

In the circuit shown in Fig. 2 back gate of M1 is connected to V_{DD} as well as back gate of M3 is connected to Ground unlike in Fig. 1 where all the transistors are connected with varying inputs. Because of these fixed back gates in the proposed design the power consuming transitions will be less which results in to less switching activity and hence less power consumption in compare to its peer designs. The aspect ratio of all the transistors has been chosen (1/1), increasing beyond this increases the power consumption as well as on-chip area with no betterment in threshold loss. Hence, to achieve low power design such aspect ratio i.e.; (1/1) is the best suitable option.

IV. SIMULATIONS AND COMPARISON

Both the circuits have been simulated using EDA tool at 45nm process technology in sub threshold region with same testing conditions.

A. *Variation with Voltage*

For performing sub threshold operation supply voltage is taken less than the threshold voltage. The input voltage variation range is from 0.16V to 0.26V. Comparison is taken at room temperature i.e. 25°C and 100MHz frequency.

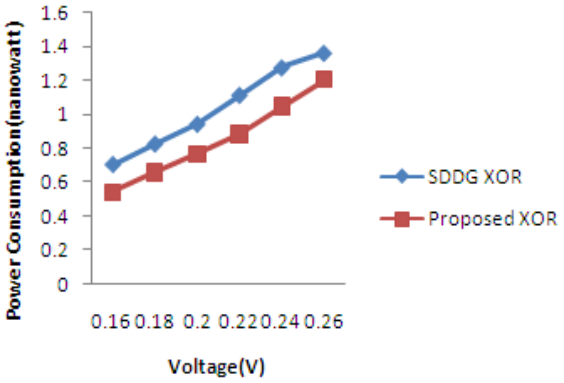

Fig. 3 Power Consumption with increasing Voltage

The graph shown in Fig. 3 illustrates that the power consumption of proposed IDDG 3T XOR is approximately 21% less than the SDDG XOR cell which experimentally supports the text in Section III. Therefore, the proposed XOR cell can be a better option for low power device design.

B. *Variation with frequency*

On increasing the operating frequency power consumption also increases as both the performance parameters are proportional to each other [9], the same has also been supported by the simulation results plotted in the graphical form in Fig.4. For performing sub threshold operation input voltage has been taken 0.2V at room temperature 25°C. Frequency variation range is taken from 100MHz to 350MHz.

In Fig. 4 it is shown that power consumption changes with varying Frequency. Initially at 100 MHz the difference in power consumption of the two designs is less but as the frequency increased this gap also increases significantly. This as a result depicts that the proposed design will be a better option for high frequency applications.

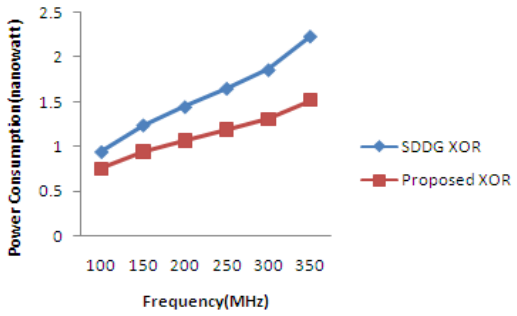

Fig. 4 Power consumption with varying Frequency

C. *Variation with Temperature*

Variations with temperature are compared at constant frequency 100MHz and input voltage 0.2V. Temperature variation range is taken from -10°C to 80°C.

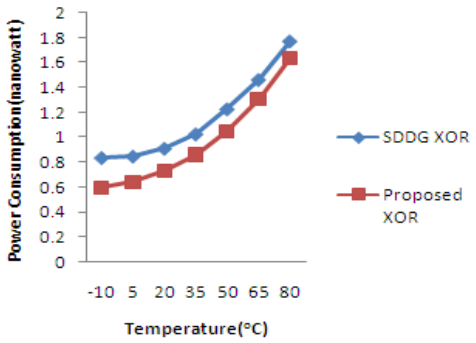

Fig. 5 Power consumption with increasing Temperature

As the simulations have been carried out in sub threshold region i.e.; voltage applied is much less than the threshold voltage of the MOSFETs, therefore, electric field generated is also less. At

low electric field current and temperature are proportional with each other. Hence, as a result power consumption increases with increase in temperature [10].

Fig. 5 shows that increase in temperature shrinks the gap between power consumption of IDDG XOR cell and SDDG XOR cell is but keeping the proposed design at lower scale i.e.; 15% less as compared to SDDG 3T XOR Gate design. Therefore, the proposed XOR cell is more temperature sustainable in comparison to SDDG cell.

V. CONCLUSION

To implement new topologies, conventional MOSFET devices have been replaced with Double Gate MOSFET devices which show improved performance. By simulation results it has been demonstrated that IDDG MOSFET is more promising for future ultra-low power systems in comparison to SDDG MOSFET. Comparison of SDDG XOR gate with proposed IDDG XOR cell show that the XOR designed using IDDG MOSFET outperforms in sub threshold operation. The circuits have been compared at 45nm technology in sub threshold region for various operating conditions. The analysis of the simulated results confirms the practicability of IDDG MOSFET technique in digital circuits design.

REFERENCES

[1] Gordon E. Moore, "Cramming more components onto integrated circuits" Electronics, Volume 38, Number 8, April 19, 1965.

[2] Ankita Wagadre and Shashank Mane, " Design & Performance Analysis of DG-MOSFET for Reduction of Short Channel Effect over Bulk MOSFET at 20nm" *2248-9622, Vol. 4, Issue 7(Version 1), pp.30-34, July 2014.*

[3] S. Mukhopadhyay, H. Mahmoodi and K. Roy, "A Novel High-Performance and Robust Sense Amplifier using Independent Gate Control in sub-50-nm Double Gate MOSFET," IEEE Transactions on Very Large Scale Integration (VLSI) Systems, vol. 14, no. 2, pp. 183-192, Feb. 2006.

[4] V. K. Yadav and A. K. Rana, "Impact of Channel Doping on DG-MOSFET Parameters in Nano Regime- TCAD Simulation," International Journal of Computer Applications, vol. 37, iss. 11, pp. 36-41, Jan. 2012.

[5] Srinivasa Rao. Ijjada, Raghavendra Sirigiri, B.S.N.S.P. Kumar, V. Malleswara Rao, "DESIGN OF HIGH EFFICIENT & LOW POWER BASIC GATES IN SUBTHRESHOLD REGION," International Journal of Advances in Engineering & Technology, Vol. 1,Issue 2,pp.215-220, May 2011.

[6] S. Singh, T. Sharma, K. G. Sharma and B. P. Singh, "PMOS based 1-Bit Full Adder Cell," *International Journal of Computer Applications*, Vol. 42, No. 15, pp. 6-9, March 2012.

[7] M. Reyboz, O. Rozeau, T. Poiroux and P.Martin, "Asymmetrical Double Gate (ADG) MOSFETs Compact Modeling," *LETI-CEA*, Grenoble, France, 2005.

[8] S. R. Chowdhury, A. Banerjee, A. Roy and H. Saha, "A High Speed 8 Transistor Full Adder Design using Novel 3 Transistor XOR gates," *World Academy of Science, Engineering and Technology*, Vol. 2, No. 10, pp. 685-691, 2008.

[9] Neil H. E. Weste & David Money Harris, "CMOS VLSI Design,"Pearson Education, Inc., Fourth Edition, 2011.

[10] D. Wolpert and P. Ampadu, "Managing Temperature Effects in Nanoscale Adaptive Systems," DOI 10.1007/978-1-4614-0748-5_2, Springer Science + Business Media, LLC 2012.

A STEP TOWARDS REALIZATION OF GRAPHENE FOR DIGITAL ELECTRONICS

[1]Anju Gupta, [2]Dr.R.S.Pande
[1]Assistant Professor, Shri Ramdeobaba college of Engineering and Management , Nagpur
[2]Professor, Shri Ramdeobaba college of Engineering and Management , Nagpur
[1]guptaam@rknec.edu,

***Abstract*—Graphene has shown high mobility, high saturation velocity, high gain, good thermal and electric properties still it is not found suitable to replace the silicon technology. The reason behind this is the lack of band gap and no current saturation. This paper reviews the different techniques used for inducing band gap in the material so that it can be used for logic purpose as well as its characteristics which makes it suitable for storage purpose**.

***Index Terms*—band gap**

I. INTRODUCTION

Si technology is reaching to its physical limit. The scaling of CMOS results in short channel effect which limits further scaling. Hence researchers are searching for new materials which can be used in place of Si. Many materials available each one has their own limitation. The Graphene is also one of the materials which can replace Si in near future. Graphene has good mobility, temperature stability which can be used as channel material in MOSFET. Graphene is band less material which makes it unsuitable for switching function [2]. But it shows good RF characteristics which makes it suitable for RF application. But still research is going on to make it suitable for digital function.

II. Limitation of graphene for logic function

Due to absence of Band gap graphene transistor cannot be used for switching function. Wide research is going on to make the graphene transistor suitable for switching function some of them mentioned below.

A. By dimension constraining

Different techniques used for inducing the band gap the most popular is constraining one dimension of large-area graphene thus forming narrow graphene nanoribbon (GNRs) [3],[4].The band gap depends on chirality one with chirality (16,0) shows 0.71eV band gap but with chirality (14,0) shows 0.13eV . GNR MOSFETs with on-off ratios exceeding 10^6 have successfully been fabricated [1]. However, ribbons having a width well below 10 nanometers
are needed for a gap ensuring good switch-off [6, 1] and this represents a serious processing challenge.

The two ideal GNR types are armchair (ac) and zigzag (zz) nanoribbons. It has been predicted that these two GNR configurations show a bandgap (EG) that depends on the GNR width roughly according to band gap is inversely proportional to ribbon width [4]. The gap opening has been verified experimentally for ribbons with widths down to about 1 nm [4]. But it has also seen by introducing band gap mobility decreases in large amount. Moreover, the gap opening in GNRs is accompanied by a dramatic mobility reduction and irregular ribbon edges deteriorate transistor performance. A recent experiment [3] demonstrated that all sub-10 nm GNRs are semiconducting due to the edge effects, which make them more attractive for electronic device applications. Both the results indicate that the 3NN (Third Neighbor neighbor)interaction and the edge bond relaxation effects both result in a decrease of the band structure-limited velocity a high energies.3NN interaction and the edge bond

relaxation are responsible for opening a band gap with roughly equal contribution from each effect. For an AGNR(Arm chair GNR) with an index of *m*=3*p*, the band gap decreases and the ON current increases whereas for an AGNR with an index of *m*=3*p*+1, the quantum capacitance increases and the ON current decreases[7] [4].

B. By doping

If undoped, a bilayer of graphene sheets is considered a semimetal, a material in which the conduction and valence bands slightly overlap in energy. When the researchers first synthesized their bilayer graphene films onto the silicon carbide substrate, the graphene became a weak n-type semiconductor, having a slight excess of negatively charged electrons; the interface layer acquired an excess of conduction electrons from the substrate, creating a small bandgap. Potassium atoms deposited onto the graphene donated their valence electrons to the graphene's surface layer, initially closing the bandgap. However, as the potassium deposition continued, the bandgap was reopened by the excess of electron charge-carriers on the graphene's surface layer. Progressive potassium deposition further enhanced the *n*-type doping. These results demonstrate that by controlling the carrier density in a bilayer of graphene, the occupation of electronic states near the Fermi level (*E*F) and the magnitude of the gap between the valence band and conduction band can be manipulated. This control over the band structure suggests the potential application of bilayer graphene to switching functions in electronic devices with a thickness of only two atomic layers [5].

C. By applying electric field to bilayer graphene

As with monolayer graphene, bilayer graphene also has a zero bandgap and thus behaves like a metal. Previously, in 2006, researchers at the ALS observed a bandgap in bilayer graphene in which one of the layers was chemically doped by adsorbed metal atoms. But such chemical doping is uncontrolled and not compatible with device applications but a bandgap can be introduced if a perpendicular electric displacement field is applied to the two layers; the material then behaves like a semiconductor. A team of researchers from Berkeley has engineered a bandgap in bilayer graphene that can be precisely controlled from 0 to 250 meV. With precision control of its bandgap over a wide range, plus independent manipulation of its electronic states through electrical doping, dual-gated bilayer graphene becomes a remarkably flexible tool for Nano scale electronic devices. Researchers then tried to tune[5][12]. But when such a field is applied with a single gate (electrode), the bilayer becomes insulating only at temperatures below 1 K, near absolute zero—suggesting a bandgap value much lower than predicted by theory.

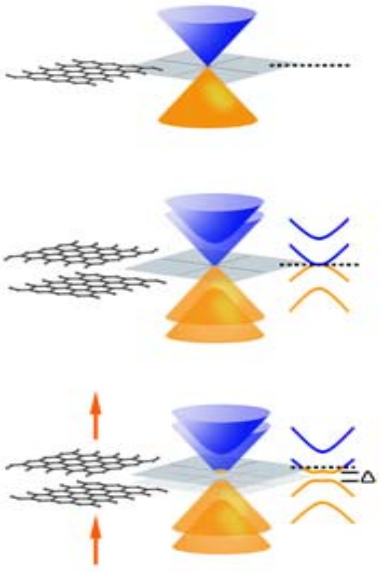

Fig. 1 Schematic depictions of graphene crystal structure (lattices), conduction band (blue cones and curves), valence band (yellow cones and curves), and Fermi level (dotted lines). Top: Monolayer graphene. Center: Bilayer graphene. Bottom: A bandgap (Δ) is induced in bilayer graphene by an external electric field (arrows).

To better understand exactly what was happening electronically, the Berkeley team built a two-gated bilayer device, which allowed them

to independently adjust the electronic bandgap and the charge doping. The device was a dual-gated field-effect transistor (FET), a type of transistor that controls the flow of electrons from a source to a drain with electric fields shaped by the gate electrodes. Their nano-FET used a silicon substrate as the bottom gate, with a thin insulating layer of silicon dioxide between it and the stacked graphene layers. A transparent layer of aluminum oxide (sapphire) lay over the graphene bilayer; on top of that was the top gate, made of platinum.

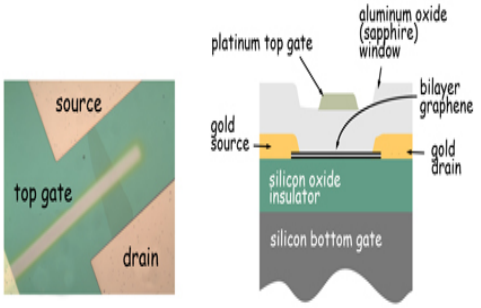

Fig. 2 double gate graphene transistor

But the theory and experiments the performance improvements achievable use bilayer graphene as channel material in field effect transistors for analog applications as compared to digital applications. Bilayer graphene provides larger output resistance than monolayer graphene, which translates in both higher voltage gain and higher maximum frequency oscillation

D. Substrate-Induced Band-Gap Opening in Epitaxial Graphene

A multi-institutional collaboration under the leadership of researchers with Berkeley Lab and the University of California, Berkeley, have now demonstrated that growing an epitaxial film of graphene on a silicon carbide substrate results in a significant band gap, 0.26 electron volts (eV), an important step toward making graphene useful as semiconductor[8].

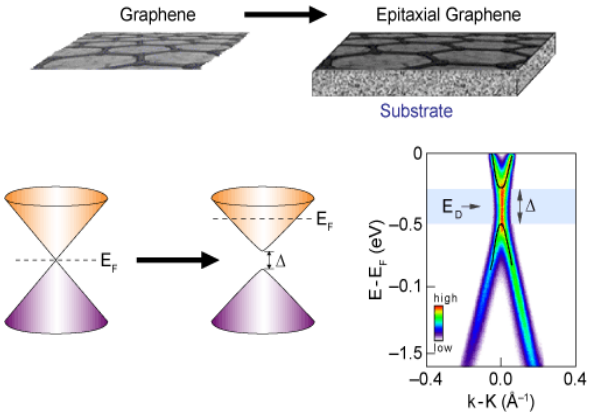

Fig. 3 Left: In graphene's electronic band structure, the conduction (orange) and valence (purple) bands just meet at the Fermi energy (E_F), so there is no band gap. Right: When a graphene layer is grown on a silicon carbide substrate), broken symmetry opens a gap (□) between the valence and conduction bands around the so-called Dirac energy (E_D), as shown in the ARPES intensity map (lower right), but below the Fermi energy.

The team found that the size of the energy gap decreased with thickness and all but disappeared at four layers. Next on the agenda are finding ways to control the width of the band gap, perhaps by using a different substrate material with a different graphene–substrate interaction strength, and to move the Fermi energy from the conduction band into the band gap to allow transistor action.

E. Large Bandgap Opening Between Graphene Dirac Cones Induced by Na Adsorption onto an Ir Superlattice.

Marco Papagno,1 Stefano Rusponi,2 Polina Makarovna Sheverdyaev investigate the effects of Na adsorption on the electronic structure of bare and Ir cluster superlattice covered epitaxial graphene on Ir(111) using angle-resolved photoemission spectroscopy and scanning tunneling microscopy. At Na saturation coverage a massive charge migration from sodium atoms to graphene raises the graphene Fermi level by about 1.4 eV relative to its neutrality point. They

find that Na is adsorbed on top of the graphene layer and when coadsorbed onto an Ir cluster superlattice it results in the opening of a large bandgap of Na/Ir/G =740 meV comparable to the one of Ge and with preserved high group velocity of the charge carriers[9].

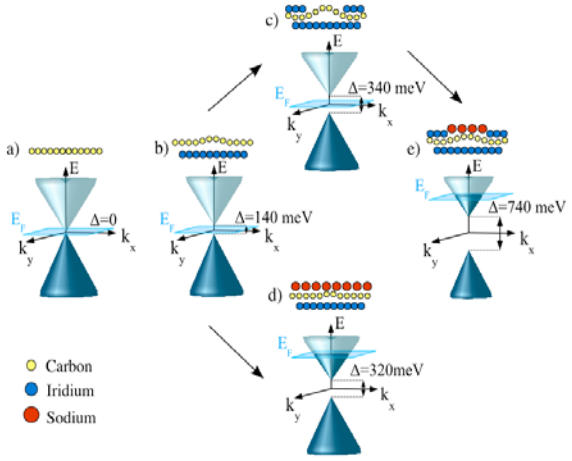

Fig. 4 Figure 1 Side view sketch of the atomic structure and of the π and π* bands dispersion close to the*K*-point of graphene Brillouin zone and to the Fermi level *EF* for (a) freestanding graphene (b) G (c)Ir/G (d) Na/G and (e)Na/Ir/G.

F. Opening of a band gap in graphene by physisorption of porphyrin molecules.

Arramel1*, Andres Castellanos-Gomez1,2, Bart Jan van Wees1 report a robust method to open a gap in graphene via noncovalent functionalization with porphyrin molecules. Two type of porphyrins, namely, iron protoporphyrin (FePP) and zinc protoporphryin (ZnPP) were independent physisorbed on graphene grown on nickel by chemical vapour de- position (CVD) resulting in a bandgap opening in graphene. Using a statistical analysis of scanning tunneling spectros- copy (STS) measurements, they demonstrated that the magnitude of the band gap depends on the type of deposited porphyrin molecule. The π-π stacking of FePP on graphene yielded a considerably larger band gap value (0.45 eV) than physisorbed ZnPP (0.23 eV). They proposed that the origin of different band gap value is governed due to the metallic character of the respective porphyrin[10]. The presence of porphyrin molecules physisorbed on the graphene substrate induces a semiconducting behavior in the surrounding graphene layer up to 10 - 20 nm far from the molecules. Interestingly, the magnitude of the bandgap opened in graphene can be controlled via the selection of the metal core of the porphyrin molecules that determines the graphene-molecule interaction. They believe that this work will open more opportunities to build other hybrid systems based on the noncovalent π-π stacking of aromatic molecules on graphene.

G. Placing Graphene sheet with boron nitride sheet

This technique involves placing a sheet of graphene a carbon-based material whose structure is just one atom thick on top of hexagonal boron nitride, another one-atom-thick material with similar properties[11]. The resulting material adds the band gap while shares graphene's amazing ability to conduct electrons. Graphene is an extremely good conductor of electrons, while boron nitride is a good insulator, blocking the passage of electrons. A high quality semiconductor can be made suggested by MIT team. To make the hybrid material work, the researchers had to align, with near perfection, the atomic lattices of the two materials, which both consist of a series of hexagons. The size of the hexagons (known as the lattice constant) in the two materials is almost the same, but not quite: Those in boron nitride are 1.8 percent larger. So while it is possible to line the hexagons up almost perfectly in one place, over a larger area the pattern goes in and out of register. At this point, the researchers say they must rely on chance to get the angular alignment for the desired electronic properties in the resulting stack. However, the alignment turns out to be correct about one time out of 15, they say. But by this technique the band gap obtained is not sufficient graphene device to use in digital electronics. Graphene and boron nitride hexagons almost perfectly align, merging their properties .The qualities of the boron nitride

bleed over into the graphene," Ashoori says. But what's most "spectacular," he adds, is that the properties of the resulting semiconductor can be "tuned" by just slightly rotating one sheet relative to the other, allowing for a spectrum of materials with varied electronic characteristics. Others have made graphene into a semiconductor by etching the sheets into narrow ribbons, Ashoori says, but such an approach substantially degrades graphene's electrical properties. By contrast, the method appears to produce no such degradation but the band gap is not sufficient to use graphene for digital electronics.

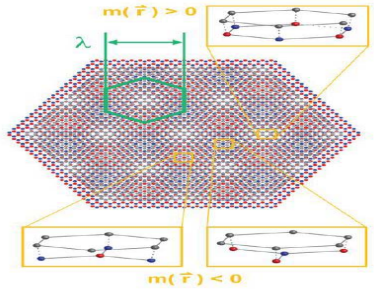

Fig. 5 Insulating states and superlattice minibands in a graphene/hBN heterostructure. Schematic of the moiré pattern for graphene (gray) on hBN (red and blue), for zero misalignment angle and an exaggerated lattice mismatch of ~10%. The moiré unit cell is outlined in green. Regions of local quasi-epitaxial alignment lead to opposite signs of the sublattice asymmetry, m(r), in different regions. (Credit: B. Hunt et al./Science.

III. NEGATIVE RESISTANCE

Guanxiong Liu, Sonia Ahsan, Alexander G. Khitun, Roger K. Lake and Alexander A. Balandin propose complimentary designs for 2-port GNR based negative resistance devices. They proposed negative resistance devices exhibit very high peak to valley current ratios (10^{14}), which is essential in digital applications. Graphene logic circuitry is based entirely on the intrinsic NDR effect in graphene and benefits from graphene's high electron mobility and thermal conductivity. The devices are highly configurable, and their properties can be adjusted and optimized by the selection of voltages applied and the gate WF values. The fabrication and integration of n- and p-type devices are simple and cost effective due to the similarities between their structures[4][13] This approach overcomes the absence of the energy band gap in graphene. The negative differential resistance appears not only in the large scale graphene transistors but also in the downscaled devices operating in the ballistic transport regime. The results may lead to a conceptual change in graphene research proving an alternative route for graphene's applications in information processing[13].

Santosh Khasanvisand , Pritish Narayanan propose a novel Graphene NanoRibbon crossbar (xGNR)exhibiting negative differential resistance (NDR) showed considerable advantages in terms of power dissipation, area and write performance[14].

IV: High density of states and work function

There has been strong demand for novel nonvolatile memory technology for low-cost, large-area, and low-power flexible electronics applications .Graphene flash memory (GFM) has the potential to exceed the performance of current flash memory technology by utilizing the intrinsic properties of graphene, such as high density of states, high work function, and low dimensionality. GFM can fabricate by growing the graphene sheets by chemical vapor deposition and integrated them into a floating gate structure. GFM displays a wide memory window of~6 V at significantly low program/erase voltages of 7 V. GFM also shows a long retention time of more than 10 years at room temperature [15]. Multi-layer graphene sheets have higher work function and higher density of states compared to single layer graphene (SLG) and lower conductivity along c-axis. A memory window of 6.8V for 1 second programming is obtained at ±18program/erase voltage. Number of electrons stored in MLG sheets after 18V programming voltage is calculated as 9.1 x 1012 cm-2 which is higher than the density of states in SLG, suggesting the suitability of MLG for multi level data storage flash memory devices.

Graphene quantum dot memory has many advantages over the polysilicon trapped memory.

Polysilicon trapped memory are affected by the local defects which can be reduced in the quantum dot memory. But it has seen increasing the size improves the erase speed and stability (27nm) but decreasing the size increases the program speed (12nm). Even other advantage on using the graphene material as trapped layer is the flexibility. It can be deposited over the flexible substrate material and flexible memory is possible to use with flexible device [17].

Resistive memories based on metal oxide thin films have been extensively studied for application as next generation

Nonvolatile memory devices. However, although the metal oxide based resistive memories have several advantages, such as good scalability, low-power consumption, and fast switching speed, their application to large-area flexible substrates has been limited due to their material characteristics and necessity of a high-temperature fabrication process. Graphene oxide is also useful for fabricating a flexible resistive switching memory device .The switching operation of graphene oxide resistive switching memory (RRAM) is governed by dual mechanism of oxygen migration and Al diffusion. However, the Al diffusion into the graphene oxide is the main factor to determine the switching endurance property which limits the long term lifetime of the device [16].

In terms of performance, a very high on-off power ratio makes graphene-based memory very attractive in terms of performance; a very high on-off power ratio makes graphene-based memory very attractive. While phase-change memories, which are currently, considered the most promising technology for data storage, have an on-off power ratio of 10 to 1. Graphene-based memory is believed to have an on-to-off power ratio of one million to one. Further, their heat generation is extremely low, eliminating the need to use heat sinks, which are usually a part of any storage system used for high-density storage [17].

III Conclusion

Graphene material has tremendous potential to use next generation semiconductor material but lack of band gap was one of the biggest hindrances. Lot of the research is going on in this direction but still no fruitful solution is found. Intensive research needed to increase band gap by optimizing the process and technique. Graphene has potential to be used as next generation storage element.

REFERENCES

[1] X. Li, X. Wang, L. Zhang, S. Lee, and H. Dai, Science, vol. 319, 1229 (2008).

[2] Majumdar, K, Murali, K.V.R.M., Bhat, N., Fengnian Xia and Yu-Ming Lin. “High On-Off Ratio Bilayer Graphene Complementary Field Effect Transistors.” : *Electron Devices Meeting (IEDM) 2010 IEEE International,* December2010

[3] Li, X.; Wang, X.; Zhang, L.; Lee, S.; Dai, H. Chemicallyderived, ultrasmooth graphene nanoribbon semiconductors.Science **2008**, 319, 1229 1232.

[4] Computational Model of Edge Effects in Graphen Nanoribbon Transistors R. Nicole, “Title of paper with only first word capitalized,” J. Name Stand. Abbrev., in press.

[5] T. Ohta, A. Bostwick, T. Seyller, K. Horn, and E. Rotenberg, “Controlling the electronic structure of bilayer graphene,”Science **313**, 5789 (2006).

[6] F. Schwierz, Nature Nanotechnology., vol. 5, 487 (2010).

[7]SPei Zhao1, Mihir Choudhury2, Kartik Mohanram2, and Jing Guo, “ Computational Model of Edge Effects in Graphene NanoribbonTransistor,” Accepted: 14 September 2008©Tsinghua Press and Springer-Verlag 2008.

[8] S.Y. Zhou, G.-H. Gweon, A.V. Fedorov, P.N. First, W.A.De Heer, D.-H. Lee, F. Guinea, A.H. Castro Neto, and A. Lanzara, "Substrate-induced bandgap opening in epitaxial graphene," Nature Materials **6**, 770 (2007).

[9] Marco Papagno, Stefano Rusponi,Polina Makarovna Sheverdyaeva,Sergio

Vlaic,MarkusEtzkor,"Large Bandgap Opening Between Graphene Dirac Cones Induced by Na Adsorption onto an Ir Superlattice".
[10] Arramel, Andres Castellanos-Gomez,Bart Jan van Wees,"Band Gap Opening of Graphene by Noncovalent π-π Interaction with Porphyrins", Graphene, 2013, 2, 102-108

http://dx.doi.org/10.4236/graphene.2013.23015 Published Online July 2013 (http://www.scirp.org/journal/graphene) scientific research.
[11] B. Hunt et al., Massive Dirac Fermions and Hofstadter Butterfly in a van der Waals Heterostructure, Science, 2013, DOI: 10.1126/science.1237240.
[12] Y. Zhang, T.-T. Tang, C. Girit, Z. Hao, M.C. Martin, A. Zettl, M.F. Crommie, Y.R. Shen, and F. Wang, "Direct observation of a widely tunable bandgap in bilayer graphene," *Nature* **459**, 820 (2009).
[13] Guanxiong Liu, Sonia Ahsan, Alexander G. Khitun, Roger K. Lake and Alexander A. Balandin," Graphene-Based Non-Boolean Logic Circuits," G. Liu et al., UC Riverside (2013)
[14] Santosh Khasanvis, K. M. Masum Habib, Mostafizur Rahman, Pritish Narayanan,Roger K. Lake and Csaba Andras Moritz,"Hybrid Graphene Nanoribbon-CMOS Tunneling Volatile Memory Fabric,"khasanvis@ecs.umass.edu, andras@ecs.umass.edu
978-1-4577-0995-1/11/$26.00_c 2011 IEEE.
[15] Augustin J. Hong ,Hyung Suk Yu, Jesse D. Fowler "Graphene Flash Memory,"VOL. 5 ' NO. 10 ' 7812–7817 2011,www.acsnano.org
[16] Seul Ki Hong,1 Ji Eun Kim,2 Sang Ouk Kim,2 and Byung Jin Cho1,"a Analysis on switching mechanism of graphene oxide resistive memory device
; published online 22 August 2011) JOURNAL OF APPLIED PHYSICS 110, 044506 (2011)
[17] Md. Nahid Hossain and Masud H Chowdhury, "Graphene Nanotechnology for the Next Generation Nonvolatile Memory".

HIGH FREQUENCY AND AREA EFFICIENT DIGITAL CONTROLLED OSCILLATOR USING NAND GATES

[1]Anju Gupta, [2]Dr.R.S.Pande
Assistant Professor, Shri Ramdeobaba college of Engineering and Management , Nagpur
Professor, Shri Ramdeobaba college of Engineering and Management , Nagpur
[1]guptaam@rknec.edu

Abstract— **This paper reviews on different techniques used to increase the range and frequency of DCO of the all phase locked loop PLL which is the main Requirement of the todays era. The new techniques should be required to reduce the power consumption and for increasing the frequency range .In this paper three transistor based NAND gate is used to design digital controlled oscillator. . Three bit three stage ring DCO with NMOS network gives output frequency [3.39 – 5.35] GHz with power consumption of [0.308 – 0.471] mW. five bit three stage ring DCO with NMOS network gives output frequency [3.65 – 6.11] GHz with power consumption of [0.304 – 0.469] mW. Three bit five stage DCOs with NMOS network shows output frequency of [2.31 – 3.19] GHz with power consumption of [0.534 – 0.672)mw. It is found that increasing the no of bits increases the frequency range as compared to increasing the no of stages.**

Index Terms— DCO,PLL,NMOS

I. INTRODUCTION

The wireless communication industries has grown tremendously in recent years, leading to strong demand for faster ,smaller low consuming circuits. Frequency synthesis is the part of the wireless system. Phase locked loops are widely used in frequency synthesis applications [1], [2].

For many portable applications such as mobile and laptop the acquisition time of PLL is very important so the design of PLLs with minimum acquisition time is the primary goal of this work .A Phase Locked Loop (PLL) is a feedback system that compares the output phase with the input phase to produce an output signal that has the same phase as that of an input signal. PLL's are found in many applications such as reference generation, frequency synthesis, frequency multiplication, FM demodulation etc. As the frequency of operation increases, the need of generating signals that are in phase lock with input (i.e. Fast varying signals) is becoming a problem. There are two types of PLL's 1.Analog PLL 2.Digital PLL. Analog PLL consists of

phase detector, charge pump ,loop filter ,voltage controlled oscillator and frequency divider. But analog PLL has many limitations such as difficult to integrate with design, low speed, occupy large chip area, power consumption, very sensitive to noise, stability . The second type of PLL contains phase frequency detector time to digital converter digital controlled oscillator and frequency counter. Digitally controlled oscillators (DCOs) are the replacement of analog voltage control oscillators (VCOs) in digital PLL systems [6]-[9]. These type of PLL is known as All phase dial phase locked loop DPLL systems which has fast frequency locking, full digital control and good stability [5]. In deep submicron CMOS

technology fully digital control oscillators have become highly attractive circuit components. Different designs for digital controlled oscillators have been reported over varied operating frequency range. In the design delay elements are arranged in ring structure [8], [10], [11]. The Schmitt trigger current driven Digital controlled oscillators [7] , [9], require large number of MOS transistors. Current starved ring oscillators consume large area and with more hardware complexity requires large area [5], [8].

Delay element is important element of the oscillator. The different techniques are used to implement it as reported in literature [12] Two parameters modulate the output frequency of ring oscillator structure. One is propagation delay time of each delay stage and second is total number of delay stages in close ring structure. In DCO structures the oscillating frequency is determined by digital input vector applied to DCDE. Controls switch network of NMOS/PMOS transistors are placed at the sources/drain of NMOS/PMOS transistor of inverter delay cell. Depending upon the condition of input vector, the equivalent resistance of switch network changes and delay of particular stage changes which further modulates the output frequency [5].

In recent years power consumption and output frequency range have become significant performance criteria [12] in DCO system design. Increasing demand of handheld devices like cellular phones, notebooks, personal communication devices have aggressively enhanced the attention for power efficiency. In battery operated communication systems power consumption has also become more significant factor due to exponential increase in data rates. Power consumption in very large scale integration (VLSI) systems includes dynamic, static power and leakage power. Dynamic power consumption results from switching of load capacitance between two different voltages and is dependent on frequency of operation. Static power is contributed by direct short circuits current component between supply (Vdd) & ground (Vss) and it is dependent on leakage currents components. Controlled oscillator is the major components of PLL system and also accountable for most of the power consumption of PLL system. The operating frequency can be increased with more capacitance loading which further adversely affects the total power consumption of oscillator. At circuit level power efficiency can be improved with an optimized design. Optimization are possible in different ways like reduction of switching activity, capacitance and by reducing the short circuit currents etc. This paper proposes novel DCO circuits with NAND gate based inverter delay cell used in ring topology. Here, switch network of transistors are added with inverter based delay cell to control the oscillator frequency. Proposed DCO circuits avoid the analog tuning voltage control and provide the design flexibility with higher power efficiency.

This paper is organized as follows: first section describes delay cell using three transistor NAND gate based three stage DCO .Section II describes 5 stage NAND gate based DCO. Simulation results and discussion have been described in section III. Section IV concludes the work.

II DCO DESCRIPTION

Digitally controlled delay elements (DCDE) are the heart on any DCO structure. The designs of DCO in this paper are based on digitally controlled inverter delay elements connected in ring topology. Three transistor NAND gate working as inverter has been utilized as delay element [3],[4]. One input terminal of NAND gate is connected to Vdd and input signal is applied to second terminal and this circuit works as an inverter. Binary weighted MOS transistors as shown in fig. 1 have been used in switch networks and delay of each stage has been controlled by binary bits applied to these transistors. With changing bit patterns different transistors are selected with unequal width and resistance of transistor network changes accordingly which further modulates the delay of circuit. Changing delay produces different

frequency components as controlled by digital input word.

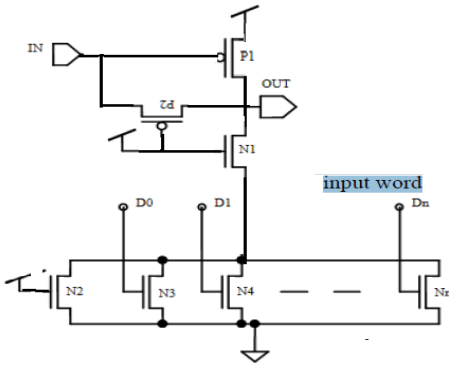

Fig. 1 Delay Cell with NMOS switch network

The delay cell has been proposed using NMOS switching networks as shown in fig. 1. Number of bits can be increased or decreased as per the need of frequency tuning. Gate length of all transistors has been taken as 0.18µm. In NAND based inverter section, width of P1 and P2 has been taken as 1.26µm whereas width of N1 has been taken as 0.24µm. DCO structure with three delay cells having 3-bit control has been shown in figure 2. Switch networks having four NMOS transistors are connected with source terminal of transistor N1 of each delay cell. Four NMOS transistors [N2-N5] are binary weighted with first transistor having Vdd supply at gate terminal to provide path for current conduction. Three control bits [D0-D2] are applied to three binary weighted NMOS transistors [N3-N5].

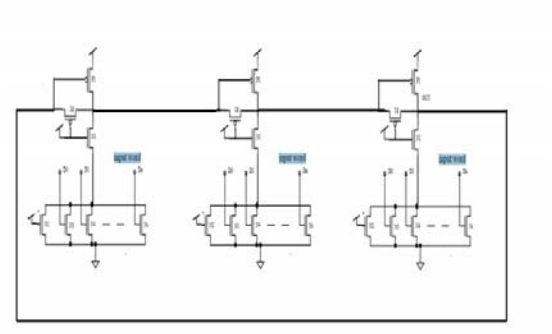

Fig. 2. 3 stage Delay cell with three bit control

III .RESULTS AND DISCUSSIONS

The results have been obtained using Microwind 2.3d software with 180 nm process technology with supply voltage of 1.2V. Power consumption and output frequency has been obtained with different control bits [000 - 111]. In 3-bit NMOS switch network DCO the resistance decreases with varying bit pattern from 000 to 111 and the delay of circuit also reduces. With decrease in delay the output frequency increases with subsequent rise in power consumption. Figure 4 shows the mask layout of 3 bit controlled DCO with NMOS switching network. Tables 1,2,3, show the results of 3-bit controlled DCO,5 bit controlled DCO and 3 bit controlled 5 stage DCO with NMOS switch network. Figures 5,7,9 show the output frequency of 3 bit 3 stage DCO , 5 bit controlled DCO and 3 bit controlled 5 stage DCO.

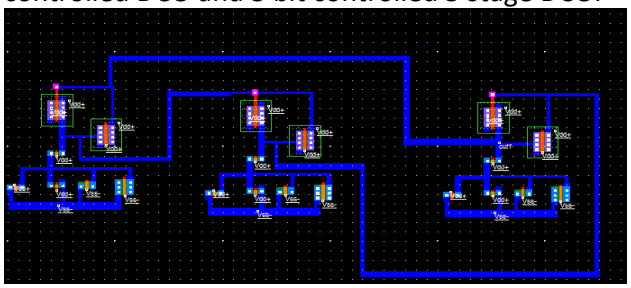

Fig 4 Mask layout of 3 bit controlled 3 stages DCO

Control Word	Frequency(GHz)	Power Consumption
000	3.39	0.308mW
001	4.26	0.379mW
010	4.68	0.415mW
011	4.92	0.438mW
100	5.11	0.454mW
101	5.22	0.460mW
110	5.29	0.466mW
111	5.35	0.471mW

Table 1 3 bit controlled 3 stage DCO

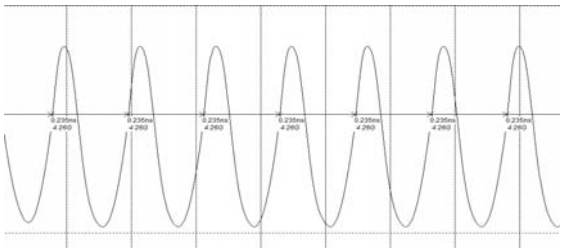

Fig. 5. Output frequency of 3 bit controlled 3 stage DCO

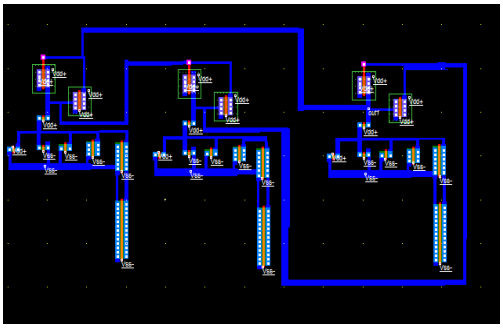

Fig. 6. Mask layout of 5 bit controlled 3 stages DCO

Control Word	Frequency(GHz)	Power Consumption
00000	3.65	0.304mW
00111	5.74	0.469mW
11111	6.11	0.501mW

Table 2. Frequency and power variation with control word for 5 bit controlled 3 stage DCO

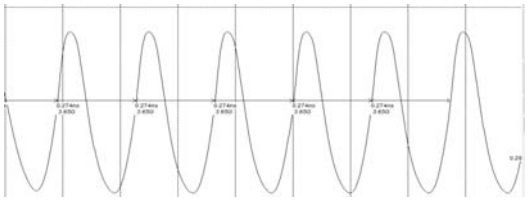

Fig.7. Output frequency of 5 bit controlled 5 stage DCO

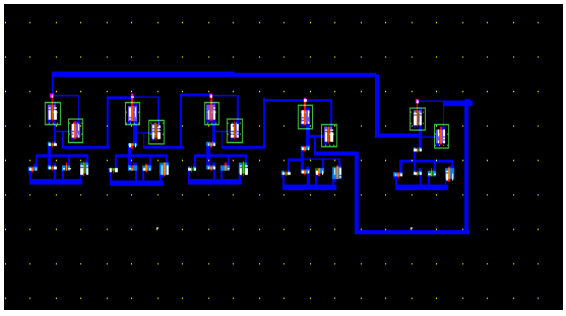

Fig. 8. Mask layout of 3 bit controlled 5 stages DCO

Control Word	Frequency(GHz)	Power Consumption
000	2.31	0.534mW
011	2.99	0.632mW
111	3.19	0.672mW

Table 3. frequency and power variation with control word for 3bit controlled 5 stage DCO

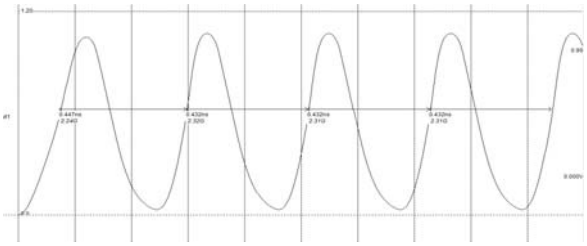

Fig 9. Output frequency of 3 bit controlled 5 stage DCO

IV. Conclusion

The new structures for digital controlled oscillators (DCOs) with NAND gates based delay cell having full digital control are reported in this paper. Three, and five bit controlled DCO have been implemented with proposed delay cells. Resistance of switch network has been varied by digital control bits and delay of circuit has been modulated. Three bit three stage ring DCO with NMOS network gives output frequency [3.39 – 5.35] GHz with power consumption of [0.308 – 0.471] mW. five bit three stage ring DCO with NMOS network gives output frequency [3.65 – 6.11] GHz with power consumption of [0.304 – 0.469] mW. Three bit five stage DCOs with NMOS network shows output frequency of [2.31 – 3.19] GHz with power consumption of [0.534 – 0.672] mW. From this it is concluded that dco implementation using NAND based increases the frequency range but at the cost of increase in power consumption.

References

1] I.Hwang, S.Lee, S.Lee and S.Kim,"A digitallycontrolled phase locked loop with fast locking scheme for clock synthesis applications," in IEEEInt.Solid-State circuits Conf.Dig.Tech.Papers,Feb.2000, pp.168-169.

[2] Ching-Che Chung and Chen-Yi Lee,"An All-Digital Phase-Locked Loop for High-Speed Clock Generation," IEEE JOURNAL OF SOLID STAESCIRCUITS, VOL.38, NO.2, FEBRUARY2013.

[3] M. Bharath Reddy 1, M. Sai Sarath Kumar 2, B. Suresh Kumar 3" ,DESIGN OF ALL DIGITAL PHASE LOCKED LOOP (D-PLL) WITH FAST ACQUISITION TIME, IJRET:", International Journal of Research in Engineering and Technology ISSN: 2319-1163 | pISSN: 2321-730.

[4] Manoj Kumar1, Sandeep K. Arya1 and Sujata Pande" ,Digital Controlled Oscillator Design with Novel Transistors XOR Gate," International Journal of Smart Home Vol. 6, No. 1, January, 2012.

[5] J. Dunning, G. Garcia, J. Lundberg, and E. Nuckolls, "An all-digital phase-locked loop with 50-cycle lock time suitable for high-performance microprocessors", IEEE J. Solid-State Circuits, Vol. 30 **(1995)** April, pp. 412–422.

[6] Jen-Shiun Chiang and Kuang-Yuan Chen, "The design of all digital phase locked loop with small DCO hardware and fast phase lock", IEEE transactions on circuits and systems-II, Vol. 46, No. 7 **(1999)** July, pp. 945-950.

[7] Jun Zhao and Yong-bin Kim, "A low power 32 nanometer CMOS digitally controlled oscillator," IEEE SoC Conference **(2008)** September, pp. 183-186.

[8] R. Saban and A. Efendovich,"A fully-digital, 2-MB/sec CMOS data separator," IEEE International Symposium on Circuits and Systems, Vol. 3 **(1994)** June, pp. 53–56.

[9] R. Fried, "Low-power digital PLL with one cycle frequency lock-in time for clock syntheses up to 100 MHz using 32,768 Hz reference clock", IEEE international ASIC Conference Exhibit **(1996)** September, pp. 291–294.

[10]Yu-Ming Chung and China-Ling Wei, "An All-Digital Phase-Locked Loop for Digital Power Management Integrated Chips", IEEE International Symposium on Circuits and Systems **(2009)** May, pp. 2413-2416.

[11] A.Tomar, R.K. Pokharel, O. Nizhnik, H. Kanaya, and K. Yoshida, "Design of 1.1 GHz Highly Linear Digitally-Controlled Ring Oscillator with Wide Tuning Range", IEEE International Workshop on Radio-Frequency Integration Technology **(2007)** December 9-11, pp. 82-85.

[12] F. Baronti, D. Lunardini, R. Roncella, and R. Saletti, "A self calibrating delay-locked delay line with shunt capacitor circuit scheme", IEEE J. Solid-State Circuits, Vol. 39, No. 2 **(2004)** February, pp. 384–387.

An Overview of InP/GaAsSb/InP DHBT in Millimeter and Sub-millimeter Range

[1]Er. Ankit Sharma, [2]Dr. Sukhwinder Singh
[1]Research Scholar PEC University Of Technology, Chandigarh INDIA
[2]Supervisor, Assistant Professor PEC University Of Technology, Chandigarh INDIA
Email: [1]ankitdit2011@gmail.com, [2]sukhwindersingh@pec.ac.in

Abstract— We present an overview of Dual Heterojunction Bipolar Transistor approaching Gigahertz frequencies based on latest device technology. Highlights include the best reported data from GaAsSb Dual Heterojunction Bipolar Transistor. We will discuss the best reported cut of frequency in DHBT. Short review of the journey from BJT to DHBT is also discussed with their advantages and disadvantages.

Index Terms— DHBT, GaAsSb, HBT, InGaAs, InP.

1. INTRODUCTION

In electronics industry, Silicon has been first choice from last few decades. But due to lack of linearity and degradation of current gain in silicon based BJT devices operate in microwave frequency, Group III-V based NpN heterojunction bipolar transistor have achieved tremendous performance in term of microwave frequencies of operation and higher current gain because of their superior material properties, such as higher electron mobility and unique bandgap alignment.

NPN HBT differ from BJT in term that emitter is replaced by a material with larger bandgap than base. This leads to a lowering of barrier for electron injection into base, but an increased barrier for holes which prevents their back injection into emitter, resulting in higher current gains. As a result base can be made thinner and doped higher than emitter to reduce the base resistance and further increase its high frequency performance. Earlier there were difficulties in develop, defect free III-V materials but advancement in epitaxial growth technologies, such as Molecular Beam Epitaxy (MBE) and metal organic Chemical Vapor Deposition (MOCVD) shows the full potential of HBTs. Recently, InP/GaAsSb/InP DHBT has shown highest cutoff and maximum oscillation frequencies of 428 GHz & 621 GHz respectively recorded for any DHBT.

Development of double heterojunction bipolar transistor is driven by increasing demand for higher data rates in optical and wireless communication network. These DHBT devices exhibit electron mobility several times higher than those achievable by present known devices. Tremendous growth in research and development effort are being made for semiconductor integrated circuit composed of

field effect transistor and bipolar junction transistor using compound semiconductor material such as GaAsSb, InGaAs, and InP. Example of such semiconductor devices are DHBT, HBT, High Electron Mobility Transistors. In this paper, we present review of DHBTs. Section 2 refer to journey from BJT to InP/GaAsSb/InP DHBT, Section 3 refer to high frequency operation of InP/GaAsSb/InP DHBT, Section 4 refer to conclusion.

2. JOURNEY FROM BJT TO INP/GAASSB DHBT

2.1 Homojunction Bipolar Transistor

Review of basic operation of homojunction BJT is important before the discussion of InP/GaAsSb DHBTs. Emitter, Base and Collector of BJT is made up of silicon material. Doping of same type is used for emitter and collector. Slightly change in base current controlled the flow of current from emitter to collector [1]. Let us assume npn transistor for explaining the functioning of transistor. Injection of minority carrier across the junction in forward bias plays significant role in the operation of BJT's. For normal operation base-emitter junction is forward bias and base-collector junction should be reverse bias. In forward bias, concentration of minority carrier in base at base-emitter junction is amplified by a factor exp (qv/kt). Width of base region should be less than diffusion length of electron [1][2]. Electron injected into base from emitter must diffuse across base to collector without excessive recombination with majority carrier's holes in base. High electric field in reversed bias base-collector junction attracts minority carriers electron of base when they reach base collector junction and form collector current. Band diagram of BJT in thermal equilibrium is shown in Fig1.

Solving the carrier continuity equations, the base current and the collector current are given as follows: [1][2].

$$I_B = \frac{qA_E D_{pE}}{X_E} \frac{n_{iE}^2}{N_E} \exp\left(\frac{qV_{BE}}{KT}\right) \quad (1)$$

$$I_C = \frac{qA_E D_{nB}}{X_B} \frac{n_{iB}^2}{N_B} \exp\left(\frac{qV_{BE}}{KT}\right) \quad (2)$$

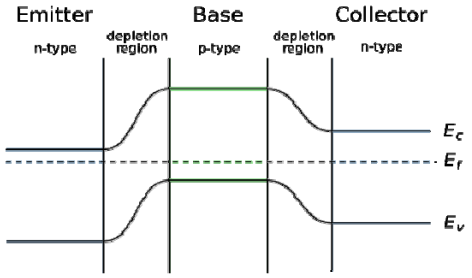

Fig. 1 Band diagram of an npn homojunction bipolar transistor under thermal equilibrium.

From the analysis of above two expressions, we get that in order for collector current to be greater than base current, it is necessary that emitter doping exceed base doping. In doing so, we have trade-off an important transistor design parameter. For keeping base doping at a lower value means that base resistance will be high. This can be compensated by widening the base, but it will cause significant effect on base transit time thus lowering the device maximum frequency of operation. Therefore, for a fixed base doping level, current gain of BJT can be increased initially by increasing the emitter doping. But significantly emitter bandgap narrowing occurs when emitter doping is around $N_E \sim 10^{18}/cm^3$, causing current gain to degrade.

Therefore in homojunction BJT there is conflicting set of requirements, where base doping cannot be increased without sacrificing current gain. This limits the operation of BJT to low frequency amplifiers and oscillators. The performance of HBT can be significantly better

than that of BJT, if we dope base high and at same time comparatively reduce emitter doping, which is more feasible because of wide band gap emitter in HBT. This is where HBT have made tremendous progress in term of frequency of operation in millimeter band.

2.2 Heterojunction Bipolar Transistor

Heterojunction bipolar transistor (HBT) uses differing semiconductor materials for emitter and base regions, creating a heterojunction. Advantage of heterojunction bipolar transistor compare to homojunction transistor lies in the possibility of increasing frequency performance while maintaining high gain. Emitter injection efficiency depends upon relative doping of emitter and base as well as on base/emitter band difference. Electrons are injected thermally into base from emitter and diffuse across base and electric field in base-collector depletion region sweep them into collector at high speed.

Hole injection from base into emitter region is reduced, because valence band has greatest potential barrier compare to conduction band. Hence lower doping density required for emitter in comparison to base besides maintaining gain. Base thickness reduced which result in improvement of unity gain cutoff frequency and maximum oscillation frequency, higher current amplification, lower base resistance, lower base emitter capacitance and high early voltage [1] of HBT in millimeter range. HBT is used in modern ultrafast circuit, generally radio frequency (RF) system and in high power efficiency application. For example RF power amplifiers in phones.

Heterojunction are of two types. Abrupt heterojunctions and Graded heterojunction. In abrupt heterojunction, two different semiconductors with different bandgap are brought together and interface is abrupt, i.e. composition changes abruptly. In graded heterojunction, composition is gradually changed across heterojunction and suppression of energy band spikes due to energy band edge discontinuity seen at abrupt heterojunction interface. Here we are considering abrupt heterojunction for research work. Shown in Fig. 2 is an abrupt emitter-base heterojunction in an npn HBT [1].

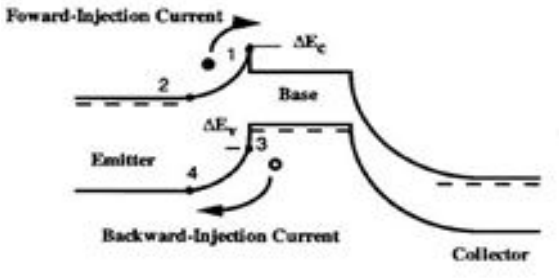

Fig. 2 Band diagram of NPN HBT under normal forward active mode.

Generally conduction band of emitter lies above that of base. Ratio of electron to hole current across emitter-base heterojunction i.e. current gain, is given as: [1].

$$\frac{I_n}{I_p} = \beta_{max} = \frac{N_E}{N_B}\frac{v_{nb}}{v_{pe}}\exp\left(\Delta E_g/kT\right) \qquad (3)$$

Where NE and NB represent emitter and base doping respectively. Vpe and Vnb represent thermal velocity of hole and electron in emitter and base respectively. Δ E_g is bandgap difference between base and emitter. Current gain has exponential dependent on valence band discontinuity ΔE_V between base and emitter for npn devices [1]. Emitter injection efficiency is ideally unity, irrespective of doping level of base and emitter [2]. Maximum current gain is obtained when negligible recombination in base and $\Delta E_V = \Delta E_G$. When $E_V > \Delta E_G$ then emitter-base energy bandgap difference increases I_n/I_p ratio by a factor of exp (ΔE_V / kt) relative to that of

BJT. Valence band Δ E_V discontinuity at heterojunction replaces E_C in equation (3) and related to current gain as follows: [1].

$$\frac{I_n}{I_p} \sim \exp\left(\Delta E_v / kT\right) \qquad (4)$$

Spike in conduction band at emitter-base junction causes injection of electron into base region with a high velocity (~10^8cm/s) that exceeds the saturation velocity. This results in a highly efficient and very fast electron transport through base. Tremendous developments in material growth technologies have enabled precise control of layer thickness, doping and possibility to change composition by replacing one with another III-V semiconductor material. So that HBT can be designed for high frequency of operation.

2.3 Double Heterojunction Transistor

HBT is suitable for low voltage operation. For high voltage operation, it is necessary to improve the breakdown voltage. One can use double heterojunction bipolar transistors, having base-collector heterojunction in addition to emitter-base heterojunction. The second heterojunction has the effect of improving the breakdown voltage through the use of material with high forbidden band width (like InP) for the collector. Use of same material for emitter and collector forms a double heterojunction transistor. Collector form by wide bandgap material causes suppression of hole injection efficiency from base to collector [2]. Material like InP have shown excellent transport and thermal properties than conventional GaAs and other materials.

2.4 InP Based Heterojunctions

InP based HBT can perform best in millimeter and sub-millimeter band compare to any other solid state devices [3]. Comparison of InP over GaAs and Si semiconductor is shown in Fig.3 [4]. Fig. 3(a) represent InP HBT have lower turn on voltage than other semiconductor devices due to small bandgap of base. Fig. 3(b) represent InP HBTs have a higher breakdown voltage at a given collector doping, while Fig. 3(c) represents InGaAs and InP have higher electron mobility than GaAs. Finally, Fig. 3(d) represents InP HBT has a larger thermal conductivity than GaAs, though less than that of Silicon. Larger thermal conductivity of InP HBT results in the lower device heating [5]. InP devices are compatible with long wavelength laser and led sources. This allows for direct integration and tight coupling of light sources and also use in transmitter/receiver circuitry [5]. Lower surface recombination velocity of InP-based HBTs results in a reduction of surface leakage currents and improved gain at low current densities, enhancing the ability to scale down devices to smaller dimensions for LSI implementation [3]. InP based devices have the significantly lower 1/f noise and higher power added efficiency (PAE) than GaAs devices which is extremely important for portable devices like mobile phones [3]. As a result InP-based devices dominate over other conventional devices in millimeter and sub- millimeter band. Earlier InGaAs, because of narrow band gap is used as base in InP-based heterojunction devices. Outstanding features of InGaAs such as mobility, electron saturation velocity, Scaling and minimization of collector area junction have shown good result in InP/InGaAs-based single HBTs in term of cut-off frequencies in millimeter range [6].Now the question arises, why we are moving to GaAsSb when InGaAs is performing well. Low break down voltage due to narrow collector gap in InGaAs was the major drawback of InP/InGaAs HBT [7].

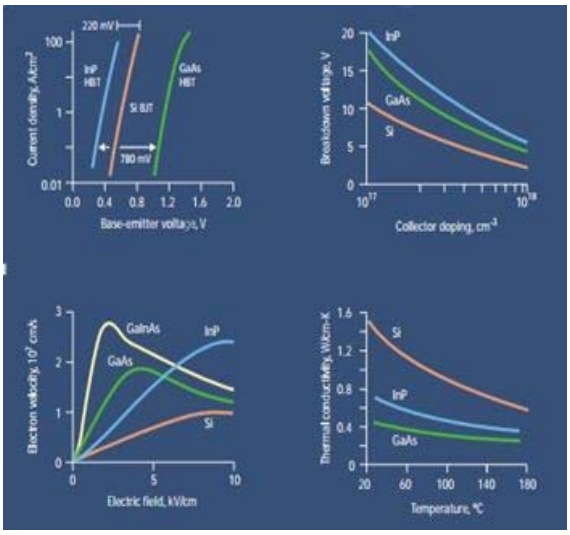

Fig. 3 Comparison of material properties of InP, GaAs and Silicon [4].

This drawback is over come by using an wide bandgap AlInAs or InP collector layers in the double heterojunction transistor [8][9]. But AlInAs or InP collector has shown collector current blocking problem caused by conduction band discontinuity between InGaAs base and wider bandgap InP collector. Fig.4 shows conduction band energy diagram in various doping and/or composition grading schemes developed for base-collector region to overcome this blocking effect [10].For InP collector, a blocking barrier of 0.25 eV must be overcome between base and collector as shown by curve (a) in Fig.4 where the base-collector discontinuity ΔE_C increase the transit time of electron minority carriers, and reduce HBT performance in term of frequency and current gain. Fig. 4(b) shows reduction in blocking effect and improvement in current gain by using an undoped InGaAs spacer layer between base and collector. Fig. 4(c) shows using of compositional grading to minimize blocking effect. Fig. 4(d) shows favorable band lineup for InP/GaAsSb DHBT.

Grading methods discussed in [8, 9, 10] introduce significant epitaxial growth complexity and impose stringent uniformity and repeatability requirements on the epitaxial growth. Even these grading schemes are not best method for eliminating collector-blocking effect at base collector interface, because high collector current densities cause a retarding potential, eventually degrading transistor performance [11]. Specifics of any grading and/or doping schemes at the base/collector junction need to be considered carefully because they can have a dominant impact on DHBT performance at high current densities [12]. GaAsSb base layer provides an excellent solution for collector blocking effect occurring in InGaAs-based DHBT designs.

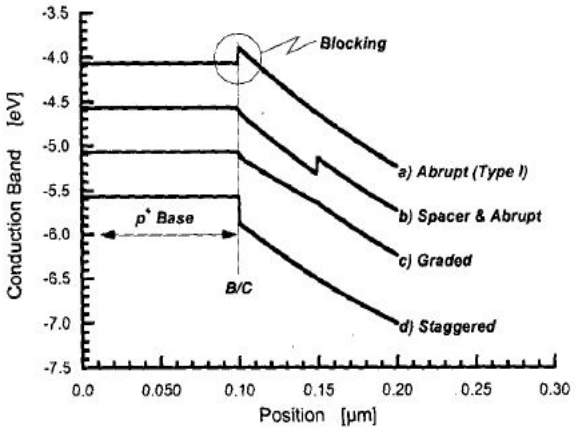

Fig. 4 Conduction band profiles of B/C junction in dhbt [10].

2.5 InP/GaAsSb/InP Double Heterojunction Bipolar Transistors

Replacing InGaAs from base layer by GaAsSb and formation of type II bandgap at base-collector junction in GaAsSb/InP HBT has shown a better solution for the collector blocking problem as shown in Fig. 4(d) [13][14]. Electrons travels from base-collector depletion region with a high velocity exceeding their saturation velocity, a phenomenon known as velocity overshoot [1]. Hence InP/GaAsSb

DHBTs benefit from two fundamental advantages over InP/InGaAs DHBTs.

(1) No graded transition layers require at collector- or emitter-base junctions, hence simplifying growth of epitaxial layers.

(2) C-doped GaAsSb feature high doping efficiency [15] and displays little or no H-passivation effects [11].

Also low diffusivity and good donor properties of Carbon doping ensures that base-collector junction is precisely and permanently self-aligned to GaAsSb/InP interface leading to stability and improves device characteristics. At 300 K, $GaAs_{0.51}Sb_{0.49}$ conduction band edge is above that of InP by 0.15 eV and valence band discontinuity is 0.78 eV [16][17] causes non-blocking conduction band profile at the base-collector heterojunction. Here compositional grading is also not required. Earlier, lots of difficulties were facing like developing GaAsSb layers with low resistivity, mobility of GaAsSb is roughly 50-60% of that in InGaAs for a given concentration. These devices had f_T and f_{MAX} performance of around 30GHz and 45GHz, respectively [18][11].

These results discouraged further development using this material system for a while. While there is a conduction band barrier at emitter-base junction impeding electron injection into base from emitter, effect is not fatal and high performance InP/GaAsSb DHBTs have been reported [19]. Recent developments have shown impressive performance gains in terms of cut-off and maximum oscillation frequency of operation. Recently Type-II InP/GaAsSb DHBT with f_{MAX} of 621 GHz and simultaneous f_T of 428 GHz has been demonstrated [20]. The present transistors are the first InP/GaAsSb DHBTs with an f_{MAX} in excess of 600 GHz. Results also show f_T/f_{MAX} = 470/540 GHz [21]. MOCVD grown, Carbon doped, abrupt heterojunction, InP/GaAsSb/InP DHBTs feature a very small VCE offset voltage < 0.1V and a low turn-on voltage of V_{BE} of 0.4 V at a current density of J_C =1 A/cm^2, by taking advantage of the staggered band lineup at the InP/GaAsSb interfaces [7]. Minority carrier electron mobility in the p-doped base is the order of 600-800 cm^2/Vs. This is low when compared to similarly doped InGaAs layers with electron mobility of 2000-3000 cm^2**/** Vs in InP/InGaAs HBTs. This lower mobility necessitates the use of thinner bases for GaAsSb than InGaAs to achieve comparable base transit times. However, to maintain acceptable base sheet resistance and high maximum oscillation frequency, higher base doping is necessary. This requirement for higher doping is solved by GaAsSb affinity for Carbon doping and low H-passivation effects [13].

3. HIGH FREQUENCY OPERATION OF InP/GaAsSb DHBT

3.1 InP/GaAsSb DHBT Energy Band Diagram

InP/GaAsSb DHBT consists of lattice matched $GaAs_{0.51}Sb_{0.49}$ base ($E_G \approx 0.72$ eV) and InP based emitter and collector region ($E_G \approx$ 1.35eV). Heterojunction between InP and GaAsSb has Type II band alignment. Equilibrium energy band diagram is shown below in Fig 5 (a) and schematic cross section view of Triple mesa device structure (b). Valence and conduction band discontinuities are $\Delta E_V \approx 0.73$ eV and $\Delta E_C \approx 0.10$ eV. The carrier flow vertically across emitter, base, collector by their respectively transport mechanism. A schematics representation of cross section of a standard DHBT is shown in Fig 6. The device consists of emitter, base, collector and sub collector mesas. A heavily N doped sub collector region is used in order to reduce collector series resistance.

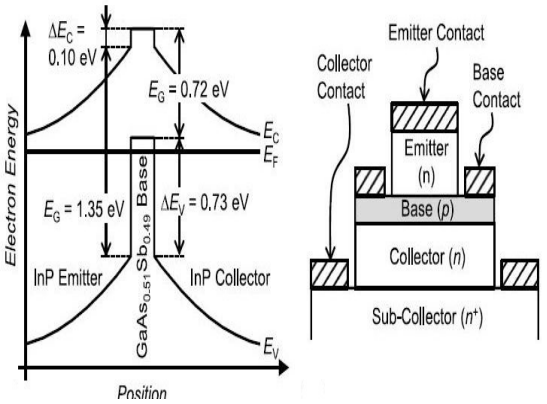

Fig. 5 Energy Band Diagram of an InP/GaAsSb (a) and schematic view of mesa structure (b).

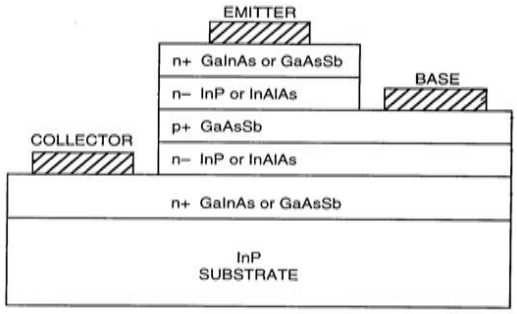

Fig. 6 InP/GaAsSb dhbt schematic diagram

3.2 Current Gain Cutoff Frequency

Cutoff frequency f_T is defined as frequency at which magnitude of common emitter short circuit gain h_{21} decreases to unity. Expression of h_{21} as a function of frequency f is shown below: [1].

$$\beta_{ac} = \frac{\beta_{dc}}{1+jw\beta_{dc}(C_p+C_{jc})/g_m} \qquad (5)$$

Where C_p is total input capacitance, C_{jc} is base collector junction capacitance and g_m is transconductance of device.

For finding f_T , $|\beta_{ac}| = 1$

$$\tau_{EC} = \frac{1}{2\pi f_T} \qquad (6)$$

Where $\tau_{EC} = \tau_e + \tau_b + \tau_{sc} + \tau_c$

Where, τ_{EC} is the total HBT input response delay time, τ_e is the emitter charging time, τ_b is the base transit time, τ_{sc} is the space charge transit time, and τ_c is the collector charging time. Relation between cutoff frequency and common emitter current gain is shown in Fig. 7 shows current gain calculated for constant emitter collector transit time and values of β ranging from 10 to 100.

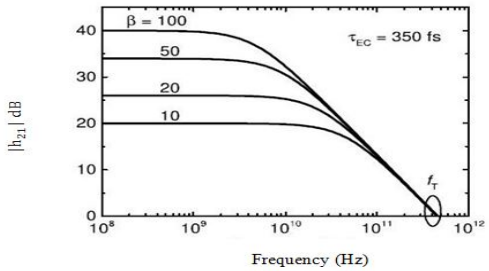

Fig. 7 Common–emitter short circuit gain $|h_{21}|$ versus frequency with current gain β.

3.3 Maximum Oscillation Frequency

Unilateral power gain of transistor is the power gain after transistor plus loss less network. It is define as the frequency at which mason's unilateral power gain U is reduced to unity. The expression of U is given below: [22]

.

$$U = \frac{f_T}{8\pi f^2 (R_B C_{BC})_{EFF}} \qquad (7)$$

Where f is the frequency and $(R_B C_{BC})_{EFF}$ is an effective time constant. The expression of maximum oscillation frequency f_{MAX} is given below: [23].

$$f_{MAX} = \sqrt{\frac{f_T}{8\pi RbCc}} \qquad (8)$$

Where R_b is base series resistance and C_c is collector junction capacitance. Increasing R_b does not affect Ft, while the increased C_c has minor affect on f_T. However both has a more pronounced effect on f_{MAX}.

3.4 Doping of base in DHBT

Compound used for the formation of base is GaAsSb. Various base grading schemes improve current gain compared to uniform doped baseline. C doping grade improve device DC current gain. DHBT with built-in electric field in the base has improved DC current gain and high speed characteristics over DHBT without built-in electric field. Built-in voltage can be introduced by either doping grading or composition grading in the base [24]. There are at least four ways to implement base grading in GaAsSb/InP DHBTs:

1. $In_xGa_{1-x}As_ySb_{1-y}$
2. $Al_xGa_{1-x}AsSb$
3. $GaAs_ySb_{1-y}$ Compositional Grading
4. GaAsSb: C Doping Grade

It is difficult to simultaneously control both composition grading in $In_xGa_{1-x}As_ySb_{1-y}$ and $Al_xGa_{1-x}AsSb$ produces unnecessary higher turn on voltage than rest of grading schemes. Hence GaAsSb: C doping grades improve DC current gain. In the given Fig. 8, base thickness is constant. Relation between DC current gain and base sheet resistance is obtain to evaluate effectiveness of certain base grading scheme.

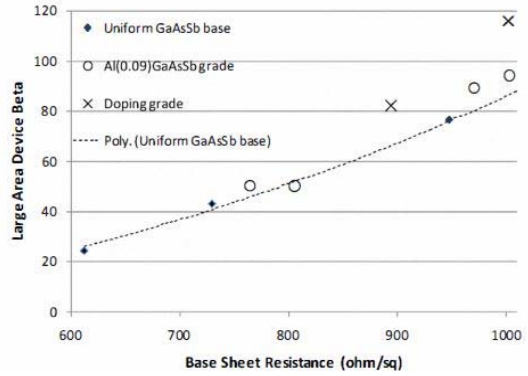

Fig. 8 Effectiveness of various base grading schemes

compared with $GaAs_{0.8}Sb_{0.2}$ baseline [25].

3.5 Diffusion Coefficient And Base Transit Time

Emitter-collector delay in InP/GaAsSb DHBT is given by equation (9). Using single pole approximation of $h_{21}(f)$ of small signal T-model, the total delay time τ_{EC} is estimated as a sum of internal delay times [25]:

$$\tau_{EC} = \tau_T + (C_{je} + C_{jc})\frac{nkT}{qI_C} \quad (9)$$

Where $\tau_T = \tau_B + \tau_C + (R_C + R_E)C_{jc}$

Delay time τ_T followed quadratic equation versus base thickness W_B as shown in fig 9.

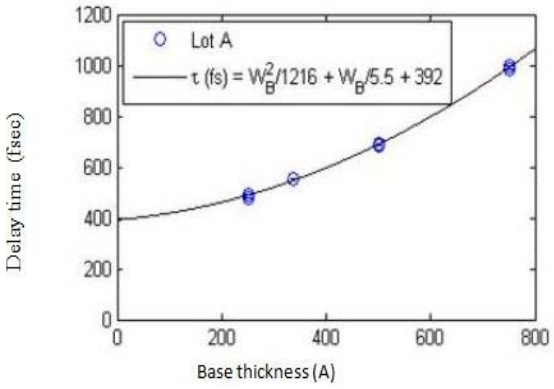

Fig. 9 Delay time τ_T versus base thickness W_B [26].

Base thickness is given by [26].

$$\tau_B = W_B^2/2D_{nB} + W_B/V_{exit} \quad (10)$$

Minority carrier diffusion coefficient in ultrafast speed HBT is calculated from above equation 10. There is currently no estimate for exit velocity V_{exit} of electrons in GaAsSb/InP transistors during non equilibrium transport, but the value of 5.5E7 cm/s, which was extracted for InGaAs/InP DHBTs by Monte Carlo simulation, is a viable approximation and was used to enhance the quadratic fit shown in Fig 9.

4. CONCLUSION

Continuously increasing demand for higher data rates in optical and wireless communication network working in gigahertz frequencies causes tremendous growth in research and development efforts. In this

review paper we have discussed the device well suitable for sub-millimetre and millimetre band. Homojunction bipolar transistor cannot function efficiently due to increase in transit time of electron from emitter to collector in gigahertz frequency band. Heterojunction transistors have solved this problem. The performance of Heterojunction bipolar transistor is evaluated in term of breakdown voltage, transit time, doping type of base.

InP based DHBT dominates the HBTs in removing the collector blocking effect and also in enhancing the collector breakdown voltage. Type II InP/GaAsSb/InP Double Heterojunction Bipolar Transistors have shown best result in term of cutoff frequency, maximum oscillation frequency, high linearity and low noise ever reported by any solid state device in high frequency operation.

REFERENCES

[1] W Liu, Handbook of III-V Heterojunction Bipolar Transistor, John Wiley and Sons, Inc, 1998.

[2] H. Kroemer, “Heterojunction Bipolar Transistor and Integrated Circuits”, Proc. of IEEE, vol.70, No 1. pp. 13-25, 1982.

[3] O. Osamu, H. Hasegawa, High Speed Semiconductor Devices –Physics and Technology, John Wiley and Sons, New York, 1999.

[4] G. Raghavan, M. Sokolich and W.E. Stanchina, “Indium Phosphide ICs Unleash the High Frequency Spectrum“, IEEE Spectrum, vol.37, No 10, pp 45-49, 2000.

[5] P.M. Asbeck, “Bipolar Transistor”, High Speed Semiconductor Devices, S.M. Sze editor, New York, Wiley 1990,pp. 335-397.

[6] J.W. Rodwell, M. Urteaga, T. Mathew, D. Scott, D. Mensa, Q. Lee, J. Guthrie, Y. Betser, Suzanne C. Martin, R.P. Smith , S. Jaganathan, S. Krishnan, S.I. Long, R. Pullela, B. Agrawal, U. Bhattacharya, L. Samoska, and M. Dahlstrom, “Submicron Scaling of HBTs”, IEEE Trans. On Electron Devices, Vol.48, pp 2606-2624, 2001.

[7] C.R. Bolognesi , M.W. Dvorak, N. Matine, P. Yeo, X.G. Xu and S.P. Watkins, ”InP/GaAsSb/InP Double HBTs : A New Alternative for InP-Based DHBTs”, IEEE Trans. on Electron Devices, vol 48, No 11, pp 2631-2639, 2001.

[8] K. Kurishima, H. Nakajima, T. Kobayashi, Y. Matsuoka, and T. Ishibashi, ”High Speed InP/InGaAs Double Heterojunction Bipolar Transistors with Suppressed Collector Blocking”, Appl. Phys. Lett., vol 62, pp.77-79, 1998.

[9] E.F. Chor, and C.J. Peng, “Composite Step-Graded Collector of InP/InGaAs/InP DHBT for Minimized Carrier Blocking”, Electron Lett., vol 32, pp.1409-1411, 1996.

[10] M.W. Dvorak, O.J. Pitts, S.P. Watkins and C.R. Bolognesi, “Abrupt Junction InP/GaAsSb/InP Double Heterojunction Transistor with f_T as High as 250 GHz and B VCEO > 6V”, IEDM, Tech. Digest, pp. 178-182, 2000.

[11] B.T. McDermott, E.R. Gertner, S. Pittman, C.W. Seabury, and M.F. Chang, ”Growth and Doping of GaAsSb via metalorganic chemical vapor deposition of InP heterojunction bipolar transistors”, Appl. Phys. Lett. vol. 68, pp. 1386-1388, 1996.

[12] C.R. Bolognesi, M.W. Dvorak, O.J. Pitts, S.J. Watkins, T.W. Macelwee, ”Investigation of high current Effect in Staggered Line-up InP/GaAsSb/InP Heterojunction Bipolar Transistor”, Presented IEEE Electronics Devices Meeting, 2000.

[13] K.I. Anastasiou, ”GaAaSb for Heterojunction Bipolar Transistor”, IEEE Trans Elect. Devices, vol. 40, pp. 878-884, 1993.

[14] C.R. Bolognesi, S.P. Watkins, "InP based Double Heterojunction Bipolar Transistor: I t may not have to be GaInAs", Compound Semiconductors, pp. 94-99, 2000.

[15] S. P. Watkins, O. J. Pitts, C. Dale, X. G. Xu, M. W. Dvorak, N. Matine, and C. R. Bolognesi, "Heavily Carbon-Doped GaAsSb Grown for HBT ," J. Cryst. Growth, vol. 221, pp. 59–65, 2000.

[16] M. Peter, N. Herres, F. Fuchc, K. Winkler, K.H. Bachemand J. Wagner, "Band Gaps and Band Offsets in Strained $GaAs_{1-y}Sb_y$ on InP Grown by Metalorganic Chemical Vapor Deposition." Appl. Phys. Lett. vol 74. pp. 410-412, 1999.

[17] J. Hu, X. G. Xu, J. A. H. Stotz, S. P. Watkins, A. E. Curzon, M. L. W. Thewalt, N. Matine, and C. R. Bolognesi, "Type II Photoluminescence and Conduction Band Offsets of GaAsSb/InGaAs and GaAsSb/InP Heterostructures Grown by Metalorganic Vapor Phase Epitaxy," Appl. Phys. Lett., vol. 73, pp. 2799–2801, 1998.

[18] R. Bhat, W.P. Hong, C. Caneau, M.A. Koza, C.K. Nguyen and S. Goswami, "InP/GaAsSb/InP and InP/GaAsSb/InGaAsP Double Heterojunction Bipolar Transistor with a Carbon Doped Base Grown by Organo-metallic Chemical Vapor Deposition", Appl. Phys. Lett., vol. 68, pp. 985–987, 1996.

[19] M.W. Dvorak, C.R. Bolognesi, O.J. Pitts and S.P. Watkins, "300 GHz InP/GaAsSb/InP Double HBT with High Current Capacity", IEEE Electron Device Letters, vol. 22, pp. 361-363, 2001.

[20] R. Lovblom, R. Fluckiger, M. Alexandrova, O. Ostinelli, and C. R. Bolognesi, "InP/GaAsSb DHBTs with Simultaneous f_T/f_{MAX} = 428/621 GHz", IEEE Electron Devices Lett., vol 34, No.8, 2013.

[21] H. Xu, B. Wu, E. W. Iverson, T.S. Low, and M. Feng, " 0.5 THz Performance of a Type-II DHBT With a Doping-Graded and Constant-Composition GaAsSb Base", IEEE Electronics Device Letters, vol. 35, pp 24-26, 2014.

[22] M. Vaidyanathan and D.J. roulston, "Effective base-collector time constants for calculating the maximum oscillation frequency of bipolar transistors," Solid State Electronics, vol. 38, no. 2, pp. 509-516, 1995.

[23] A.P. Laser and D.l. Pulfrey, "Reconciliation of Methods for Estimating f_{MAX} for Microwave Heterojunction Transistors," Electron Devices, IEEE, Trans. , vol. 38, no. 8, pp.1685-1692, 1991.

[24] B.R. Wu, M.W. Dvorak, P. Colbus, T. S. Low, and D. Davanzos, High Current Gain of Doping-Graded GaAsSb/lnP DHBTs, IPRM conference, 2011.

[25] E. W. Iverson, T.S. Low, B.R. Wu, M. Iwamoto, D. Davanzo, Measurement of Base Transit Time and Minority Electron Mobility in GaAsSb-Base InP DHBTs, CS MANTECH Conference, 2014, 353-355.

[26] T. Ishibashi, "Nonequilibrium electron transport in HBTs", IEEE Trans. on Electron Devices, vol. 48, no. 11, pp. 2595-2605, 2001.

ANALYSIS OF SPEED CHARACTERISTICS ON VIDYA PATH CHANDIGARH- A CASE STUDY

[1]Amanpreet Kaur, [2]Bhavneet Singh, [3]Dr. Tripta Goyal
M.E. Student, M.E. Student, Associate Professor
(Department of Civil Engineering, PEC Uni. Of Tech.)
[1]Akaur1991@yahoo.com, [2]somysingh@gmail.com, [3]goyaltripta@yahoo.com

Abstract- Speed is considered as a quality measurement of travel as the drivers and passengers will be concerned more about the speed of the journey than the design aspects of the traffic. It is an important parameter in transportation as it relates to safety, time, comfort, convenience, and economics. Spot speed studies are done to estimate the distribution of speeds of vehicles in a stream of traffic at a particular location. The data collected from the spot speed is to be used for assessing general speed trends and for setting speed limits. This paper presents the analysis of spot speed of the vehicles travelling on the Vidya Path, Chandigarh.

Index terms: spot speed, speed percentiles

I. INTRODUCTION

Speed defines the distance travelled by user in a given time, and this is a vibrant in every traffic movement. The actual speed of traffic flow over a given route may fluctuated widely, as because at each time the volume of traffic varies. A typical unit of speed is kilometers per hour (Kmph). Speed is considered as a quality measurement of travel as the drivers and passengers will be concerned more about the speed of the journey than the design aspects of the traffic. . It is defined as the rate of motion in distance per unit of time. Mathematically speed or velocity v is given by, v = d/t where, v is the speed of the vehicle in m/s, d is distance traveled in m in time t seconds. Speed of different vehicles will vary with respect to time and space.

Spot speed is the instantaneous speed of a vehicle at a specified location. Spot speed can be used to design the geometry of road like horizontal and vertical curves, super elevation etc. Location and size of signs, design of signals, safe speed, and speed zone determination, require the spot speed data. Accident analysis, road maintenance, and congestion are the modern fields of traffic engineer, which uses spot speed data as the basic input. Spot speed can be measured using an endoscope, pressure contact tubes or direct timing procedure or radar speedometer or by time-lapse photographic methods. **(Source: Evaluation of Traffic Characteristics: A Case Study by Arash Moahadkhani Roshandeh)**

A. Study area

Area of study is taken along the Vidya Path in Chandigarh as shown in Fig. 1. The condition of the road is average and there are many potholes and cracks which are clearly visible along the length of the road due to which there is wide fluctuation in the speed adopted by the different vehicles.

Fig. 1

B. Objective of the study

The objective of the study is to analyse the speed characteristics along the study stretch and to determine the speed percentiles, which are useful in designing and regulating the traffic.

II. DATA COLLETION

Various methods of data collection for spot speed are: (1) stopwatch method, (2) radar meter method, or (3) pneumatic road tube method. The data gathered in spot speed studies are used to determine vehicle speed percentiles, which are useful in making many speed-related decisions. Spot speed data have a number of applications which are as:

i. Determining existing traffic operations and evaluation of traffic control devices
   a) Evaluating and determining proper speed limits
   b) Determining the 50th and 85th speed percentiles
   c) Evaluating and determining proper advisory speeds
   d) Establishing the limits of no-passing zones
   e) Determining the proper placements of traffic control signs and markings
   f) Setting appropriate traffic signal timing

ii. Establishing roadway design elements
   a) Evaluating and determining proper intersection sight distance
   b) Evaluating and determining proper passing sight distance
   c) Evaluating and determining proper stopping sight distance

iii. Assessing roadway safety questions
   a) Evaluating and verifying speeding problems
   b) Assessing speed as a contributor to vehicle crashes
   c) Investigating input from the public or other officials

iv. Monitoring traffic speed trends by systematic ongoing speed studies

v. Measuring effectiveness of traffic control devices or traffic programs, including signs and

vi. Markings, traffic operational changes, and speed enforcement programs.

Data was collected manually on the study stretch for 2- wheelers and 4-wheelers using stopwatch method as shown in Table 1 and Table 2. 100 m stretch was taken on the Vidya Path.

Calculation of spot speed by stopwatch method

The stopwatch method can be used to successfully complete a spot speed study using a small sample size taken over a relatively short period of time. The stopwatch method is a quick and inexpensive method for collecting speed data.

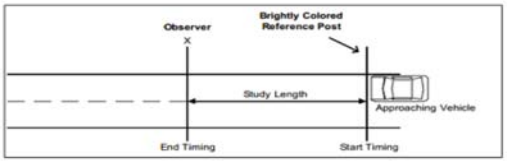

A stopwatch spot speed study includes five key steps:

a) Obtain appropriate study length.
b) Select proper location and layout.
c) Record observations on stopwatch spot speed study data form.
d) Calculate vehicle speeds.
e) Generate frequency distribution table and determine speed percentiles.

III. DATA ANALYSIS

The analysis of the study is very important to achieve the key objectives. After Data Collection, analysis is done. Collected data was compiled in tabular form and the following steps have been taken to analyse the data. Analysis is done in order to find the key parameters which may include Mean speed, 85th Percentile Speed, 98th Percentile Speed, 50th Percentile Speed, Median, Mode, Speed Variance etc. Some values are directly obtained from the data and some can be drawn from the graphs. 50th percentile speed represents the average speed of the traffic stream. The 85th percentile is the speed at which 85% of the observed vehicles are travelling at or below the particular speed. This percentile is used in evaluating/recommending posted speed limits based on the assumption that 85% of the drivers are travelling at a speed they perceive to be safe. The 98th percentile speed is the speed at which 98% of observed vehicles are travelling at or below that particular speed. The 98th percentile is the design speed.

Table 1: Spot speed study for 2-wheelers on Vidya Path Chandigarh

WEATHER:GOOD DATE: 12-NOV-2014 ROAD SURFACE:AVERAGE TIME: 3.00-4.00pm				
SPEED CLASS LIMITS (K.P.H)	MID POINT SPEED (K.P.H)	NO. OF VEHICLES	FREQUENCY %	CUMULATIVE FREQUENCY %
18-23	20.5	3	7.5	7.5
23-28	25.5	4	10	17.5
28-33	30.5	8	20	37.5
33-38	35.5	11	27.5	65
38-43	40.5	0	0	65
43-48	45.5	9	22.5	87.5
48-53	50.5	0	0	87.5
53-58	55.5	0	0	87.5
58-63	60.5	5	12.5	100

Table 2: Spot speed study for 4-wheelers on Vidya Path Chandigarh

WEATHER:GOOD DATE: 12-NOV-2014 ROAD SURFACE:AVERAGE TIME: 3.00-4.00pm				
SPEED CLASS LIMITS (K.P.H)	MID POINT SPEED (K.P.H)	NO. OF VEHICLES	FREQUENCY %	CUMULATIVE FREQUENCY %
18-23	20.5	10	25	25
23-28	25.5	5	12.5	37.5
28-33	30.5	9	22.5	60
33-38	35.5	9	22.5	82.5
38-43	40.5	0	0	82.5
43-48	45.5	4	10	92.5
48-53	50.5	0	0	92.5
53-58	55.5	0	0	92.5
58-63	60.5	3	7.5	100

A. Graphical analysis

The Cumulative percentages calculated for 2-wheelers and 4-wheelers in Table-1 and Table-2 respectively is plotted against the upper limit of the various speed groups as shown in Fig. 2 and Fig. 3. A smooth S-shape curve is obtained which is called the cumulative speed curve.

The vertical axis of the curve indicates the percentage of the number of vehicles travelling at or below the indicated speed.

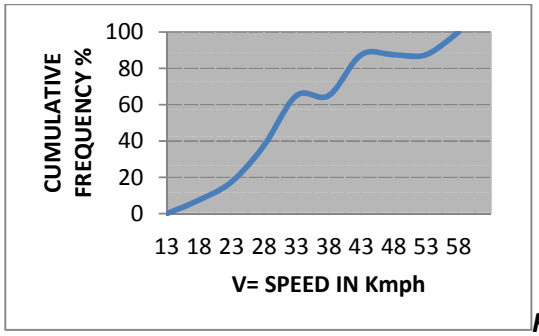

Fig. 2 Cumulative Speed Distribution for 2-wheelers

From graphical analysis, the following results have been obtained for 2-wheelers:

- **15th percentile speed- 22 Kmph**
- **50th percentile speed- 31 Kmph**
- **85th percentile speed-42 Kmph**
- **98th percentile speed-58 Kmph**

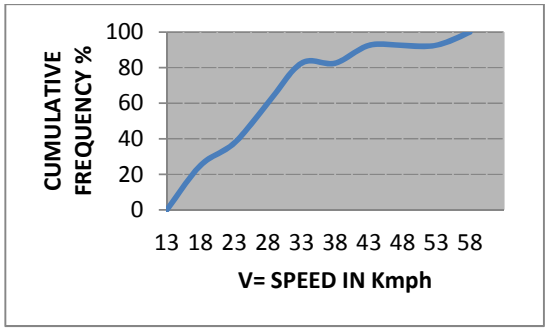

Fig. 3 Cumulative Speed Distribution for 4-wheelers

From above graph, the following results were obtained for 4- wheelers:

- **15th percentile speed- 16 Kmph**
- **50th percentile speed- 26 Kmph**
- **85th percentile speed- 40 Kmph**
- **98th percentile speed- 58 Kmph**

IV. CONCLUSIONS

The following conclusions have been drawn from the study:

1) The maximum speed limit on the road is equal to 58 Kmph for 2-wheelers as well as for 4-wheelers.
2) All the 2-wheelers and 4-wheelers plying on the road moved with a speed ranging between 13-58 Kmph.
3) Maximum 2-wheelers moved with the average speed of 31 Kmph and maximum number of 4-wheelrs moved with an average speed of 26 Kmph.
4) The 85th percentile speed i.e. the critical speed for 2-wheelers is 42 Kmph and for 4-wheelers is 40 Kmph.
5) The 15th percentile speed i.e the minimum speed for 2 wheelers is 22 kmph and for 4- wheelers is 16 Kmph.

REFERENCES

[1] Arash Moradkhani Roshandeh, Mahmood Mahmoodi Nesheli, and Othman Che Puan, “Evaluation of Traffic Characteristics: A Case Study,” International Journal of Recent Trends in Engineering, Vol. 1, No. 6, May 2009.

NUMERICAL INVESTIGATION OF THE EFFECT OF MIXING ON THE PERFORMANCE CHARACTERISTICS OF A MICRO-REACTOR

Pavan N[1], Prashant V D, Tony Sebastian, Ashraf Ali B[2]
Department of Chemical Engineering,
National Institute of Technology Karnataka, Surathkal, India
Email:pavann3008@gmail.com[1], ashrafmchem@gmail.com[2]

Abstract- In this work, we investigate suitable microchannel to carry out reactions and separations. For this, various microchannel geometries are considered such as T, Y and Arrow shaped. Here, the mixing is analyzed at first by sending two fluids having different temperature. The time at which two fluids attain steady state is considered to be the mixing time. This is further verified by sending a liquid mixture with different concentrations. Mixing efficiency is quantified for these microchannels and found Arrow to be the suitable reactor to investigate the progress of reaction. The resulting flow behavior in these system enhances reactions. The mixing was found to be better when the angle formed between inlet and outlet channel is in the range of 90° and -45°.

Index Terms- CFD , Microchannel, Mixing efficiency, Simulation.

INTRODUCTION

Over the past decade, microfluidics has developed at a fast pace. The main driving forces for this research are applications in several emerging technological areas such as chemical synthesis, micro separation processes, nanoparticle synthesis, and polymerization reaction [1]. The main advantage of this system is the increase in surface area to volume ratio with the decrease of the system feature size of micro-devices and some physical phenomena which are insignificant in the macro domain become prominent in the micro domain. Mixing is a transport process for species, temperature, and phases to reduce inhomogeneity. Various studies have been carried out to understand mixing in microchannels [2-7]. The characteristic channel width are of 100 to 500 µm. The channel height is of the order of channel width. In comparison to molecular size scales, the length scale and volume scale of micromixers are very large. This fact leads to two key characteristics of micromixers. Firstly, designing micromixers relies on manipulating the flow using channel geometry or external disturbances. Secondly, while micromixers bring advantages and new features into chemical engineering, molecular level processes such as reaction kinetics remain almost unchanged.

A. Soleymani et.al. [3] carried out numerical and experimental investigations of liquid mixing in T- type micromixers. They considered mainly T-type channels with different geometrical parameters such as aspect ratio, mixing angle and throttle size. Here simulations were performed for different operating conditions. The prediction shows that the development of vortices and it is essential to

achieve good mixing performance. Furthermore, it has been shown that the development and occurrence of vortices strongly depends on flow rate. It was found that with increase in flow rate, the flow pattern changes from stratified to vortex and then to engulfment flow. The mixing efficiency is found to be higher during engulfment flow.

John T. A., and Adeniyi L., [8] investigated on T-shaped channels. The performance of such a channel is analyzed by the RTD.

The performance of mixing in different micro-channel geometries has been further analyzed by K. D. P. Nigam et.al [7]. They used both active and passive mixers. The effect of different geometries (rectangular, circular, and triangular) on friction factor, laminar-to-turbulent transition, and the effect of roughness are analyzed in their study. The differences in the uncharacteristic behavior of the transport mechanisms through micro-channels due to compressibility and rarefaction, relative roughness effects were discussed. The micro-mixers were quantified based on Reynolds number (N_{Re}) and Peclet number (N_{Pe}) and mixing characteristics.

Computational fluid dynamics (CFD) is an important tool for the development of micro-fluidic system. CFD has been used extensively to investigate and understand flow regimes in micro-channels [10-11]. Here, the flow in micro-channel is predicted by Computational Fluid Dynamics (CFD) to find suitable micro-channel to carry out reactions and separations. The micro-channels considered have different mixing angles and it is analyzed by commercial software Ansys Fluent 13. The aim of our article is to analyze and quantify mixing in such microchannels for various N_{Re} using 2D model.

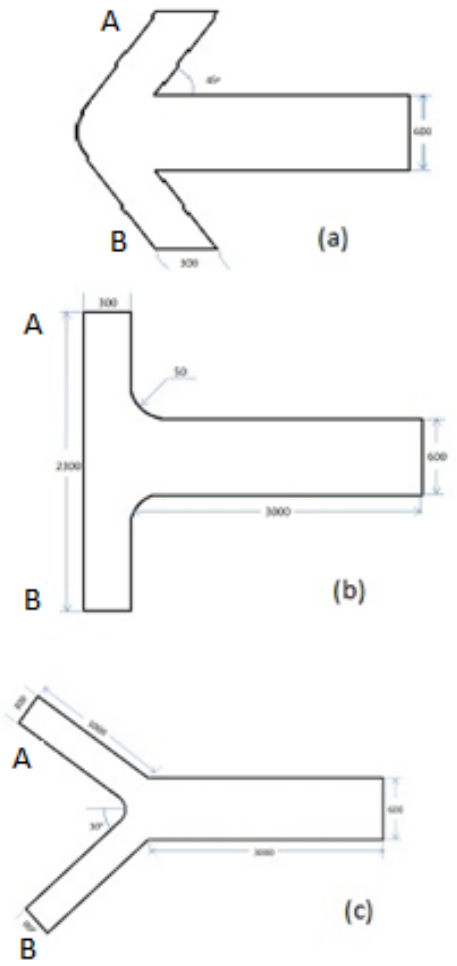

Fig. 1. Schematic representation of (a) Arrow, (b) T and (c) Y-Shaped microchannels. A and B are the inlets. (all dimensions are in mm)

I. CFD Modelling

Newtonian liquid in microchannels can generally be described by Navier-Stroke equation and continuity equation [9].

$$\frac{\partial V}{\partial t} + V.\nabla V = -\frac{1}{\rho}\nabla p + \vartheta\nabla^2 V$$

(1) $\nabla . V = 0$

(2)Where V is the velocity vector, ρ is the density of the fluid, p is pressure and v is kinematic viscosity of the fluid. The species transport on the other hand can be described by diffusion- convection equation.

$$\frac{\partial C}{\partial t} + (V.\nabla)C = D\nabla^2 C$$
(3)

where C and D are concentration and diffusion coefficient of the species, respectively. The energy balance for the system can be described by the energy equation [12].

$$\rho C_p\left(\frac{\partial T}{\partial t} + (V.\nabla)T\right) = k\nabla^2 T$$
(4)

where C_p is the specific heat, k is thermal conductivity coefficient and T is temperature of the fluid.

II. Simulation Methodology

To simulate such micro-channels, no slip boundary condition was imposed on the walls of the microchannel and a gauge pressure of zero was considered at the outlet of the channels. A uniform velocity profile was specified by setting the desired mass flow rate at the inlet zones.

The CFD results may depend strongly on the employed mesh. In order to check grid independency three different meshes employing roughly (i) 312, (ii) 25177 and (iii) 100850 grid cells, revealing that the intermediate one is sufficient to describe hydrodynamics with a good accuracy. It has therefore been retained (10^{-5} m) for all the further simulations.

Second order upwind discretization is adopted in the CFD together with the SIMPLE algorithm for pressure-velocity coupling. A typical CFD simulation requires roughly 2 days of computing time on a standalone desktop PC (2 GB RAM, 32 bit, Pentium IV processor). Here transient simulations were performed with a time step of 10^{-4} s for integration. The simulation are carried out for the flow time of 1 sec, the system usually attained steady state at 0.16 sec.

III. Results and Discussions

A. Heat transport in liquid phase

To investigate the flow field in such microchannels, calculated fields of the major flow variable are first discussed. Figure 2 shows contours of velocity magnitude predicted by CFD for N_{Re} of 180. Here velocity magnitude is maximum at the center of the microchannel as expected. dead zones are present in Arrow and T shaped microchannel when comapred to Y shaped microchannel.

To analyze the performance of micro-channel, hot water (360 K) is passed through one inlet (A) and cold water (300 K) through another inlet (B). The physical properties of water considered are shown in Table 1.

Property	**Value (SI units)**
Density (ρ_w)	998.2 kg/ m^3
Viscosity (μ_w)	1.003e -3 kg/m s
Thermal Conductivity (k_w)	0.6 w/m K
Specific Heat Capacity (C_{pw})	4182 J/kg K

Table 1. Physical properties of water considered.

To understand mixing in such microchannel, variation of temperature in the microchannel is analyzed. Here the time at which two liquids attain steady state is considered to be the mixing time. To analyze quantitatively, the spatial variation of temperature at two cross sections along x=1000E^{-6} m and 2000E^{-6} m are studied. For N_{Re} of 180 as shown in Figure 3, it is observed that there is no significant change in temperature across the channel as temperature between the two inlet of the microchannel is very small.

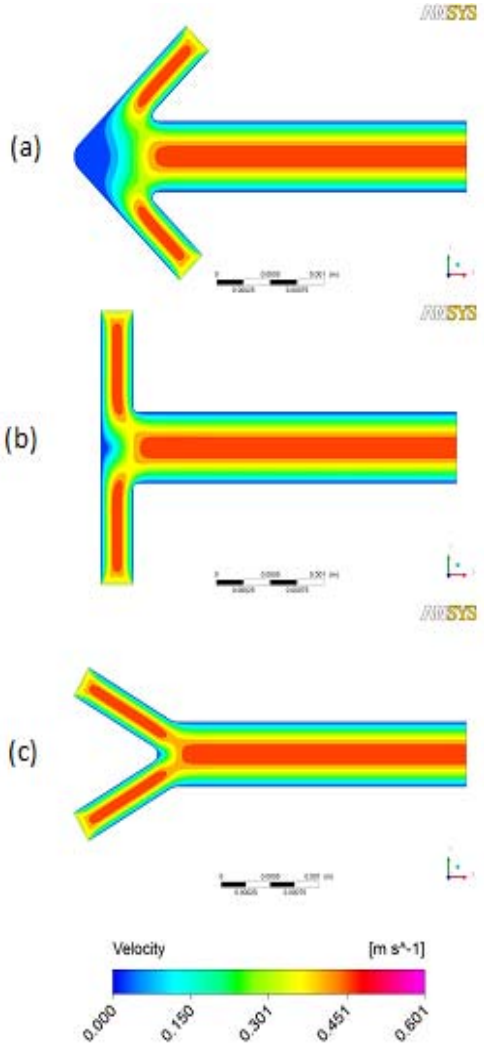

Fig. 2. Comparison of velocity contours for various geometries of micro-channels (a) Arrow (b) T and (c) Y-Shape.

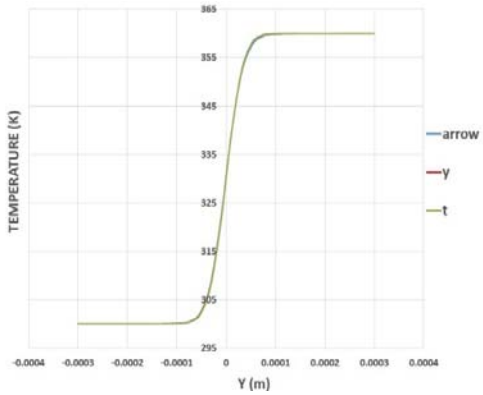

Fig. 3. Spatial variation of Temperature along X = 1000eE^{-6} m in the microchannels.

B. Species transport in gas phase

To find suitable microchannel, further nitrogen and oxygen gases are admitted as into the microchannel. Through inlet A, 0.2 and 0.8 mole fraction of oxygen and nitrogen, respectively are passed and through inlet B inversed mole fractions as that through inlet A is passed. The physical properties of the mixture are as shown in Table 2.

Transport properties	Value (SI units)
Density (ρ_g)	1.225 kg/ m^3
Viscosity (μ_g)	1.72E $^{-5}$ kg/m s
Diffusion Coefficient (D)	2.88E^{-5} m^2/s

Table 2. Physical property of gaseous mixture considered.

The spatial variation of concentration of the oxygen at 1000E-6 m and 2000E^{-6} m is analyzed for the microchannels as shown in Figure 4. It is observed that no significant variation was present even when the concentration gradients at inlets were kept large. Observations made can be explained by strong molecular diffusion over the convective transport at this Reynolds number.

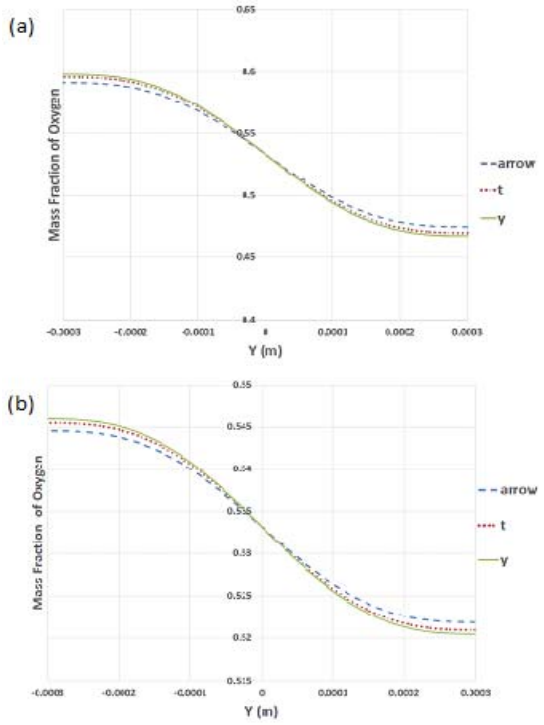

Fig. 4. Spatial **v**ariation of concentration at (a) $1000E^{-6}$ m and (b) $2000E^{-6}$ m in the micorchannels.

C. Species transport in liquid phase

The liquid phase species transport system is considered further to investigate the performance of micro-channel. Here, the inputs A and B have the same properties as that of water but are treated as two different liquids with a diffusion coefficient of $2E^{-7}$ m^2/s. In order to quantify the extent of mixing at a certain distance along the mixing length, mixing efficiency α is defined by

$$\alpha = 1 - \sqrt{\frac{\sigma^2}{\sigma^2_{max}}} \qquad (5)$$

Where σ^2 is variance of concentration and σ^2_{max} is the maximum variance of concentration present in the mixture. Here α=1 for perfect mixing and α=0 for no mixing in the micro channel.

The previous simulations had a strong influence of molecular diffusion and hence the diffusion coefficient of the system was set to $2.0E^{-7}$ m^2/s. The simulations are performed for various N_{Re} starting from 24 to 360. The mixing efficiency α is calculated at two cross sections, one at a distance of $1000E^{-6}$ m and another at $2000E^{-6}$ m as seen in Figure 1. The calculated values are shown in Table 3 and Table 4.

Reynolds Number, N_{Re}	Microchannels		
	T-Shaped	Y-Shaped	Arrow-Shaped
24	11.21	10.86	13.24
30	9.74	9.45	11.45
60	6.37	6.19	7.46
90	4.97	4.84	5.83
120	4.16	4.08	4.90
180	3.23	3.21	3.84
240	2.70	2.71	3.23
300	2.35	2.38	2.83
360	2.09	2.15	2.55

Table 3. Percentage of Mixing Efficiency for various Reynolds numbers for considered geometries at a cross sectional distance of $1000E^{-6}$ m.

Reynolds Number, N_{Re}	Microchannels		
	T-Shaped	Y-Shaped	Arrow-Shaped
24	17.40	17.08	19.38
30	14.83	14.57	16.41
60	9.48	9.34	10.37
90	7.39	7.30	8.08
120	6.20	6.14	6.79
180	4.84	4.82	5.32
240	4.06	4.07	4.48
300	3.54	3.56	3.92
360	3.16	3.20	3.52

Table 4. Percentage of Mixing Efficiency for various Reynolds numbers for considered geometries at a cross sectional distance of $2000E^{-6}$ m.

It is observed that the arrow shaped channel has a better mixing efficiency due to larger dead space as observed in figure 2. In all the cases mixing efficiency (α) has been found to decrease with increase in Reynolds number in all the channels. This is due to the dominance of diffusive effect over convective. These results are concordant with the previous researcher's [3] results.

IV. SUMMARY AND CONCLUSION

Mixing in micro-channels has been investigated quantitatively for various micro-channel using CFD and an approximated 2D model. To carry out this, two fluids with different temperatures are admitted through the inlets of such channels. Here, spatial variation of temperature along the line is considered for investigation. The observations made were inconclusive to decide on the best microchannel due to the strong influence of molecular diffusion.

This is further verified by sending two liquid having different concentration. The system was also influenced greatly by molecular diffusion.

For better understanding of the system, two materials with low diffusion coefficient are considered. On simulating this system and quantifying the mixing, it was observed that arrow shaped channel was better than the other considered channels. Here, Reynolds number was varied from 24 to 360. The residence time decreases as velocity is increases and hence mixing efficiency decreases. These observations were observed in 3D models also; hence making the approximation of microchannels to 2D models is valid.

REFERENCES

[1] Burns, J. R. and Ramshaw C., (1999), "Development of microreactor for chemical production". Chem. Eng. Res. Des. , 77, 206.

[2] Auro A. S. and Sushanta K. M., (2008) "Modelling and Simulation of Microscale Flows", Modelling and Simulation, Giuseppe Petrone and Giuliano Cammarata (Ed.), InTech, 283-316.

[3] A. Soleymani, E. Kolehmainen, I. Turunen, (2008) "Numerical and experimental investigations of liquid mixing in T- type micromixers", Chem. Eng. Journal, 135S, S219-S228.

[4] Chiara G., Mina R., Elisabetta B., and Roberto M., (2012) "Effect of inlet conditions on the engulfment pattern in a T-shaped micro mixer", Chem. Eng. Journal, 185-186, 300-313.

[5] Engler, M., Kockmann, N., Kiefer T., and Woias, P.(2004), "Numerical and experimental investigations on liquid-liquid mixing in static micromixer". Chem. Eng. J., 101, 315.

[6] Joelle A., Montse F., VladimirJ., (2010), "Current methods of characterizing mixing and flow in microchannels", Chem. Eng. Sc., 65, 2065-2093.

[7] V. Kumar, M. Paraschivoiu, K.D.P. Nigam, (2011) "Single-phase fluid flow and mixing in microchannels", Chem. Eng. Sci., 66, 1329–1373.

[8] John T.A., Adeniyi.L., (2009), "Numerical and experimental studies of mixing characteristics in a T- junction microchannel using residence-time distribution ", Chem. Eng. Sc., 64, 2422-2432.

[9] Nam. T.N., (2008), "Micromixers: fundamentals, design and fabrication ", William Andrew Inc., USA.

[10] Siva Kumar R. C., Sreenath K., and S. Pushpavanam, (2010), "Experimental and Numerical Investigations of Two-Phase (Liquid-Liquid) Flow Behavior in Rectangular Microchannels", Ind. Eng. Chem. Res., 49, 893-899.

[11] Siva Kumar R. C., Sreenath K., and S. Pushpavanam, (2009), "Screening, Selecting, and Designing Microreactors", Ind. Eng. Res., 48, 8678-8684.

[12] Bird R.B., Stewart W.E. and Lightfoot E.N., (2004), "Transport Phenomena", John Wiley, Singapore (2nd edition).

COMPARATIVE STUDY OF THERMAL PERFORMANCE OF INSULATED LIGHT ROOFS IN TROPICAL CLIMATE

M.Ponni[1], Dr.R.Baskar[2]

[1] Research scholar, Department of Civil & Structural Engineering, Annamalai University, Chidambaram-608 001, Tamil Nadu, India.

[2]Associate Professor, Department of Civil & Structural Engineering, Annamalai University, Chidambaram-608 001, Tamil Nadu, India.

[1]E- mail: ponnim_cdm@yahoo.co.in, [2]E-mail: rajarambaskar@rediffmail.com,

Abstract: Thermal performance of a building depends on many factors. It is associated with solar insolation, the type of roof, type of wall, orientation, colour of paint given to the walls, and the motion of Earth around the sun. The building elements, roof and wall play an important role in the thermal reception from the solar insolation. Residential buildings consume more energy for heating and cooling. A residential building should not be a mere shadow maker. It should be a less energy consumer. It should provide a good thermal experience. To reach this aim the indoor environment should be feasible. The indoor environment depends on the indoor temperature and the indoor relative humidity. If the indoor temperature increases then the relative humidity will be decreased. Now the occupants feel thermal discomfort. So control over the indoor temperature is a must. The quantity of heat entering the inside the building can be modified through Roof and wall insulation. In this study, to get a better thermal performance roof insulation is alone considered. Two side by side modules of the same size and orientation were constructed with different insulated roofs. The construction of walls and floor are having the same dimension. Polyurethane readymade panels are used as roof material in one of the modules and named as PUD module. The polyurethane panel is an industrial product. The other module is provided with a newly designed roof called Double Decker (DOD). Both the roofs are having intermediate insulation. Thermal performance of the newly designed roof is better than the industrial product in the summer peak hours. The cost of the DOD is relatively less. The study has been carried out from September 2013 to August 2014, in the tropical climate.

Key words: DOD, Indoor temperature, PUD, Relative humidity, Thermal comfort, Thermal performance.

I. INTRODUCTION

Energy consumption in buildings is also increasing at an unprecedented rate, as more and more buildings are designed in lightweight materials like Galvanized sheets, Asbestos sheets, glass and aluminium giving little importance to the passive methods of heat control and human adaptation to comfort. It is well known now that buildings with poor adaptive opportunities often produce

intolerable indoor conditions within, and consume high energy.

In the residential buildings, indoor thermal discomfort has been very challenging and it depends on, one or more of the materials used either as ceiling or wall or making doors or roofing support or combination of all. The ceiling materials are made by different materials with different thermal conductivity, thermal absorptivity, thermal diffusivity and thermal resistivity. Heat propagated into indoor space is partly through ceiling and partly through walls by the process of conduction, convection and radiation. Shortage of conventional energy source and enhancing energy cost has caused the re-examination of the general design practice Hence, the major focus of researchers, policy makers, environmentalists and building architects has been on the conservation of energy in buildings. Energy efficiency in buildings can be achieved through a multipronged approach involving adoption of bioclimatic architectural principles responsive to the climate. Use of materials with low embodied energy and effective utilization of renewable energy sources should be carried out to power the building. Studies of various countries have shown that buildings with wooden structures require less energy and emit less CO2 during their life cycle than buildings with other type of structures.

The energy efficient roofs so far designed costs too high, and they do not reach the common. Most of the heat developed by the solar radiation in the roof and wall is transferred into the occupant zone. The sun is the primary source of thermal energy. Roof receives the solar radiation directly from the sun light and it becomes a secondary source of heat. The east wall receives heat directly up to the noon and the west wall receives heat directly after the noon. The two walls also becomes the secondary source of heat. The floor of a building does not heated directly by the sun light in most of the buildings. The roof and walls become secondary heat sources. As soon as the roof and walls emit heat radiations into the building, the heat is transferred to the indoor air. Regarding light roofs the indoor temperature of a building closely follows the outdoor temperature.

II. BACK GROUND OF THE STUDY

The Tropics is regarded as a region where the human evolved and comfort has been often taken for granted, built environments are increasingly becoming issues of public concern. The tropical outdoor environment has been regarded as important as indoors in the life of the populace. This tendency has put increased demand on the comfort requirements in the design of buildings. Comfortable outdoor spaces have a significant bearing on the comfort perception of the indoor ambience. The demand for comfort conditions in buildings are significantly increased as a result of exposure to uncomfortable outdoors [1]. Generally the tropical zone is defined as the area of land and water between the Tropic of Cancer (latitude 23.5^{o} N) and the Tropic of Capricorn (latitude 23.5^{o}S).Occupying approximately 40% of the land surface of the earth, the tropics are the home to almost half of the world's population. There are variations in climate within the tropic. However 90% of the tropical zones embody hot and humid climatic regions, whether permanent or seasonal. The remaining 10% is desert like, and characterized as hot and dry climate [2].

The higher thermal resistance systems containing bulk insulation within the timber frame, the measured result for a typical installation was as low as 50% of the thermal resistance determined considering two dimensional thermal bridging using the parallel path method. This result was attributed to three dimensional heat flow and insulation installation defects, resulting from the design and construction method used. Translating these results to a typical house with a 200 m2 floor area, the overall thermal resistance of the roof was at least 23% lower than the overall calculated thermal resistance including two dimensional thermal bridging [3]. Providing

insulation for walls and roof in a building increases their thermal resistance and limits conductive heat flow through the building envelope. The building envelope insulation is a main component because it plays a major function in the energy consumption. The building's roof, windows, walls and floors lead the flow of energy between the indoor and the outdoor of the building. The envelope insulation is very important, and it is the best solution in order to have an efficient and less consuming energy building. [4].

Thermal insulation has a dual nature. It decreases daytime the extra heat that come to a building, but prevents the building from cooling down at night. Based on their study, this dual nature makes insulation inappropriate for buildings with natural climate control. Perhaps the solution is to first define the cooling load at the design phase and then making decision whether this cooling load would be decreased by applying thermal insulation in the building or by using passive means of control [5]. Many studies have also quantified the energy savings from improved insulation. Retrofitting exterior masonry wall insulation from R-3 to R-13, energy consumption reduces by 9 -15% in Arizona [6].

Requirements for energy efficiency in a building envelope surrounding the heated and cooled parts of the building is generally set based on resistance or contribution to heat transparency through a unit of the construction, respectively R-value or U-value. [7]. A study of a typical un-insulated masonry house in the hot and humid climate of Bangkok, Thailand indicated 3-4% annual energy savings from light-weight walls with R-11 batt insulation and from cement tile roof with R-11 batt insulation [8]. A study of a house in Bangkok showed 8% of total energy reduction from light-weight concrete block walls with R-10 exterior insulation, and 9% reduction from similar wall construction with R-10 interior insulation [9]. Wall insulation does not significantly affect reducing heating and cooling load in buildings. He stated that adding 50 mm of polystyrene as wall insulation only causes in 1.7 % 33 [10]. Structural control of a modern building are its main parts such as walls, roof, floors and glazed materials (glass) in openings. The ability of a building enclosing elements to conduct heat from one side of the wall to the other is the thermal transmittance denoted as U value for the element [11].

Mineral wool, also known as rock wool, is an insulation material produced from steel slag. The slag, a by-product of steel manufacturing containing of dirt and limestone, is combined with other chemicals, heated and turned into a fibrous material that is a good insulator. It defined as a permanent insulation because it does not rot; burn or melt, and it does not absorb moisture, and does not maintain mould or mildew. It is available in batts or as a loose-fill product that can be blown into walls and ceilings. It can also be installed between wall studs by using a mesh screen across one side of the studs, letting floor to ceiling filling with a technique virtually the same as with blown-in cellulose. Because of its greater density and water resistant properties, mineral wool performs as a vapour barrier and, unlike fiberglass, does not need an additional vapour barrier to be effective (ORNL 2002) [12].

The major importance of good insulation of the roof in tropical climate is thickness and colour of insulation. In general, 5cm insulation is being used for red and blue tiled roofs, which is inadequate. Therefore, insulation thickness needs to be at least 8cm (the value for medium colours) and to use polystyrene as insulation rather than mineral wool. Mineral wool is fairly cheap but not very well adapted to tropical climates: it loses its thermal properties when it absorbs ambient humidity. In another experiment more than 3˚C have been observed between a dwelling with a well- insulated roof and with no insulation [13].

III. RESEARCH DESCRIPTION

The earlier research efforts have investigated the thermal performance of various roofing systems. In this study an attempt has been made to quantify the influence of insulation on indoor ambient

temperature. The two modules have same floor, wall area and orientation. The size of the module is 3mx 3m x 3m. The galvanized sheets used in the modules have the same thickness of 0.21 mm. The walls have a thickness of 230 mm made up of brick and cement mortar. Two angles are used as purlins. It is a low sloped roof and is maintained to be 2˚. Walls of the modules are white washed and the flooring is done with cement mortar.

First Module (PUD):

The first module was constructed with Polyurethane panels of length 3660 mm and breadth 1000 mm is used as roof, which is an industrial product. The thickness of the Poly Urethane Decker is 35 mm and the thickness of the sheets is 0.35 mm. The white painted panels reflects the solar radiation on one hand and on the other hand polyurethane prevents heat entering the inside of the building.

Second Module (DOD):

The roof of the second module was newly designed. The design was carried out in four steps. In the first step, first roof was made using galvanised sheets. In the second step wooden reapers of size 3000 mm X 50 mm X 25 mm were arranged over the roof. The spacing between the reapers is 200 mm. In the third step packed mineral wool roll was spread. Thickness of the mineral wool is 50 mm. In the fourth step galvanized sheets were set over it as second roof. The two roofs are separated by 100 mm to 122 mm. Since light roofing system have two light roofs enclosing the wooden reaper and mineral wool, it was named as Double Decker. Since the sheets are trapezoidal, air gap of 11 mm above and below the mineral wool pack and wooden reapers is formed. The air vents created are the passage for the air and takes away the heat produced between the galvanized sheet and the mineral wool bed. Likewise the air vents created between the lower roof sheet, the wooden reaper and the mineral wool bed is also drains away the heat produced by convection. The mineral wool, wooden reapers and the air enclosed in the gaps are serving as insulators. This assembly possesses three insulators wooden reapers, mineral wool and air gap. Mineral wool has a low thermal conductivity among the building materials used (K= 0.04 W/m K).

Fig.1 Mineral Wool

Fig.2 Double Decker

Fig.3 Polyurethane Decker

IV. EXPERIMENTAL PROCEDURE

The experiments were carried out in Chidambaram, Tamil Nadu, 11˚24´N latitude and longitude 79˚44´E.The location is characterized by hot and humid weather. The modules, used in this study are exactly identical in terms of their geometry, orientation, area and climate conditions. DOD and PUD are reflective roof material. All the modules are fully instrumented. To measure the Indoor Ambient Temperature and Relative Humidity Single channel data logger is used. In six hours

interval (6, 12, 18hr) the roof, wall and floor temperatures are measured by means of Infra-Red Thermometer. Roof, wall, floor and indoor and outdoor ambient temperature and relative humidity field data have been catalogued for eleven months for two different insulated roofing systems exposed to weathering on an indoor and outdoor test facility. The data are plotted for the time period between September 2013 and August.2014.

V. RESULT AND ANALYSIS

Fig.4 shows the Mean Monthly indoor ambient temperature by 6 hours for the observation period. This figure shows that the indoor ambient temperature of the DOD module is higher than the PUD module from September to March 2014. After March to July the indoor ambient temperature of DOD module is lesser than the PUD module. But the variation of indoor temperature between the two modules during the months of September to March is 0.44.the variation during the months between March to July is 0.2 to 0.4˚C. The indoor temperature decreases from September to December.2014 and then increases to a maximum during the summer months of June and July.2014.

Fig.5 shows the Mean Monthly indoor ambient temperature by 12 hours for the observation period. This figure shows that the indoor ambient temperature of the DOD module is lesser than the PUD module from September to July 2014. But the variation of indoor temperature between the two modules during the months of September to July is from 0.4 to 1˚C.

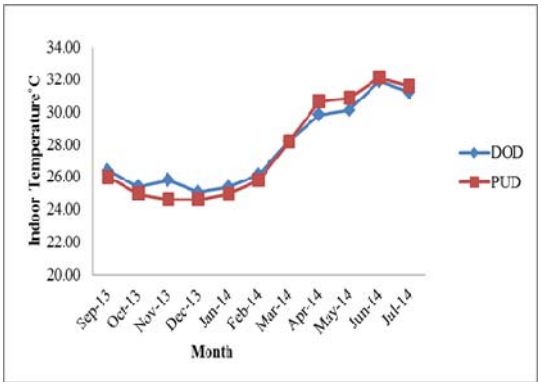

Fig.4 Mean Monthly indoor ambient temperature by 6 hours

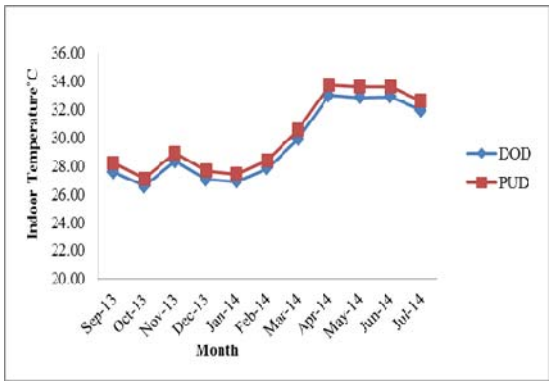

Fig.5 Mean Monthly indoor ambient temperature by 12 hours

Fig.6. shows the indoor ambient temperature of the modules by 18 hours. The variation of the temperature is alike as the 6 hours temperature performance.

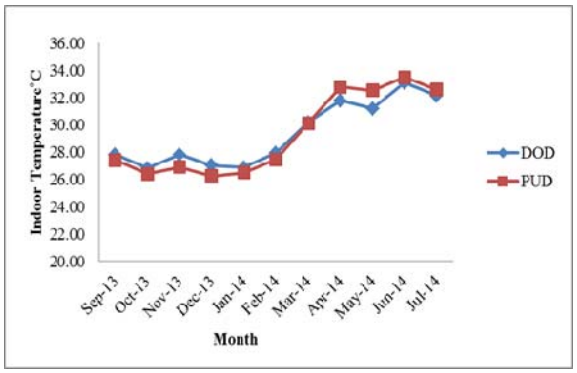

Fig.6. Mean Monthly indoor ambient temperature by18 hours

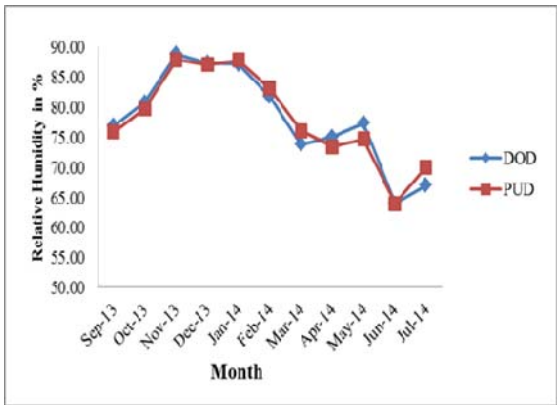

Fig.7 Indoor Relative humidity of the two modules by 6 hours

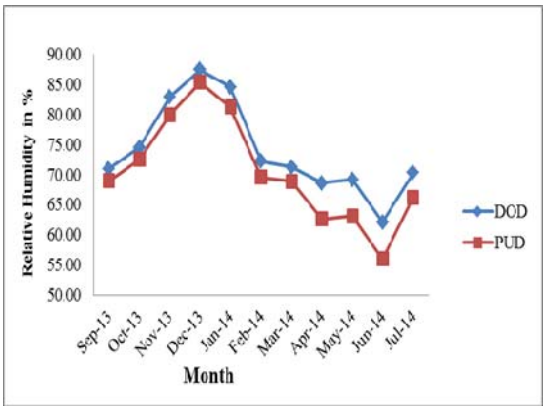

Fig.8 Indoor Relative humidity of the two modules by 12 hours

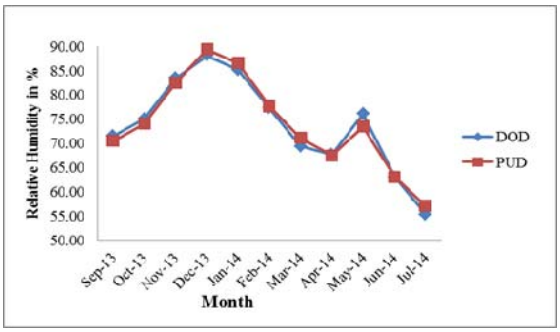

Fig.9. Indoor Relative humidity of the two modules by 18 hours

Fig.7 & 9 shows the Indoor Relative humidity of the two modules by 6 hour and 18 hour during the monitoring period. Relative humidity during these periods is showing a little difference. Measurement during 12 hours Fig.8 shows an obvious difference. The relative humidity increases from September and reaches a maximum in December and then deceases up to June. From June to July there is an increase. During the winter months DOD module attains a maximum of 87.5% and the PUD module attains a maximum of 85.5%. During the summer months the PUD module reaches minimum of 56% and the DOD reaches a minimum of 62%. The variation in the relative humidity is appreciable.

VI. CONCLUSION

In this Study two insulated roofs have been engaged. Insulated roofs are highly effective in reducing the indoor temperature. The PUD and DOD module performs well. The DOD performs in a better way than the PUD module during the summer months. The indoor temperature of DOD is 7 - 9 ˚C lesser than the outdoor temperature. The indoor relative humidity is appreciable during the summer months in the insulated roofs. The DOD has a higher relative humidity of 6% than PUD during summer. The cost of PUD roof per square meter is Rs.1500/- Whereas the cost of DOD roof per square meter is Rs. 1000/- Hence the newly designed roof is comparatively less cost. Regarding the thermal performance and cost effectiveness the DOD roof is superior to the other one.

REFERENCE

[1] Ahmed, KS. (2003). Comfort in urban spaces: defining the boundaries, of outdoor thermal comfort for the tropical urban environments. Energy Build. 35:103–110.

[2] Baish, M.A. "Special Problems of Preservation in the Tropics," Conservation Administration News 31 (Oct. 1987): 4-5

[3] Belusko M, Bruno F, Saman W. Investigation of the thermal resistance of timber attic spaces with reflective foil and bulk insulation, heat flow up. Appl Energy 2011; 88:127–137.

[4] Taylor B.J and Imbabi M.S , The application of dynamic insulation in buildings, Renewable Energy, 1998, pp. 377-382.

[5] Gut, P. & Ackerknecht, D. 1993. Climate Responsive Building: Appropriate Building Construction in Tropical and Subtropical Regions. Switzerland: SKAT.

[6] Ternes, M.P., K.E. Wilkes and A. McLain. 1994. Cooling Benefits from Exterior Masonry Wall Insulation. Home Energy Magazine 11(2): 33-35.

[7] B. Yesilata, P. Turgut, A simple dynamic measurement technique for comparing thermal insulation performances of anisotropic building materials, Energy and Buildings 39 (2007) 1027–1034.

[8] Chulsukon, P. 2002. Development and Analysis of a Sustainable, Low Energy House in a Hot and Humid Climate. Ph.D. Dissertation. College Station, TX: Texas A&M University.

[9] Rasisuttha, S. and J. Haberl. 2004. The Development of Improved Energy Efficient Housing for Thailand Utilizing Renewable Energy Technology. Presented at SimBuild 2004, First National Conference of IBPSA-USA. Boulder, CO.

[10] Tham, K.W. 1993. Conserving Energy without Sacrificing Thermal Comfort. Building and Environment, 28 (3): 287-299.

[11] Madueke, A.A.L and Opoko, A.P. (1998): Thermal Response to outside at Temperature and Solar radiation of a NBRRI Model house with a flat roof in Kano, Nigeria J. Physics Vol. 10, 108-113.

[12] ORNL. 2002. DOE Insulation Fact Sheet. DOE/CE-0180/ with Addendum 1. Oak Ridge, TN: Oak Ridge National Laboratory.

[13] F. Garde, L. Adelard, H. Boyer, C. Rat, Implementations and experimental survey of passive design specifications used in new low-cost housing under tropical climates, Energy and Buildings 36 (2004) 353–366.

GENERATION OF INDIAN LIGHT MUSIC USING AUDIO PROGRAMMING LANGUAGE

[1]Chidambara Kalamanji
[1]Professor, Department Of Computer Science & Engineering, PES Institute Of Technology, Bangalore- India
[1]chidambara@pes.edu

Abstract : This paper is related to the application of technology for art specifically for Indian music. It is a proven fact that computers are extensively used in the life cycle of music namely music creation, generation, recording, performance and analysis. Traditional way of creation and generation of music making use of skilled artists is being replaced, in recent years, by computer assisted approach. Many software tools are available for music composition, generation. One of the latest potential technologies is to use Audio Programming languages to compose, generate and perform music. Interestingly this technology helps to achieve three things namely (EEE) Enrich the listener's experience, Empower & Enhance the creativity of the musicians. These languages are widely used in Western & European countries. But it is yet to be innovatively explored for Indian music since there are certain challenges have to be addressed. This paper shares the Engineering approach of creating Indian light music, experimented using the audio programming language namely ChucK. Three sample music compositions are presented as a proof of how an amateur musician could be empowered to create Indian music with the help of technology. Objective of presenting this work is to invite the interested researchers to join hands with the author to explore many possibilities to 'add value' to Indian music.

Index Terms—Audio programming, ChucK, Indian light music, Melody matrix, Percussion matrix

MOTIVATION:

Music is a divine art accepted by every human being in the world. I'm an Electronic Engineer, technologist and also an amateur music composer involved in Indian light music. With in me, there has been a **dialogue**, consistently from my young age, **between the Engineer and musician**. Musician is looking for solutions for certain problems and Engineer is passionate about solving musician's problems. Many ideas, rather wish list, used to spark with in me to blend technology for music art.

"Music world is giving me so much; In turn, what can I, as technologist, give back" was the urge to enter in to the exciting domain called **CompuMusic** – (Computer for Music). I was happy to know that there is a music technology community worldwide both in academics and industry contributing lot in terms of research and development. As a result, a spectrum of computer based products, tools based on variety of technologies have been developed. Musicians are utilizing these products mostly in the Western and European countries. **Motivation for me has been to apply and adapt these technologies for Indian light music. The work presented through this paper is just a humble beginning in this direction.**

INTRODUCTION

There are two aspects in the present work.

1.Music

2.Technology.

Let me give a brief overview of the musical aspects first.

MUSIC CREATION METHODS (Fig.2).

Basically, music is the combination of human voice and instruments**.** Musical instruments are of two types -melody instruments and percussion instruments. If stage performance by actual singing, playing real traditional instruments is ***one face of the coin***, recording the music in variety of storage devices and playing using computers, MP3 players and other gadgets is ***the other face.***

We may classify music creation / generation process in to Real and Virtual. **Real music** is the music created by singing and actually playing **real instruments.** Other method which is quite widely used especially in commercial entertainment music sector is to use technology. Technological approach is nothing but making use of computers and **electronically synthesized** music using **virtual instruments** which may be called as **virtual music.**

Computer based music or **CompuMusic** can be classified as :

1. Make use of software tools called **Record Edit Sequence** tools. More than 20 software tools like audacity, Protool, Cubase are used typically in recording studios by music composers and arrangers.
2. Recent technology which is the topic of discussion in this paper is to use Computer Programming Language specifically called as **Audio Programming Language.**

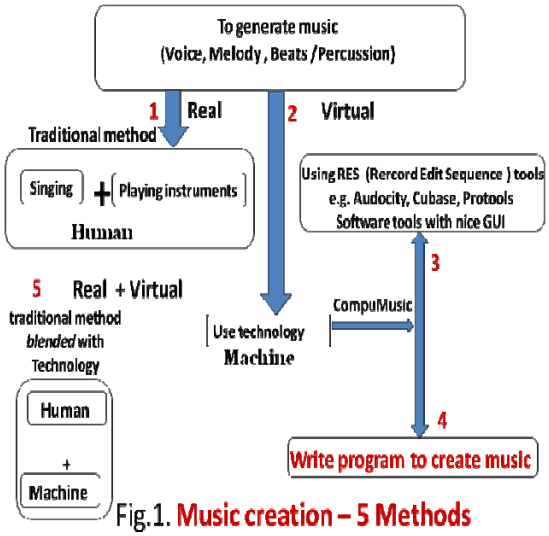

Fig.1. Music creation – 5 Methods

WHAT IS INDIAN LIGHT MUSIC?

Thousands of **genres** are used worldwide in different contexts. A **music genre** is a conventional category that identifies pieces of **music** as belonging to a shared tradition or set of conventions. In India main genres of music are **classical, semi classical, light, folk and popular(like movie music)** In classical music there two types namely **Hindustani and Carnatic.**

The basic concepts of classical music includes

- *shruti* (microtones),
- *swara* (notes),
- *alankar* (ornamentations),
- *raga* (melodies improvised from basic grammars),

  and
- *tala* (rhythmic patterns used in percussion).

Classical music follows strict rules, grammar and aesthetics in terms of conforming to raga and tala.

But in light music, anything pleasant to hear and suiting the occasion is accepted. It doesn't impose strict rules to conform to a raga, tala

and rendering. **However implicitly or explicitly Indian light music is a kind of derivative of classical music. Music composition is based on a raga, but with lots of flexibility and freedom.**

Mostly in the recorded music domain, music creation cycle goes through the following steps**(Fig.2)** :

1.Write lyric.
2.Compose basic tune.
3.Arrange instrumental music.
4. Perform.
5.Record.

Ultimately it reaches the listener either directly or through recorded media.

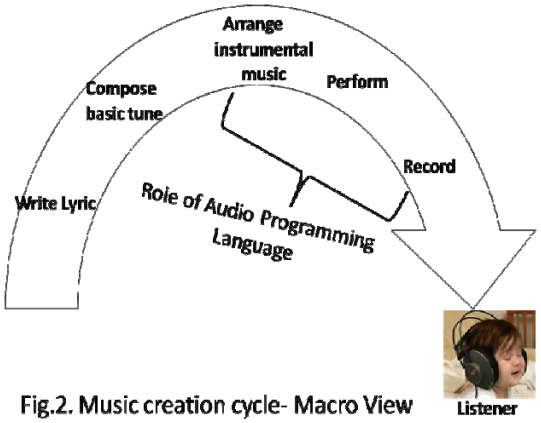

Fig.2. Music creation cycle- Macro View

Typically Audio programming languages have a role compose, arrange instrumental music, and even during performance.

Building blocks of computer generated music [Fig.3]

As shown in Fig.3, typical recorded music is a combination of multiple tracks namely:

a) Voice b) Instrument *c) Special effects*

Instrument track is comprises

a) Melody track
b) Beats/Percussion track.
c) Chord track

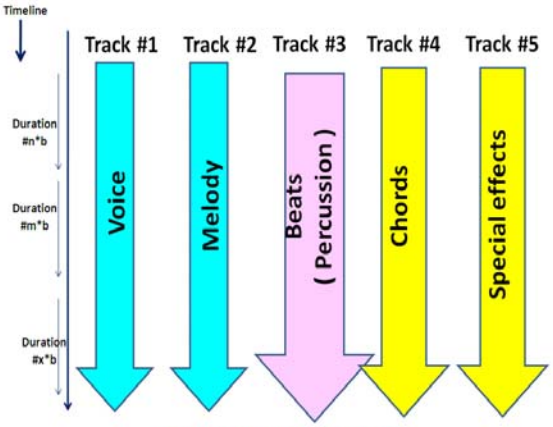

Fig.3 Music design process

Our work focuses only on creating instrument track, since voice track is created through actual singing by the artists.

Main step is to create a **'blue print'** of the final music which is called as **'Score sheet'** in western music terminology.

As shown in Fig… the score sheet represents the flow of all the three tracks on a timeline.

Melody track includes music created using one or more real or virtual instruments like Mandolin, Flute, Guitar, Violin etc.,

Beats/Percussion track includes music created using one or more real or virtual instruments like Tabala, Mridangam, Ghatam, Drums etc.,

Chord track is a special melody track that includes harmonic set of three or more notes of an instrument like Guitar, that is heard as if sounding simultaneously.

Of course, it is not mandatory to have all the tracks; depends on the context and composer's ideas.

PROCESS OF COMPUTER MUSIC GENERATION [FIG.4]

Computer music generation follows a structured way in three phases:

1. Design (Composition)
2. Engineering
3. Implementation (realization of engineered music)

It may be noted that as a novice, when I started music generation projects, I didn't follow any structured approach. It was a random and iterative approach of course with intuition. After completing couple of projects, I realized that real good music can be generated by properly following these 3 phases.

Music design (can also be called as composition) involves basic tuning of the main melody instruments and deciding what **timbre** of instruments to be used (string, reed, blow, bowing…). Same thing applies to percussion instruments; Composer may decide whether to use Indian classical instruments like Tabla, Mridangam or folk style instruments like Dholak, khanjira or western instruments like drums, snare, hihat etc.,

Music design is a creative work manually done by the composer. As in any art form, intuition, imagination and visualization are the natural elements of design.

Music engineering is to decide the specific musical instrument to be used. **Obviously music engineering has to be done based on music design.** For example, if the result of music design is **string instrument,** music engineering decides whether it should be **sitar, guitar, mandolin or veena.**

Output of the Music design and engineering is a score sheet as shown in Fig.5. Score sheet is a kind of 'blue print'. Score sheet comprises :

a) Multiple melody tracks, each based on a specific melody instrument. Each melody track is characterized by what is known as **Melody Matrix** (explained in subsequent sections).

b) Multiple beats (percussion) tracks, each based on a specific percussion instrument. Each track is characterized by what is known as **Percussion Matrix** (explained in subsequent sections)

Music composition is done manually and music generation is done by writing and executing computer program using the **object oriented programming language called ChucK.**

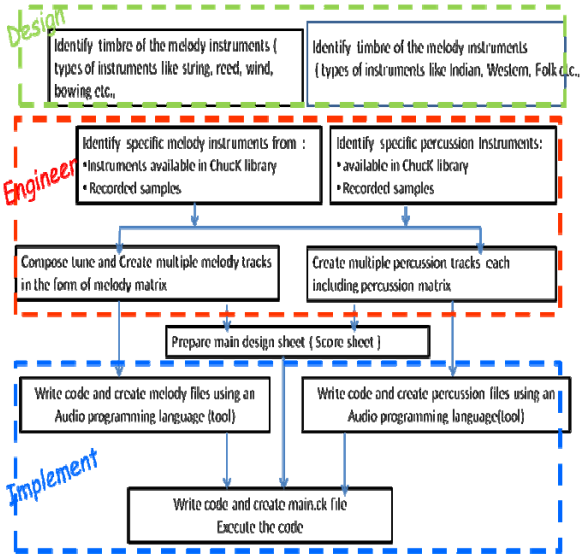

Fig.4-Music Generation phases - Design, Engineer & Implement

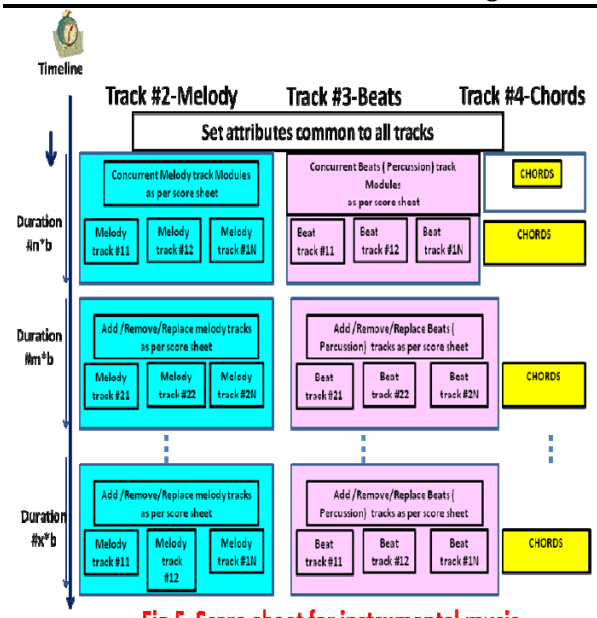

Fig.5. Score sheet for instrumental music

MELODY MATRIX [Table.1]

Melody matrix is the core of music composition that is referred by the programming language to generate music.

	Note	Duration (seconds)	Gain(Number)	Other attributes**
BMU	N1	d*	1	
	N2	2d	1	
	N3	4d	2	
BMSU	N4	3d	0.5	
	N5	2d	0.5	
	N6	8d	1	
	N7	6d	1	
	N8	d	2	

*d – duration of Basic Melody Unit (BMU)
**other attributes : Echo, Reverb, Fading
•Basic Melody Unit (BMU) is the Note (Swara) with a predefined frequency.
•Duration of Basic Melody Unit (BMU) – is defined as per the needs of the composition
•A melody track is made up of Multiple BMUs
•BMUs are grouped into Basic Melody Sequence Unit (BMSU)

Table1. Melody Matrix

A song is nothing but a series of notes (*swaras* as they are called in Indian music), each played for a specific duration. Technically each note generates a electrical / electromagnetic signal vibrates the diaphragm of the speaker to produce sound. Melody matrix gives the attributes of every note to be played. Mandatory attributes are

- Note number (indicates what frequency has to be generated)
- Duration (how long the note to be played)
- Gain (the intensity or volume of the note)

Optional attributes are to give special effect to each note like

- Reverb
- Echo
- Fading effect

Computer program picks the element of each row in the matrix and produces the melody of that instrument.

Basic Melody Unit (BMU) and **Basic Melody Sequence Unit (BMSU)** are the two elements giving a structure to the matrix.

BMU is the note (swara) with a predefined frequency . d is the duration of BMU in seconds, which decides the tempo of the track. BMUs are grouped in to Basic Melody Sequence Unit (BMSU). In other words, BMSU is a pattern of n number of notes. A melody track is made up of multiple BMSUs. **BMSU is the basis to decide the Percussion track in terms of number of beats per cycle.** BMSUs can be of different lengths as shown in Fig.5

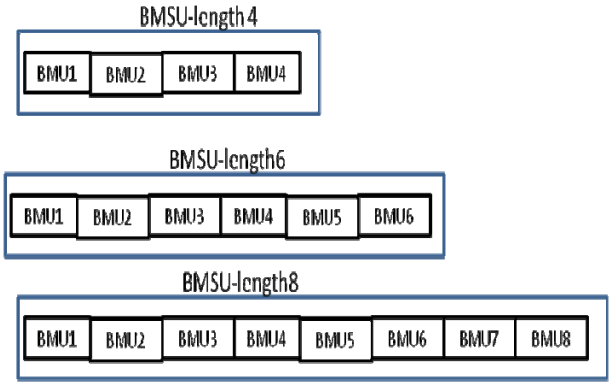

Fig.6. BMSUs of different lengths

PERCUSSION MATRIX [Table.2]

Percussion matrix also follows the same principle as in Melody matrix.

	Beat	Duration (seconds)	Gain (Number)	Other attributes**
BPU	B1	d*	1	
	B2	2d	1	
	B3	4d	2	
BPSU	B4	3d	0.5	
	B5	2d	0.5	
	B6	8d	1	
	B7	6d	1	
	B8	d	2	

*d – duration of Basic Percussion Unit (BPU)

**other attributes : Echo, Reverb, Fading

•Basic Percussion Unit (BPU) is one unit – (e.g. in Tabla, it is called as *theka, bol)*

•Duration of Basic Percussion Unit (BPU) – is defined as per the needs of the composition

•A percussion track is made up of Multiple BPUs

•BPUs are grouped into Basic Percussion Sequence Unit (BPSU)

Table2. Percussion Matrix

Percussion matrix is the basis to generate the rhythmic pattern of beats. Mandatory attributes are

- Beat number
- Duration (how long the note to be played)
- Gain (the intensity or volume of the note)

Optional attributes are to give special effect to each note like

- Reverb
- Echo
- Fading effect

Computer program picks the element of each row in the matrix and produces the percussion sound of that instrument.

Basic Percussion Unit (BPU) and Basic Percussion Sequence Unit (BPSU) are the two elements giving a structure to the matrix.

BPU is the basic unit of percussion beat. d is the duration of BMU in seconds, which decides the tempo of the track. BPUs are grouped in to Basic Percussion Sequence Unit (BPSU). In other words, BPSU is a structured sequence of beats as shown in Fig.6. A percussion track is made up of multiple BPSUs. It is extremely important that **BPSU is designed to synchronise the melody track.**

So for the discussion has been on the process of music generation, irrespective of the programming language to be used. Let me discus now the vital component – Audio programming language used in our work namely ChucK.

Chuck – AUDIO PROGRAMMING LANGUAGE-OVERVIEW

What is ChucK?

ChucK is a **"open-source" , object oriented programming language** designed specifically for **real-time sound synthesis** and **music creation.** "Real-time" means that ChucK synthesizes the sound as you are hearing it (rather than just playing back a sound file, although ChucK can also do that), and often in response to signals and gestures from the "outside world," such as you typing on the keyboard, moving the computer mouse, manipulating a joystick or other game controller, playing the keys on a musical keyboard connected to your computer, or a host of other things that are available to hook up to our computers.

Not just for sound and music, ChucK is also good for controlling and/or interacting with almost any type of real-time computer media and art, such as graphics, robots, or whatever can communicate with your computer.

ChucK is designed specifically to allow and encourage **"on-the-fly" programming,** which means you can add, remove, modify and edit, and layer segments of code at any and all times, hearing the results instantly, without interrupting other sounds being synthesized and heard.

Most other languages require you to compile, run, and debug code in a fashion that doesn't let you hear what you're doing immediately. In fact, almost all computer languages (such as C,

C++, Java, etc.) are not designed specifically from the ground-up for sound, music, and other real-time tasks. **But ChucK makes immediate, real-time sound a priority.**

ChucK was initially created by Ge Wang when he was Perry's graduate student at Princeton University and now an Assistant Professor at Center for Computer Research in Music and Acoustics, Stanford University.

Why ChucK?

• **It's all about time.** Time is at the core of how ChucK works, and how one works with ChucK to make sound. Why such emphasis on time? **Sound/music is a time-based phenomenon;** without the passage of time, there would be no sound. By controlling how and when we do things through time, it's a different and powerful way to work with sound at every level – every molecule of it.

• **It's text, plain and simple.** For example, to generate **1 second music tone of the melody Indian instrument Sitar,** following 4 lines are sufficient.

Sitar s=>dac;
400=>s.freq;
1=>s.noteOn;
1::second=>now;

• **It's fun and immediate.** It is designed to be a fun language and environment to work in, to experiment in. You can synthesize sounds, make fantastical automations, map physical gestures (e.g., with controllers) to sound, network different computers together, and even analysis to computational make sense of sound.

• **It's free.**

ChucK has been in development and non-stop use for more than 10 years, and it continues to evolve. It's open source, which really means it belongs to everyone whocare to use it, modify it, fix it, improve it, or extend it.

• ChucK has many features as in any other popularly used language like JAVA, C, C++.

EXPERIMENTS & RESULTS

More than 10 Indian music compositions were successfully tested. Out of them 3 compositions are presented in this paper. Corresponding MP3 files are attached.

Music #1

Category	**Popular Indian patriotic song**
Language original song	Indian national language- Hindi
Title	"saare jahaa se accha"
Duration	54 seconds
Voice track	Nil
Number of melody tracks	3
Melody instruments used	Mandolin, Flute, Rhodey,
Available in ChucK library (unit generator)	Mandolin, Flute, Rhodey,
Number of percussion tracks	
Percussion instruments used	ModalBar, Drums, tabla , *'Gejje'*
Available in ChucK library (unit generator)	
Sampled (Recorded) sound	Drums
	Tabla
	"Gejje"

Music #2

Category	Popular Kannada old movie song from movie 'Gandhada Gudi'
Language original song	Regional language of Karnataka - - Kannada
Title	-'Naavaaduva nudiye kannada nudi'

Duration	100 seconds
Voice track	Nil
Number of melody tracks	2
Melody instruments used	Mandolin, Clarinet
Available in ChucK library (unit generator)	Mandolin, Clarinet
Sampled (Recorded) sound	Nil
Number of percussion tracks	2
Percussion instruments used	Modalbar, *"Gejje"*
Available in ChucK library (unit generator)	
Sampled (Recorded) sound	Drums

Music #3

Category	Folk style
Language original song	Not applicable – Instrumental music
Title	'Naavaaduva nudiye kannada nudi'
Duration	4 Minutes
Composed by	Prof.Chidambara Kalamanji
Voice track	Nil
Number of melody tracks	3
Melody instruments used	Mandolin, Flute, Rhodey
Available in ChucK library (unit generator)	
	Mandolin
Sampled (Recorded) sound	Nil
Number of percussion tracks	4
Percussion instruments used	Tabla, Gejje, Dholak, Drums and some other folk instruments.
Available in ChucK library (unit generator)	Modal bar
Sampled (Recorded) sound	Drums, Tabla, "Gejje"

SAMPLE ChucK PROGRAMS

PROGRAM#1- GENERATION OF PERCUSSIN SEQUENCE - TABLA

```
//-------------------------------------------------------
----------------------------------------
// This module generates Beat(Percussion) sequence
// Written by Prof.Chidambara, PESIT, Bangalore, India.
// Language used is ChucK;
//Instrumental music generated : Tabla - Popular Indian instrument used both in Classical and Light music.
// Approach : Since this instrument is not avalabele as part ChucK libaray ( Unit Generator)
// Already recorded samples of Tabla ( max 1 sec)  in the form of .wav files are used
// Algorithm :
//1) Create temporary buffers; 2)Copy the .wav file from the hard disk to temporary buffer 3) Play.
// Sequence of the files played will generate Tabla pattern .
// In this program 4 beats per cycle is generated.
// Input : .wav files in a floder ( preferable to have in current folder )
// Output : Music - Tabla sound pattern
//-------------------------------------------------------
----------------------------------------
// Initialisation
SndBuf mySound1 => dac; // Create buffer1
SndBuf mySound2 => dac; // Create buffer2
SndBuf mySound3 => dac;//Create buffer3
SndBuf mySound4 => dac;// Create buffer4
```

```
0.25=> float tempo;// variable for the
duration of each beat
// Name the path for the recorded Tabla files
me.dir()+ "/wavefiles/TB1NA.wav"=> string
FileTB1NA; // Name for the path of the .wav
file corresponding to beat1;
me.dir()+ "/wavefiles/TB1SUR.wav"=> string
FileTB1SUR;// Name for the path of the .wav
file corresponding to beat2;
me.dir()+ "/wavefiles/TB2CLSGE.wav"=> string
FileTB2CLSGE;// Name for the path of the
.wav file corresponding to beat3;
me.dir()+ "/wavefiles/TB1OPNGE.wav"=> string
FileTB1THAP;// Name for the path of the .wav file
corresponding to beat4;

fun void PlayTabla() // Function to play 4
beats in sequence
 {
  while(true)
   {
    FileTB2CLSGE => mySound1.read; // Read
the .wav file to buffer1
    0.75=>mySound1.gain;// set the gain
    0=> mySound1.pos;// start from the
begining of the buffer and play
    tempo::second=>now; // for the duration
defined by the variable tempo.

    FileTB1SUR => mySound2.read; // Read
the .wav file to buffer2
    0.75=>mySound2.gain;// set the gain
    0=> mySound2.pos;// start from the
begining of the buffer and play
    tempo::second=>now;//for the duration
defined by the variable tempo.

    FileTB1NA => mySound3.read;// Read the
.wav file to buffer3
    0.75=>mySound3.gain;// set the gain
    0=> mySound3.pos;// start from the
begining of the buffer and play
    tempo::second=>now; // for the duration
defined by the variable tempo.

    FileTB1THAP => mySound4.read;//Read
the .wav file to buffer4
    0.75=>mySound4.gain;// set the gain
    0=> mySound4.pos;// start from the
begining of the buffer and play
    tempo::second=>now;//for the duration
defined by the variable tempo.
   }
} // End of function that plays Tabla beat
sequence

// Main program; calls the function to play
tabla
PlayTabla();
```

PROGRAM#2-GENERATION OF PERCUSSIN SEQUENCE – MODAL BAR

```
//-------------------------------------------------------
---------------------------------------
// This module generates Beat(Percussion)
sequence
// Written by Prof.Chidambara, PESIT,
Bangalore, India.
// Language used is ChucK;
//Instrumental music generated : Modal Bar
// Approach : This instrument is  avalabele as
part ChucK libaray ( Unit Generator)

// Algorithm :

// Modal Bar is played continuously at a set
tempo.
// Input : Nothing
// Output : Music- Beats
//-------------------------------------------------------
-----------------------------------------
// Initialise
 ModalBar bar => dac;
 0.5=>bar.gain; // volume set
 10=> bar.preset; //Select the sound
(timbre)required. Value assigned will decide
the sound generated.
 0.25=> float Tempo;// duration set; ( which
also sets the tempo)
 61=> int pitch;// set the pitch of the
instrument.
```

```
fun void PlayModal()// function to play
continuosly beats.
{
  while(true)
    {
     Std.mtof (pitch)=>bar.freq;
      1.0 => bar.noteOn;
      Tempo*2::second=>now;
    }
}

PlayModal();
```

PROGRAM #3-GENERATION OF MELODY – INDIAN PATRIOTIC SONG "SAARE JAHAASE ACCHA"

```
//-----------------------------------------------------------
-----------------------------------------------------------
---------
// This module ( Melody Track ) plays the first
line ( Pallavi) of the song  "SAARE JAHAASE
ACCHA"
// Written by Prof.Chidambara, PESIT,
Bangalore-30 Nov 2014
// Using Audio Programming Language : ChucK
// Input Data : Melody Matrix
// Output : Music
//-----------------------------------------------------------
-----------------------------------------------------------
-----------

//Select instrument
  Mandolin m=> dac; //
  0.5=>m.gain;// Intensity of sound
  0.25 =>float KTempo;// Variable to control
the duration each note and the tempo of the
song.
  0.95=> float DutyCycle;// Variable to control
the on duration and off duration of each note.

  KTempo*DutyCycle=>float OnDur; // set On
duration of each note.
  KTempo*(1-DutyCycle)=> float OffDur; //
set off duration of each note.
// Melody matrix [2X2]: Each row [ Midi Note
number, Duration ]; This matrix represents the
main part of this song.
SA    RE    -     JA    HA    SE
[[    [64,1], [63,1] [61,1], [63,2], [60,1],

A     CH    A
[61,2], [61,2], [999,2]  @=>  int  notepallavi[][];//
64,2],

  NotePallavi.cap()=> int NoteTotal;// Total
notes in the matrix

// Function to play the notes of the Melody
matrix using the instrument Mandolin
fun void PlayMandolin()
{
  for(0 => int i; i<=NoteTotal-1; i++) // Loop
that selects each note one by one and plays.
   {
            NotePallavi[i][0]=> int note1; //
select the current note
              if
               (note1==999)// if it is 'silent'
              don't note off. 999 in the matrix
              represents silence.
                 {
                    <<< "silence">>>;//
Dispaly that it is a silence
                     0=>m.noteOn;

  NotePallavi[i][1]*OnDur::second => now;//
both On duration and off duration of the note
to be silent
                      0=>m.noteOn;

NotePallavi[i][1]*OffDur::second => now;
                 }

             else // if the note is not silent,
play the note;

              {
                  <<< "Playing Mandolin
Note">>>; // display that mandolin note is
played
                   NotePallavi[i][0] =>
Std.mtof => m.freq; // pick the note number (
MIDI ) format; Convet in to frequency.
                  1.0 => m.noteOn; // Play
note in this frequency
```

```
NotePallavi[i][1]*OnDur::second => now; //
Play for the duration specified ( second
element ) in the row;
                    0=>m.noteOn;

NotePallavi[i][1]*OffDur::second => now;//
Second part of the note; silence
                }
    }
        0=>m.noteOn;
        <<< " Mandolin Pallavi is over">>>;//
when all notes are played, display;
}  // End of function

//Main program

PlayMandolin();// Call the function to to play
all the notes of the matrix
me.exit(); // exit
```

CONCLUSION

"Enrich the listener, Empower the musician and Enhance the creativity using audio programming language" was the statement made in the beginning of this paper. **Could this be achieved?. Answer to this is 'YES'.**

Enrich the listener: When the music created and generated through this mechanism was sent to some of the listeners, excellent feed back was received. They have expressed that some patterns of music were unique which couldn't be possible through real music.

Empower the musician: Author himself is the proof for this. Author is just an amateur music composer, not a professional musician. Only playing keyboard was the skill set possessed. Playing percussion or playing any other instrument was not known. As can be listened from the three music clippings presented, an orchestra of melody and percussion could be created *(of course, there is a lot to improve).* Using audio programming language ChucK has empowered an amateur musician.

Enhance creativity: ***No doubt, human creativity can not be replaced by machines. How can a machine be creative when it can do only the things programmed by the humans?.*** This logic is true. But while experimenting using ChucK, many innovative melody and percussion pattern design ideas were triggered which was nothing but enhancing the authors creativity.

Quality of music generated as part of the experiment may not be as good as a professional music created in a studio. But it may be treated as a 'proof of concept' that has shown the potential of this interdisciplinary approach that can be explored by the CompuMusicians. **Through this paper, author invites the interested, passionate individuals to join in the journey of CompuMusic.**

References :

[1] Prof.H.M.Padalikar,"When Science Facilitates Art Designing A Computer Based System To Simulate Music Rendered by Tabla", International journal of Multidisciplinary Approach and Studies, Volume 01, No.5, Sep-Oct 2014, ISSN NO::2348-537X

[2] Ajay Kapur, Perry Cook, Spenser Salazar, Ge Wang, ""Programming for Musicians and Digital Artists – Creating music with ChucK", Page No 4-5, Manning publications.

[3] Ge wang and Perry Cook, " The Chuck Manual 1.2.1.3"

Online references:

[3]http://ravikumarv.wordpress.com/2010/06/13/indian-classical-vs-light-music/

[4] http://www.musicgenreslist.com/

[5] Wikipedia

SMS BASED PERSON'S LOCATION CHECKING SYSTEM FOR ANDROID MOBILES USING GPS AND GPRS

[1]Purvi N Jardos, [2]Viral V Kapadia
MCA Dept. The Dharamsinh Desai University of Nadiad,
Computer Science & Engg Dept.The M S University of Baroda
Email:purvi.jardos@gmail.com,
kapadia_viral2005@yahoo.co.in

Abstract - Purpose to develop the system is to keep track of your family members and close person's location using smart phone by just sending simple SMS(Short Message Services).Locating of the mobile device uses two technologies via General Packet Radio Service (GPRS) and Global Positioning System (GPS). The person's location can be tracked using a mobile phone which is equipped with an internal GPS receiver or mobile internet connectivity which is useful for finding out the location of device. System is developed for android mobile devices and using android sdk, Google Play service, Google MAP API and sqlite database to log necessary required information. System is serve as requestor - capable to request for other device's location and as a provider - capable to provide location of device to pre-synchronized number using SMS(Short Massage Services). Google Map is used for mapping the device's location which is serves via SMS by provider. Log of last received location information of provider's device is maintained. System rendered with facility like any other number which is not part of synchronized number list cant access the device's location.Basic utility like modified and delete the information of requestor as well as provider.

Index Term – Google MAP , GPS, GPRS,SMS base application , Synchronization

I INTRODUCTION

Smart mobile device can either using GPS (Global Positioning system) or GPRS(General Packet Radio Service) for finding the current location of device, [1] GPS system which is a satellite based service which is available 24X7 everywhere in the whole world. GPS system can be used to get location which includes details like latitude, longitude's values .So, tracking of human . GPRS system is track location with the help of service provider network with nominal coast using Mobile phones equipped with GPS receiver or using GPRS and service provider network rather than handheld GPS receiver is cost effective and easy.

In Today's fast life everyone always wants to know that their kids, retired parents and

dear ones are safe. So it's become easy with the help of mobile device to keep in track of location of family members. Every smart phone having SMS and GPS facility.

The main purpose of develop the system is to keep track of location of your dear once as well as provide your location to your family member and dear one who request for a it , by just sending one SMS service. GPS is combined with one of the basic service of a smart phone which is GSM, more specifically SMS, in one system. System holding facility to work as a requestor which will allow requestor to send a request to get the location information of other person and show that on Google Map. System also holding facility to work as a provider which accept the request of requestor and pass on the current latitude and longitude value of device to the requestor. . On the other hand, the system at the provider's side uses GPS or GPRS service provider network to get person's location information using phone device.[4]Information such as GPS coordinates a sent to the requestor smart phone that's preregistered on the application via SMS. The communication between the two devices is done using Short Message Service (SMS). SMS offers the system unique features, which makes system to work without the need of internet connection thus allows the application to be implemented on smart phones that don't support continuous GPRS, 2G or 3G internet connectivity. The system sends the location of provider's device to requestor's device when requestor send request to check location of provider. So, the System is facilitated with functioning of requestor as well as location provider , that is it can send the request for get location of person as well as provides the location to the synchronized requestor. At the security aspect of system, location information like longitude and latitude value of current device's position only provided to when request is coming from synchronized number, So any other non-synchronized number not able to check the device/person's location. In case of finding latitude and longitude values GPS off GPRS service provider network, WIFI sensor is utilized. For open the location at Google Map only internet connectivity is required, and location information is logged by system, which will be useful to show the location on Google Map whenever internet connection available on device. System is rendered with basic utility of update and deletes the provider and requestor detail.

II RELETED WORK

[1] Existing human tracking system ,The architecture of the system is based on client server approach. at mobile device's application side that is client side GPS receiver fetches the GPS location, after calculating the exact location it further creates a GPRS packet along with the location details a running on the Android based Mobile sends this GPRS packet to the server. Server stores packet information and at server computer displays the map along with location to track the human. Limitation of system is that in order for the system to work there must be continuous internet connectivity required at mobile device.

[3]Existing system for woman tracking using GPS and GPRS , use client-server type of

architecture, in which after the registration on server and getting password. When user one the app in emergency from mobile device, GPS start to trace the phone & find the location of user with help of device, and keep sending to server using GPRS service after certain time-slab continuously. At other side Administrator's computer generates and updates the MAP for received updated location information. Location information store in database and server send the same location information via message to its family members continuously after specified time-slab. Limitation of system is there must be internet connectivity required to mobile device to continuous sending location data . Also administrator side computer required internet connectivity to receive latest location information receives from client side device.

[4] System for child tracking aimed to help locating missing or lost children. GPS is combined with one of the basic service of a smart phone which is GSM, more specifically SMS, in one system. System having two parts, parent and child application. An application at the parent side allowed parents to send a location request to a child side then retrieve the location from the request reply and shows it on a map. On the other hand, the application at the child's side gathers the necessary information of the smart phone that will be used to locate the smart phone. Information such as GPS coordinates and time are gathered and sent to the parent smart phone that's preregistered on the application. The communication between the parent and the child applications is done using Short Message Service (SMS) and application to be implemented on smart phones that don't support

GPRS, 2G or 3G internet connectivity. Limitation of system is device having a child side application cannot requests for location of other person.

III Application development

A. Requirement for the system

This system use basic SMS service and GPS service which is commonly available in every smart phones. Mainly used by family member especially parents who want to keep track of their child's location which can be provide as an when it is demanded. This system is developed using tool eclipse for android developer and android sdk.[5] Application use SQLite database to store information about the location and synchronization detail. For display the map system uses Google play service and MAP key for accessing Google MAP.[6]

B. System Architecture

Fig[1] shows the overall architecture of the system it can work as requestor as well as can work as a location provider . As requestor system can first t send request for synchronization to the provider side using SMS. At provider side system maintain the log of coming requests of synchronization and if request is accepted then requestor will get SMS of acceptance of request this way system make . Synchronization between requestor and provider for communication about the location information so SMS from other than synchonised acquire number cant d the after location information r successful synchronization, system grants requestor for requesting provider's device location via SMS. At provider side using GPS or network

service which ever available system acquire the current longitude and latitude of the provider's device and send to requestor via in SMS. At requestor side after receiving of SMS of about location information notification of location information is generated to rendered a facility to open a location in map by single click on notification whenever internet connectivity available on requestor's device . Provider's location information logged by requestor's system to facilitates to locate last known location of provider's device on Google map.

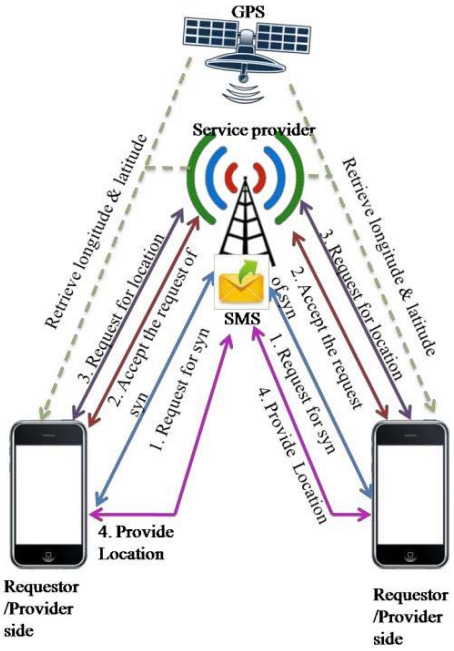

Fig[1]. System Architecture

C. Algorithm of system

1) Send request for synchronizes the number for checking location of receiver/provider using SMS. for the permission to get other device location.

2) At Receiver/provider side generate notification for synchronization, after approval of the request, send SMS of approval to requestor side.

At requestor side after getting approval SMS can request for check location of provider's device using SMS to provider' number

3) At receiver/provider side , check in database of incoming request mobile number with synchronized number. If incoming request coming from synchronized number then using GPS service or GPRS provider network service , fetch current latitude and longitude of device and send it using SMS service to same mobile number from which number request coming from using SMS service.

4) At the requestor's side after getting longitude and latitude location SMS , Generate notification and on click on notification opens Google map to locate the area. And store last receive location values for later on locate location on Google Map .

5) Other Utility like edit or delete provider and request or detail like name and synchronized SIM number stored in device is provided by system.

6) Other Facility of maintain logs for all pending synchronization requests handled by system.

D. *Application Specification*

Fig[2] having main page of system to shows the basic functionality of system requestor side as well as provider side.

Button for synchronize is for sending request for synchronize for start communication for checking and getting number. Location button for sending request for check location of synchronized number and locate on map. Location Provider button opens the list of available person's and allowed to update/delete details whom location is allowed to check . Pending button list out all coming request for synchronization. Requestor List button shows and update/delete the requestor number which can access device location. Fig[3] shows how Requestor can send request for the synchronization to other SIM number where application is installed on other device. In Fig[4] At receiver side where system is installed and gets SMS and notification is generated so on click of notification it open pending list waiting for the synchronization. Fig[5] shows the list of pending requests awaiting for the synchronization for permission to check the location of device. Fig[6 shows the list of provider to whom request to check his/her device location can be retrieved . In Fig[7] system send request via SMS for getting location of selected contact . Fig[8] requestor get the latitude and longitude values via SMS and generate the notification Fig[9] on click of notification about location values , Map is open and locate the retrieved person's location on Google Map. Fig[10] Displays list of provider for update the detail. Fig[11] displays list of requestor for update the detail. Fig[12] allowed to update the selected requestor or provider detailed and update database

Fig [2] Main page

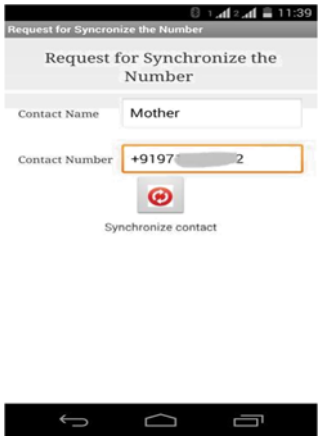

FIG[3] REQUEST FOR SYNCHRONISATION

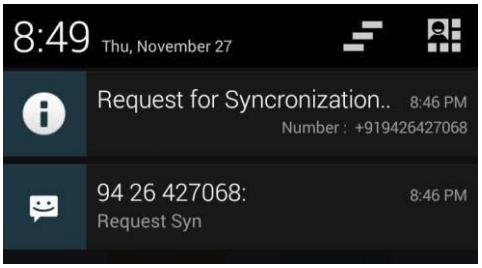

FIG[4]RECIEVER SIDE SMS RECEIVE AND NOTIFICATION GENERATE

FIG[5] LIST OF PENDING REQUEST WAITING FOR SYNCHRONISATION

FIG[6]list of location provider for display last known location or send request for current location

FIG[7]sending sms to selected contact for his/her current location of device

FIG[8]at requester side get sms of longitude and latitude value and notification generate notification

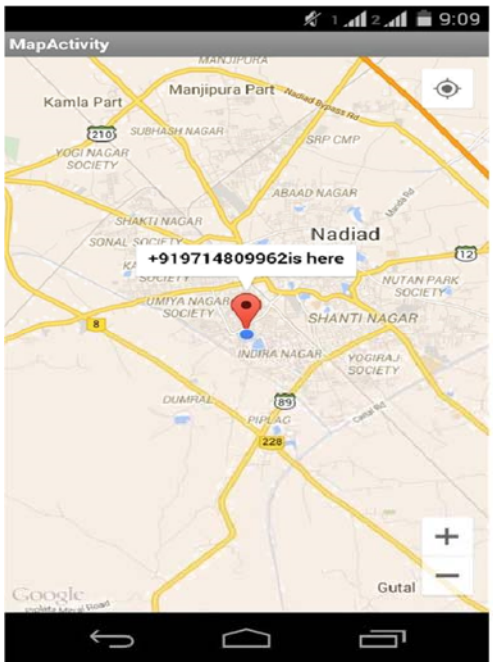

FIG[9]at requester side open map for receive latitude and longitude value

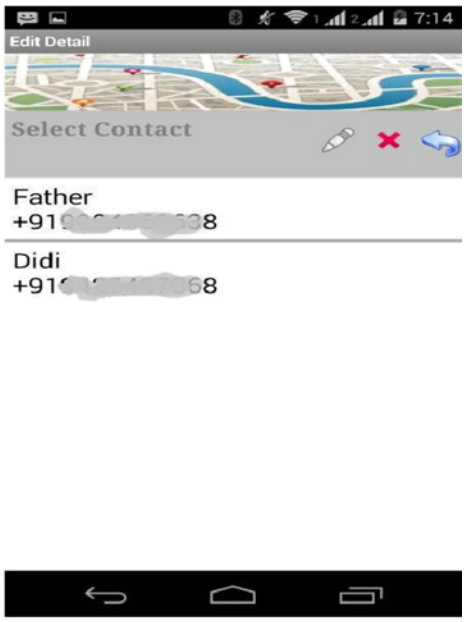

FIG[10]list of provider for edit detail

FIG[11]list of requester for edit/delete detail

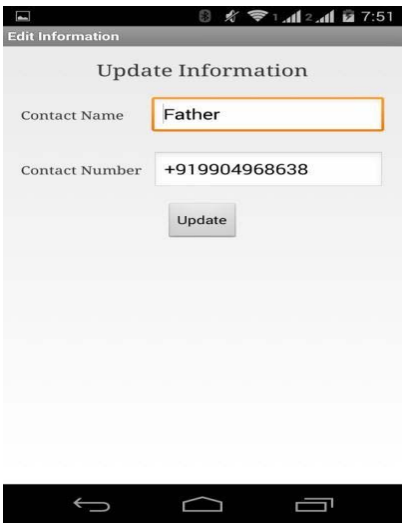

FIG[12] Update selected requester/provider detail

IV CONCLUSION AND FUTURE ENHANCEMENT

The ystem can work on basis of SMS service. So without internet network also communication for the device location between two people is made possible. System maintain the log of last know location information, used to locate on map later on whenever required. Only for display location on Google map it requires internet connectivity .Log for pending synchronization request also maintained. As security aspect only entitled synchronized number can do location request so threat of accessing device location by other than entitled synchronized number not possible. Mobile device's EMI number is also use for locate the device. System should be synchronize with sim number as well as EMI number in future enhancement. Sending location information of device to synchronized number as an alert when SIM number in particular device is changed would be the future enhancement for the system.

REFERENCES

[1]. Ruchika Gupta and BVR Reddy: " GPS and GPRS Based Cost Effective Human Tracking System Using Mobile Phones", VIEWPOINT, vol. 2 , No. 1, January-June 2011

[2]. Nilesh Dhawale, Mahesh Garad, Tushar Darwatkar , "GPS and GPRS Based Cost Effective HumanTracking System Using Mobile Phones" International Journal of Innovations & Advancement in Computer Science- IJIACS, vol. 3, Issue 4,ISSN: 2347 – 8616,June 2014

[3]. Devendra Thorat, Kalpesh Dhumal, Aniket Sadaphule, Vikas Arade, " A Cost Effective GPS-GPRS Based Women Tracking System and Women Safety Application using Android Mobile ", International Journal of Advanced Engineering & Innovative Technology, vol. 1, Issue 1, April-2014, 2-6 ISSN:2348-7208

[4]. A. Al-Mazloum, E. Omer, M. F. A. Abdullah, "GPS and SMS-Based Child Tracking System Using smart phone" International Journal of Electrical, Robotics, Electronics and Communications Engineering, vol. 7 No:2, 2013

[5]. Android Developers for sdk at: , http://developer.android.com/sdk/index.html

[6]. Google Map api key help at: https://developers.google.com/maps/document ation/android/start

[7]Google Map key generation, https://code.google.com/apis/console